UNIVERSITY OF CALIFORNIA
RIVERSIDE

Nitrogen and Phosphorus Biogeochemistry of Watersheds Along the Western Slope of the Sierra Nevada

A Dissertation submitted in partial satisfaction
of the requirements for the degree of

Doctor of Philosophy

in

Soil and Water Sciences

by

Peter Michael Homyak

September 2012

Dissertation Committee:
Dr. James O. Sickman, Chairperson
Dr. Edit B. Allen
Dr. Michael A. Anderson

The Dissertation of Peter Michael Homyak is approved:

_____

_____

_____
Committee Chairperson

University of California, Riverside

ACKNOWLEDGEMENTS

I am extremely grateful to my advisor, Dr. James Sickman, and committee members, Dr. Edith Allen, and Dr. Michael Anderson for their guidance, support, and excitement over my research. I am very thankful to many people who helped me in the field including Kevin Skeen, Ahmed Haggag, Thomas Martin, Paul Koster, Andi Heard, and Annie Esperanza. I am also very grateful to those who helped me with laboratory analyses including Dee Lucero and Jennifer Quach who helped me with countless soil and water samples, as well as Amanda James, Myles Davis, Will Vicars, Mike Bell, and Judy Turk. I thank Woody Smith for his help using the ICP and Dave Thomason for his help with many chemical analyses and other logistics. This research was made possible by a UCR Chancellor Fellowship, NSF LTREB grant, and a UCR graduate mentorship fellowship.

DEDICATION

I dedicate this dissertation to my wife, Gabriela, who has inspired me to reach beyond any of my expectations. To my parents, Mike and Melba for their love and encouragement, and to my sister, Natalia, and Sonia and Santi for their unconditional love and support. To Juan for "keeping things real" by frequently asking when would I get a job, and to Lili, Paulina, and Pat. Lastly, I dedicate my work to Uncle Wally to whom I owe the opportunity of an education and to my very large family who have contributed in many ways to my personal growth and career.

ABSTRACT OF THE DISSERTATION

Nitrogen and Phosphorus Biogeochemistry of Watersheds Along the Western Slope of the Sierra Nevada

by

Peter Michael Homyak

Doctor of Philosophy, Graduate Program in Soil and Water Sciences
University of California, Riverside, September 2012
Dr. James O. Sickman, Chairperson

Human activities have more than tripled the amount of N and P available to ecosystems, resulting in complex effects on the environment. The objectives of this study are to evaluate the N saturation status of chaparral ecosystems exposed to elevated atmospheric N deposition and identify mechanisms for the destabilization of P in soils and lacustrine sediments that may be contributing to the eutrophication of high-elevation Sierra Nevada lakes. The N saturation status of a chaparral catchment was assessed through an N budget including atmospheric N inputs, hydrologic and gaseous N outputs, belowground N dynamics, and isotopic separation of streamwater nitrate sources. Phosphorus pools in soil and lake sediment were identified and monitored seasonally to understand how changes in physicochemical conditions and hydrology affect the transport of P to Sierran lakes. In chaparral, seasonal transitions, microbial C limitation, and the asynchrony between N availability and plant N demand modulated the kinetic N saturation of the catchment. The transition from dry to wet soil conditions induced rapid

nitrification of ammonium leading to large hydrologic and gaseous N losses. However, during the growing season, N losses were minimal highlighting the limitations of applying standard N-saturation theory to xeric landscapes. In high elevation catchments, P is tightly bound by Al and atmospheric P inputs and rock weathering during the Holocene are the primary sources of present day soil and sediment P. Lake sediments represent a strong sink for P in high elevation lakes even during periods of anoxia. During snowmelt, 27% of the soil P cycles between the inorganic and organic pools raising the possibility that changes in snowpack dynamics could potentially explain long-term trends in P supply to lakes. Although intrinsic differences exist between chaparral and subalpine catchments, they respond similarly to the Mediterranean climate of California. The loss of tight biological control of N and P during seasonal transitions in the Sierra Nevada is similar to the response of ecosystems to periodic disturbances like fire and logging. Thus, nutrient limitation of these terrestrial and aquatic ecosystems and their sensitivity to anthropogenic pollution is tightly linked to interannual and long-term changes in climate.

TABLE OF CONTENTS

LIST OF TABLES

LIST OF FIGURES

LIST OF EQUATIONS

1. Introduction

Both nitrogen (N) and phosphorus (P) are essential elements in terrestrial nutrient cycling; they often limit ecosystem productivity, and are important for the synthesis of organic compounds such as proteins, DNA, and ATP (Schlesinger, 1997). Although N and P are typically available in low quantities relative to ecosystem demand, since the beginning of industrialization, it is estimated that anthropogenic activities have more than tripled the amount of N and P available to ecosystems and in many cases these additions have resulted in indirect negative effects to the environment (Caraco, 1993; Erisman et al., 2011; Galloway et al., 2004; Vitousek et al., 1997).

Although the direct effects of human activities on natural systems are relatively well understood (e.g., acid rain lowers soil pH), the indirect effects on ecosystems are more difficult to predict, owing to the complexity associated with interpreting how interacting processes modify ecosystem dynamics. For example, N deposition can alter the magnitude and intensity of wildfires in semiarid environments by promoting the growth of exotic grasses in interspaces between shrubs that increase the amount of highly flammable fine fuel biomass (Allen et al., 1998; Rao et al., 2010). Because the effects of anthropogenic pollution can affect sensitive remote ecosystems isolated from pollution sources, it is critical to understand how these systems may respond to anthropogenic pressures through synergistic and complex mechanisms in order to ensure their preservation.

The Sierra Nevada Mountains stretch for approximately 700 km north to south and are part of a semi-continuous belt of plutonic rocks that extends from the Mojave Desert in California to northwestern Nevada (Bateman et al., 1963). Because of its Mediterranean climate, precipitation occurs mainly during winter with little to none occurring during dry summers. Temperature varies as a function of elevation (~200 to over 4,000 m) in which the average temperature for the warmest month is at least 22 C° in the foothills and 10 C° for alpine regions; on average, a 100 m gain in elevation results in a 0.6 C° decrease in temperature (Mutch et al., 2008). The Sierra Nevada is mainly composed of granitic rock which has been polished by several glacial periods starting approximately 1 million years ago and lasting until about 10,000 years ago. As a result of deglaciation, Sierran landscapes are highly eroded and characterized by U-shaped canyons from glacial melting and moraines from the deposition of eroded materials (Mutch et al., 2008). Because of the relative young age of these soils and their granitic rock parent material, soils in the Sierra Nevada are typically poorly developed and are commonly classified as Entisols and Inceptisols (Taskey, 1995). Despite poorly developed soils, altitudinal gradients and associated changes in temperature help support seven distinct vegetation zones (from west to east: foothill woodland, chaparral, lower montane forest, upper montane forest, subalpine forest, alpine, great basin woodland) with over 3,500 native vascular plant species, 650 moss species, and 280 native vertebrates (Mutch et al., 2008).

While the Sierra Nevada is not directly impacted by point sources of pollution, intense agricultural practices and growing urban centers in the San Joaquin Valley are

significantly altering rates of N (Cisneros et al., 2010) and P (Vicars et al., 2010) deposition to Sierran ecosystems, resulting in accelerated nutrient cycling, nutrient imbalances, eutrophication, and presumably vegetation type conversions. I hypothesize that the ecosystem response to anthropogenic pollution, in both chaparral and alpine environments, is influenced by "hot moments" of intense biogeochemical cycling caused by marked changes in soil moisture during seasonal transitions. These hot moments are controlled by shifts from dry soils during summer to wet conditions during winter (Miller et al., 2005), and exclusively to high elevations, from periods with deep snowpacks to saturated soils and intense hydrologic flushing during snowmelt (Miller et al., 2009). That is, hot moments during seasonal transitions can promote processes analogous to ecosystem disturbances, during which the indirect effects of anthropogenic pollution are exacerbated through accelerated biogeochemical cycling and mobilization of nutrients by microbial mineralization and transport via hydrologic pathways.

In low-elevation ecosystems of the Sierra Nevada, chaparral dominated watersheds are exposed to elevated rates of N deposition (Cisneros et al., 2010; Fenn et al., 2003c; Li et al., 2006). Although these systems are believed to be N limited (Padgett and Allen, 1999), elevated stream nitrate (NO_3^-) concentrations along with potentially elevated gaseous N losses (nitric oxide (NO) and nitrous oxide (N2O)) during seasonal transitions suggest that chaparral ecosystems are receiving N inputs in excess of ecosystem demand (Fenn et al., 2003a; Fenn et al., 1998; Fenn et al., 1996). This condition, known as N saturation (Aber et al., 1989; Stoddard, 1994), has promoted vegetation type conversions in other xeric landscapes by indirectly altering the frequency

and intensity of wildfires through chronic fertilization of exotic grasses and concomitant increases in fine fuel biomass (Allen et al., 1998; Rao et al., 2010; Wood et al., 2006). However, despite the dominance of chaparral communities in California (Keeley and Davis, 2007), their capacity for N assimilation remains uncertain, as comprehensive N budgets have not been developed. Here, an N budget is assembled for a headwater chamise-dominated catchment located in the foothills of the Sierra Nevada to 1) understand how N deposition has altered the capacity of chaparral ecosystems to assimilate N; 2) evaluate how indicators of N saturation developed in mesic sites apply to xeric landscapes; and 3) develop an understanding of how chaparral ecosystems may respond to increased anthropogenic pressures.

In contrast to ecosystems at low elevations, where chronic N fertilization negatively impacts chaparral communities (Fenn et al., 2003a), alteration of P biogeochemistry in alpine and subalpine environments appears to be driving ecosystem response to indirect anthropogenic effects (Sickman et al., 2003b). Increases in P supply to alpine lakes have resulted in mild eutrophication events and have shifted nutrient dynamics from primarily P-limited systems to increasing limitation and co-limitation by N (Sickman et al., 2003b). Although increases in atmospheric P deposition from agricultural activities in the San Joaquin Valley can explain some of the observed changes in P supply to high-elevation watersheds (Vicars and Sickman, 2011; Vicars et al., 2010), increases in P supply from the alteration of soil and lake sediment P cycles have not been investigated. Since climate change is predicted to shift precipitation patterns resulting in more rain and less snow with concomitant increases in temperature

(Kim, 2005; Knowles et al., 2006), and organic matter accumulation (Dahlgren et al., 1997; Luckman and Kavanagh, 2000), the magnitude of these changes may result in hot moments of intense biogeochemical cycling and increased nutrient loading from watershed soils and lake sediments to surface waters.

This study examines how Sierra Nevada ecosystems, of contrasting elevation and temperature, are coupled by the mechanisms to which they respond to anthropogenic pressures. Although N is examined in chaparral and P in alpine and subalpine catchments, these ecosystems remain linked by both the effect of seasonal transitions on N and P biogeochemistry and by hydrology as a vehicle for nutrient transport. To this end, chapter 2 quantifies the annual rate of NO and N_2O emissions from chaparral ecosystems, an important pathway for the export of N, as the first step in developing a comprehensive N budget for the watershed. Chapter 3 synthesizes atmospheric N inputs, hydrologic and gaseous N fluxes, and belowground N dynamics to develop a comprehensive N budget and understand the N saturation status of chaparral watersheds and the impacts of chronic N pollution. Chapter 4 focuses on alpine soils by quantifying important P pools and understand how the cycling of P may be destabilized in response to changes in soil physicochemical conditions and hydrology. Lastly, chapter 5 evaluates the rate of P supply from alpine lake sediments to lake water and develops an understanding of how anthropogenic activities may be affecting P cycling in high-elevation catchments.

2. SOIL NO AND N_2O FLUXES IN MEDITERRANEAN ECOSYSTEMS OF THE SIERRA NEVADA (CALIFORNIA): SEASONAL TRANSITIONS INFLUENCE GASEOUS N EMISSIONS

Abstract

Soil gas emissions may be an important pathway for nitrogen loss, particularly in ecosystems where abrupt seasonal transitions produce strong temporal gradients in soil moisture. I measured rates of NO and N_2O fluxes in a chaparral watershed to gain better understanding of temporal patterns of emissions and processes regulating gaseous N production in soils. Gaseous N loss for chaparral was 1.4 ± 1.2 kg N ha^{-1} yr^{-1}, of which on an annual average, soils acted as a net sink for N_2O (-0.08 kg N ha^{-1} yr^{-1}). Nitrification appeared to regulate gaseous N fluxes in chaparral during the dry summers typical of the Sierra Nevada chaparral zone. However, during the dry-to-wet seasonal transition, pulses of NO following soil wetting were indicative of abiotic processes such as chemodenitrification; fluxes of NO peaked within 20 seconds following wetting (maximum rates: 97 to 513 ng NO-N m^{-2} s^{-1}) and were generally insensitive to C_2H_2 fumigation. To determine if seasonal patterns of gas flux observed in chaparral soils were a general characteristic of Mediterranean ecosystems of the Sierra Nevada, I also measured NO fluxes during the dry-to-wet seasonal transition along an elevational gradient in the western Sierra Nevada. Along the gradient, ambient rates of NO fluxes decreased with elevation, but when soils were wetted in the autumn, the pattern reversed

(maximum rates: 18 ng NO-N m^{-2} s^{-1} at chamise, 31 ng NO-N m^{-2} s^{-1} at the mixed conifer, and 323 ng NO-N m^{-2} s^{-1} at the subalpine site), suggesting that dry soils in the subalpine zone have a large capacity for NO gas emissions following summer. These data suggest that gaseous N emissions are important components in N budgets of Mediterranean-type ecosystems. Future climate change projections and elevated N deposition may work synergistically to increase NO emissions from soils in Mediterranean ecosystems.

Introduction

Emissions of nitrogen-containing gases from soils are often not included when estimating ecosystem N budgets, presumably because hydrologic N outputs account for the majority of N inputs, or simply because few studies have actually measured these fluxes (Meixner and Yang, 2006). Gas flux data are especially sparse in the western U.S. and no measurements exist for a full one-year period in chaparral ecosystems despite the urgent need for measurements to validate emission models and to assess the nitrogen-saturation status of these ecosystems (Wu et al., 2010). Because arid and semiarid ecosystems comprise about 1/3 of the global land surface (Gurevitch et al., 2002), and climate change may act to extend this coverage (Borken and Matzner, 2009; Meehl et al., et al., 2007), it is essential to understand the contribution of dryland ecosystems to the global N budget and include N flux measurements in ecosystem budget calculations.

From the limited number of measurements, it is clear that dryland ecosystems can emit significant amounts of gaseous N from soils (Fenn et al., 1996; Hall et al., 2008; McCalley and Sparks, 2009). Biological nitrification and denitrification are known to regulate both nitric oxide (NO) and nitrous oxide (N_2O) production (Firestone and Davidson, 1989), though nitrification is generally associated with NO production, and denitrification with N_2O (Skiba et al., 1993). Nitric oxide is a byproduct of nitrification (Anderson and Levine, 1986), and is produced during the reduction of nitrite (NO_2^-) (Hall et al., 1996). Nitrous oxide is predominantly generated in the absence of O_2 as an intermediate product of denitrification (Payne, 1981), however, at low levels of O_2, ammonia oxidizers can use NO_2^- as an electron acceptor resulting in N_2O production via

nitrification (Robertson and Groffman, 2007; Yoshida and Alexander, 1970). Despite the strong role of biological processes on fluxes of gaseous N from soils, abiotic processes can also contribute to NO and N_2O emissions; however, biological production of NO_2^- is required for abiotic processes to occur (Venterea et al., 2005). Through chemodenitrification, NO_2^- can react with H^+ to produce HNO_2 followed by aqueous disproportionation to NO (Allison, 1963; Davidson et al., 1993; Venterea et al., 2005). Although chemodenitrification is favored in acidic soils (pH<5), during nitrification, both NO_2^- and H^+ may accumulate in soil microsites favoring the formation of NO, even in soils with higher than optimal pH (Davidson et al., 1993; Gelfand et al., 2009).

In arid and semiarid environments, variations in soil moisture and transitions from dry to wet soil conditions strongly influence the magnitude and timing of soil gaseous N fluxes (McCalley and Sparks, 2008, 2009). During the period immediately following wetting of dry soils it is common to detect a "hot moment" of increased gaseous N production, particularly NO (Davidson et al., 1993; Hall et al., 2008), which can account for a significant fraction of annual ecosystem N losses in desert regions (Hall et al., 2008; McCalley and Sparks, 2009). Increases in gaseous N production following soil wetting have been attributed to the rapid response of nitrifying bacteria to water availability (Davidson, 1992). Nitrifying bacteria can be well adapted to periods of stress (drought) and can quickly recover following a wetting pulse (Gelfand and Yakir, 2008; Schimel et al., 2007). Other mechanisms to explain the hot moment include: (i) the rapid catabolism of N-rich extracellular enzymes released by soil microbes following a wetting event (Fierer and Schimel, 2002), which may be metabolized to NO, (ii) chemo-denitrification

(Davidson et al., 1993; Venterea et al., 2005), or (iii) other less-understood mechanisms involving temperature-induced oxidation of N in desert soils (McCalley and Sparks, 2009).

Because arid and semiarid ecosystems contribute about 25% of the global NO production and twice the amount of NO produced by cultivated lands (Davidson and Kingerlee, 1997), it is important that studies draw comparisons between NO and N_2O fluxes, and expand beyond focusing on N_2O (Del Grosso et al., 2006). Further, because of the significance of NO emissions in arid and semiarid environments, more data are needed to understand how increases in atmospheric deposition of N and climate change may alter biotic and abiotic regulation of soil NO production. For semiarid regions, climate change is projected to intensify droughts and the frequency of extreme rainfall events (Meehl et al., *et al*., 2007), which can shift the mechanisms for catchment N export from a predominant hydrologic control to increased importance of gaseous emissions. Moreover, because atmospheric N deposition is projected to continue to increase (Galloway et al., 2004), and high soil N availability can enhance gaseous N production (Erickson et al., 2002), N losses from ecosystems can intensify during seasonal transitions or during extreme rainfall events following prolonged drought (McCalley and Sparks, 2009). Of particular concern, however, is the feedback between increased N_2O concentrations and climate change, since N_2O has a global warming potential 300 times that of CO_2, and in the stratosphere, it can catalyze the destruction of O_3 (IPCC, 2007). Increases in NO can promote reactions with hydroxyl radical and volatile organic compounds in the troposphere producing HNO_3 and other organic

nitrates causing downwind air quality problems, as well as promoting tropospheric O_3 pollution (Crutzen, 1979).

In southern California, dryland ecosystems currently receive the highest rates of atmospheric N deposition in the U.S. (from an average of 30 kg N ha^{-1} yr^{-1} in the Los Angeles basin to over 70 kg N ha^{-1} yr^{-1} in polluted sites of the San Bernardino Mountains (Fenn et al., 2003b)). In this region, chronic N fertilization has altered wildfire cycles negatively affecting chaparral and coastal sage scrub ecosystems with large-scale conversion to invasive grasses (Allen et al., 1998; Rao et al., 2010). The foothills of the western Sierra Nevada still contain large tracts of chaparral that are exposed to N deposition rates > 10 kg N ha^{-1} yr^{-1} (Fenn et al., 2003c), yet the N saturation status of these ecosystems has been poorly studied. Complete watershed N budgets for Sierra Nevada chaparral ecosystems are needed to evaluate the N-saturation status of these ecosystems and promulgate critical loads for N-deposition (Fenn et al., 2011). Recent attempts to construct chaparral N budgets suggest that inputs of N exceed ecosystem N demands, but these budgets could not be closed owing to unidentified pathways for N loss including gaseous N emissions from soils (Vourlitis et al., 2009). Thus, studies are needed to address: (i) what is the annual gaseous N export from Mediterranean-type ecosystems?; (ii) what processes regulate soil gaseous N emissions and how do they vary temporally?; and (iii) how do processes regulating gaseous N production vary among Mediterranean ecosystems of the Sierra Nevada?

To gain better understanding of rates of gaseous N production in dryland ecosystems, I measured ambient NO and N_2O fluxes from a chaparral-dominated

watershed in the Sierra Nevada over a 13-month period. Although N_2 emissions were not measured, they are presumed low, as the low water content and coarse textured soils typical of arid and semiarid regions do not favor denitrification (Anderson and Levine, 1987). I conducted additional experiments to improve understanding of the biotic and abiotic processes regulating NO emission from soils and to determine if other Sierra Nevada ecosystems (mixed-conifer forest and subalpine community) exhibit similar pulses of NO flux during transitions from dry to wet soils. To my knowledge, these are the first published field measurements of NO fluxes from the Sierra Nevada and some of the first available field NO measurements for montane regions worldwide. I hypothesize that in chaparral, gaseous N losses will be greatest during the dry to wet seasonal transition and that little to no gaseous N fluxes will be detected during the long and hot dry season that is typical of Mediterranean climates. I further hypothesize that gaseous N fluxes during transitions from dry to wet soils will decline moving upward in elevation owing to greater ecosystem N demand, lower rates of N deposition (Fenn et al., 2010), and overall wetter soils.

Materials and methods

Site descriptions

Our study was conducted in a chaparral watershed (denoted CH in figures) located along the western slope of the Sierra Nevada, within the Kaweah River drainage of Sequoia and Kings Canyon National Parks (338170 m E ,4042382 m N). The watershed is 4.3 ha and the elevation ranges from 680-700 meters a.s.l. The site is

characterized by a Mediterranean climate with hot dry summers and cool wet winters (Fig. 2.1). Annual rainfall at the nearby Ash Mountain meteorological station, (3 km west of the study site), averages 670 mm with an average maximum air temperature of 36.4 °C and an average minimum of 2.2 °C. Prior measurements indicate that the watershed receives approximately 8 to 10 kg N ha^{-1} yr^{-1} from atmospheric deposition.

Soils in the chaparral site are classified as Ultic Haploxeralfs and are sandy clay loams derived from gabbro-dioritic parent material with a well-developed argillic horizon (Huntington and Akeson, 1987). Soil pH is about 6 (Miller et al., 2005) with a C:N ratio ranging between 13 in the upper 20 cm to as low as 6.5 within a 50-100 cm depth (Chapter 3). Vegetation at the site is dominated by thick stands of chamise (*Adenostoma fasciculatum*) with annual grasses (*Bromus* species) covering the interspaces between shrubs and the understory. California mountain mahogany (*Cercocarpus betuloides*), California scrub oak (*Quercus berberidifolia*), buckbrush (*Ceanothus cuneatus*), and mountain balm (*Eriodictyon californicum*) are also present in small patches. The watershed has not burned since 1960 and therefore represents a fully mature chaparral ecosystem (Li et al., 2006).

Soil NO emissions were measured at two additional sites along an elevational gradient east of the chaparral watershed, but still within the Kaweah River drainage. The mid-elevation, mixed conifer site (denoted MC), was located near Wolverton trailhead (344862 m E, 4051058 m N; 2,260 m a.s.l.), and the high-elevation subalpine site (denoted SA) was located in the Emerald Lake watershed (350054 m E, 4051454 m N; 2,800 m a.s.l.).

Vegetation at the mixed-conifer site was composed predominantly of white fir (*Abies concolor*), red fir (*Abies magnifica*), Ponderosa pine (*Pinus ponderosa*), Jeffrey pine (*Pinus jeffreyi*), Lodgepole pine (*Pinus contorta*), and understory scrubs. The soils at the mixed conifer have not been formally classified, but have a gravely sandy loam texture with O_i horizons approximately 5-15 cm thick under forest canopy. Similar soils at locations nearby the studied site have been classified as Typic Xerumbrepts (Huntington and Akeson, 1987). At the mixed conifer site, NO fluxes were measured in soils with both north- and south-facing aspect. The north-facing sites were characterized by dense mixed conifer stands, while the south-facing sites had thinner forest cover with larger gaps between trees.

The Emerald Lake watershed is a remote subalpine basin, accessed by foot (6 miles from trailhead), and located in the Tokopah Valley which forms the headwaters to the Marble Fork of the Kaweah River. The 120 ha watershed has 21% soil cover (Entisols and Inceptisols) with the remaining area made up of rock outcrops (Huntington and Akeson, 1987). Soils are derived from granitic and granodioritic parent material, are well to somewhat excessively drained, acidic (pH < 5), poorly buffered, and have an average C:N ratio of 17 (Chapter 4). Vegetation is sparse and characterized by *Pinus contorta*, *Pinus monticola*, and low woody shrubs (*Salix orestera)* and grasses (*Calamagrostis canadensis*). The mean average temperature is 4.6°C (Leydecker A., *unpublished data*) with annual precipitation averaging 1,510 mm, of which about 90% falls as snow (Sickman et al., 2001). At Emerald Lake, NO fluxes were measured along both north- and south-facing aspects. The north-facing sites were wetter and vegetation consisted of

willow and grasses, with gravely sandy loam textured soils described as Lithic Cryumbrepts (Huntington and Akeson, 1987). The south-facing sites were steeper and dryer, with little vegetation, and with sandy clay loam textured soils described as Entic Cryumbrepts (Huntington and Akeson, 1987).

Experimental setup

Six months prior to measuring gaseous N emissions at the chaparral site, two polyvinylchloride collars (PVC) (30.48 cm diameter × 10 cm height) were inserted, in pairs, 6 cm into the ground at four locations for a total of eight collars. Collars were installed under a dense chamise stand (henceforth denoted "Chamise"), near an ephemeral stream with dense chamise cover ("Stream"), at an open meadow dominated by *Bromus* grasses ("Meadow"), and under California scrub oak ("Oak"). Soil NO and N_2O fluxes were measured from September 2009 through October 2010. During 2009, NO fluxes were measured on: October 11-12, October 16-17, November 8, November 25, and December 19. In 2010, I measured NO fluxes on: January 24-25, March 16-17, May 7-8, July 2-3, August 30-31, and September 15. Soil N_2O fluxes were measured in 2009 on November 8, November 25, and December 19, and in 2010 on January 24, March 16, May 7, July 2, August 30, and September 15.

Soil NO fluxes at the chaparral site were measured in duplicate at all four locations by placing a PVC chamber (volume = 11 L) over the previously installed PVC collars and measuring the concentration of NO inside the chamber headspace for approximately seven minutes. A tight seal was achieved between the chamber and collars with a rubber gasket. Nitric oxide concentrations were measured with a Scintrex

LMA-3 chemiluminescent NO_2 analyzer following methods described by Davidson et al., (1991), in which chamber air flowed into the NO_2 analyzer and ambient air flowed into the chamber through a vent. Because the LMA-3 analyzer measures the concentration of NO_2 in air, a CrO_3 in-line oxidizer was used to convert NO into NO_2 prior to the introduction of sample air into the LMA (this oxidizer cartridge was purchased from Drummond Technology Inc., Bowmanville, Canada). The areal flux of NO was calculated based on the physical dimensions of the chamber, the rate of change in NO concentration inside the chamber, and air temperature:

$$J_{NO} = \frac{dC_{NO}}{dt} \times \frac{VN}{ART} \qquad \text{Equation 2.1}$$

Where J_{NO} is the NO flux rate (ng NO-N m^{-2} s^{-1}); dC_{NO}/dt (ppbv NO s^{-1}) is the rate of NO increase inside the chamber calculated by linear regression; V is the chamber volume (L); N is the atomic weight of nitrogen (14.007 g $mole^{-1}$); A is the area of the chamber (730 cm^2); R is the gas constant (0.0821 L atm $mole^{-1}$ deg^{-1}); and T is the chamber air temperature (°K). The LMA-3 was calibrated in the field prior to and after each series of measurements. For calibration purposes, a standard curve was made by mixing an NO standard (0.0988 ppmv NO in N_2 gas; Scott Marrin, Riverside CA) with zero air gas (Scott Marrin, Riverside CA). The method detection limit for NO measurements was 0.02 ppbv NO. Error estimates for NO flux measurements were calculated by combing the error of the instrument (± 2.6 %) and the error resulting from the linear regression used to calculate fluxes (value varied for each measurement; 0.14 ± 0.27 % (mean ± std. dev.)).

At the chaparral site, N_2O emissions were anticipated to be low and relatively insignificant when compared to NO (Fenn et al., 1996); however, during periods in which chaparral soils are wet, significant N_2O fluxes can occur (Anderson et al., 1988). In an effort to capture the potential for N_2O emissions in chaparral, N_2O was measured only in chamise and stream collars, where presumably higher soil moisture content during the wet season, would favor the formation of N_2O (Anderson et al., 1988; Anderson and Poth, 1989). During these measurements, chamber air was withdrawn and injected into 12-mL pre-evacuated borosilicate glass vials (Exetainer). At least four samples were collected over a 30-minute period. Exetainers were filled with chamber air using a double-ended needle equipped with a shutoff valve. One end of the needle was connected to the chamber through a rubber septum, while the other end was inserted into the pre-evacuated Exetainer. Once the Exetainer was properly attached to the chamber, the shutoff valve was opened to allow chamber air to flow into the Exetainer. Nitrous oxide concentrations were determined by gas chromatography with electron capture detection and fluxes estimated by linear regression of N_2O concentrations against time and Equation 2.1. The method detection limit for N_2O measurements was 13 ppbv.

During NO and N_2O flux measurements, air and soil temperature and soil volumetric water content (θ) were recorded, as they are known to control gaseous N production in soil (Gelfand et al., 2009). During each gas flux measurement, air temperature was recorded with a digital thermometer and soil temperature was obtained by inserting a temperature probe (10 cm long) into the soil, adjacent to the collars. Soil

moisture, θ, was recorded hourly at the Meadow site using a datalogger and two Decagon EC-5 dielectric moisture-sensors installed 5 and 30 cm below the soil surface.

Wetting experiments in chaparral soils

To gain better understanding of the effects of abrupt changes in soil moisture on N gas fluxes, a series of soil wetting experiments were performed at each pair of soil collars in the chaparral study site during each sampling time. Note: Only one of the paired collars was artificially wetted during each experiment (denoted as the "Wetted" collar in figures and tables) and during subsequent wetting experiments only this same collar was wetted. Thus, over the course of the experiments one of the paired collars experienced periodic artificial and natural wetting (Wetted collar) and the other experienced only natural wetting (Unwetted collar). Gas flux measurements from artificially wetted collars were not used in the calculation of annual ambient gaseous N emissions.

During a wetting experiment, NO fluxes were measured at different time points depending on whether the collar was wetted or unwetted. Nitric oxide fluxes were measured in the unwetted collars immediately before the start of the wetting experiments; these measurements are referred to as "ambient" flux rates in figures. For the wetted collars, NO fluxes were measured at three time points: (i) prior to artificial wetting (measurements are denoted "Pre-wetting"), (ii) immediately after soils were artificially wetted (measurements are denoted "Wetting"), and (iii) on the day following wetting (approximately 16 hours post-wetting and denoted "Post-wetting"). Because these are field measurements from remote locations accessed by foot, the 16 hours are

representative of the period of time between the wetting experiment and the time at which the site was accessed the next day for a follow-up measurement. In these experiments, I used the ambient NO measurements to represent soil NO fluxes at field conditions. Soils within the ambient collars were never artificially wetted and therefore could be used, along with the Pre-wetting measurements from the water-amended collars, as reference points to compare NO fluxes from the wetted collars (i.e., NO fluxes measured at the Wetting and Post-wetting time points).

During a wetting experiment deionized water (1 L) was added slowly (ca. 45-60 sec) and evenly to the soil within the "Wetted" collar simulating a 1.4 cm rainfall event. Although the rate of water addition is clearly above the typical rate of precipitation for the catchment (Fig. 2.1), the objective of the wetting experiment was to document a potential flux of N following wetting. In all experiments, water was quickly absorbed by the soil and NO flux measurements were begun within 10-20 seconds after soil wetting. Nitrous oxide fluxes were made at only two time points: Ambient (unwetted collar) and wetting (immediately after water additions to the wetted collar), due to logistical constraints associated with the remoteness of the sites.

NO fluxes along the elevational gradient

Soil NO fluxes were measured along an elevational gradient during the summer-fall seasonal transition (September 2010) in order to capture the "hot moment" that typically occurs after the wetting of dry soil. Nitric oxide fluxes were measured on September 15 at the chaparral site, September 16 at the mixed conifer site, and September 18 at the subalpine site (Emerald Lake).

Nitric oxide measurements in chaparral were made on previously installed collars at Chamise, Stream, Meadow, and Oak sites. However, permanent PVC collars were not previously inserted into the soil at the mixed-conifer site and Emerald Lake. Because soil disturbance is known to influence N mineralization and nitrification rates (Vitousek and Melillo, 1979), NO fluxes at the mixed-conifer and subalpine sites were measured after carefully placing a temporary collar over the soil surface on which the chamber was set. Placement of the temporary collar was done with care to ensure maximum contact between the soil and collar, but avoided significant disturbance to soils below 1 cm depth. Because a perfect seal between the collar and soil surface was unlikely, NO flux measurements at the mixed conifer and subalpine site may slightly underestimate NO emissions; irregular flows of ambient air could have seeped into the chamber diluting NO. To evaluate the error introduced by use of a temporary collar, I compared replicate measurements of NO flux from the permanent collars at the chaparral meadow site with NO fluxes made with temporary collars in nearby meadow soils. The variations in NO flux among these replicate measurements were less than 30 % for both ambient and wetting measurements (data not shown). This degree of NO flux variability is less than the between-site variability typically observed at the chaparral study site (Fig. 2.2), suggesting that the use of temporary collars at the mixed conifer and subalpine sites did not produce substantial bias in the NO flux measurements.

On September 15, 2010, NO fluxes were measured at all four locations and in all collars in the chaparral watershed. In the mixed-conifer site, I measured NO fluxes at two locations under a dense mixed conifer stand with a north-facing aspect and at three

locations with a south-facing aspect with gaps in forest cover. At the subalpine site, I measured soil NO fluxes at two points with north-facing aspect and two points with south-facing aspect. Soil NO fluxes were measured using previously described methods including field calibration procedures for the LMA-3. Following soil NO flux measurements under dry soil conditions, all measurement locations (including the unwetted chaparral collars) were amended with water and measured as previously described. Nitrous oxide fluxes were not measured along the elevational gradient.

Acetylene field fumigation experiments in chaparral soils

On October 21, 2010, prior to a wetting treatment, I randomly selected four of the eight soil collars at the chaparral site and incubated them with C_2H_2 (10 Pa) for 16 hours to inhibit nitrification (Berg et al., 1982) and understand its contribution in the production of NO during dry conditions and during the initial response to wetting. The remaining four collars were not fumigated and served as references. Acetylene incubations were performed by sealing the collars with thick polypropylene plastic through which C_2H_2 was injected. After 16 hours, the plastic seal was removed and soil NO fluxes were immediately measured under dry soil conditions. Acetylene-amended collars were then wetted with 1 L deionized water saturated with 100 Pa C_2H_2 (to insure complete inhibition of nitrification), and then sampled for NO emissions within 30 seconds following water addition. Though C_2H_2 is known to degrade NO (Bollmann and Conrad, 1997), the concentrations used were sufficiently low to avoid interference with NO measurements (Davidson et al., 1993). Nitric oxide fluxes were measured in the unfumigated collars prior to and after wetting on October 21. One-tailed t-tests were

used to assess differences in NO flux rates between C_2H_2-treated and non-fumigated collars and I report average values ± 1 standard error.

Annual gaseous N flux in chaparral ecosystems

The annual gaseous N flux rate in the chaparral study site was calculated using two approaches. In the first approach, I used the average ambient NO and N_2O flux measurements made during each sampling trip (i.e., the average NO flux rate measured in the Chamise, Stream, Meadow, and Oak ambient collars) and interpolated these fluxes over a one-year period. As a measure of uncertainty, I propagated the error associated with averaging N fluxes at all four chaparral sites. Because this approach used fluxes from ambient collars only (ignoring hot moments), it likely underestimates the true gaseous N flux from chaparral.

Our second approach used linear and nonlinear regression models to incorporate the pulse of N after soil wetting, and predict gaseous N fluxes as a function of air and soil temperature and θ at 5 and 30 cm depth (these models are presented in the Results).

Results

Ambient NO fluxes in chaparral

Nitric oxide fluxes exhibited strong seasonal and spatial variation in the ambient collars at the chaparral site (Figs. 2.2 and 2.3). The highest NO fluxes measured for dry soils occurred during late summer/early autumn corresponding to the start of the dry to wet seasonal transition of 2009. Both sites dominated by chamise vegetation (collars at Chamise and Stream) had the highest NO fluxes measured on October 11, 2009 (16 ng

NO-N m^{-2} s^{-1} at Chamise; 9.4 ng NO-N m^{-2} s^{-1} at Stream), followed by the Meadow (8.7 ng NO-N m^{-2} s^{-1}) and Oak collars (2.6 ng NO-N m^{-2} s^{-1}) (Fig. 2.2). Rain fell at the chaparral study site on October 13 and 14. Flux measurements made at the ambient collars on October 16, 2009, were the highest recorded among all sites (Fig. 2.3), and presumably reflect enhanced NO fluxes typical of natural wetting of dry soil by the first precipitation event of the wet season.

During the wet season (ca. November 2009-May 2010) when soils were regularly wetted by rain events (Fig. 2.1), ambient NO fluxes remained below 1 ng NO-N m^{-2} s^{-1} and sometimes became negative (Fig. 2.2); negative fluxes may indicate NO consumption by nitrifying or denitrifying bacteria (Davidson and Schimel, 1995). On average, the Chamise and Oak collars had the highest wet season NO fluxes (0.36 ng NO-N m^{-2} s^{-1}), followed by the Stream (0.27 ng NO-N m^{-2} s^{-1}) and Meadow collars (-0.09 ng NO-N m^{-2} s^{-1}).

Ambient NO fluxes in the dry season of 2010 were not as high as the fluxes measured in October 2009, although they tended to increase as the dry season progressed and peaked in September 2010 (Fig. 2.3). On September 15, 2010, NO flux rates in the Chamise collars were 5.8 ng NO-N m^{-2} s^{-1}, followed by the Meadow collars, 2.8 ng NO-N m^{-2} s^{-1}; Stream collars, 2.4 ng NO-N m^{-2} s^{-1}; and Oak collars, 0.9 ng NO-N m^{-2} s^{-1}.

Chaparral wetting experiments

The artificial wetting of collars on October 10, 2009 enhanced the flux of NO across all sites (Fig. 2.2). Within 20 seconds following wetting, the chamber was closed and an immediate pulse of NO was observed over the 0-7 minute measurement period

(average of 294 ng NO-N m^{-2} s^{-1} for all wetted collars (Fig. 2.2)). Average NO flux from wetted collars decreased to 173 ng NO-N m^{-2} s^{-1} on October 11, approximately 16 hours after wetting. Five days after wetting, NO fluxes returned back to ambient levels. After the October 2009 experiments and continuing through the winter and spring of water year 2010, artificial wetting of soils did not generally enhance NO fluxes when compared to ambient measurements (Fig. 2.2 inset).

During the summer of water year 2010, NO fluxes in wetted collars were orders of magnitude larger than fluxes measured in ambient collars, but not as high as those fluxes measured in October 2009 (Fig. 2.2). The magnitude of the wetting NO pulse decreased over time during the summer of 2010 with each additional wetting event (Fig. 2.3; July 2 2010-Oct 22, 2010), presumably because the substrate N pool for NO production was not replenished following consecutive wetting during the dry season.

N_2O fluxes in chaparral

Soil N_2O fluxes in chaparral were low when compared to NO fluxes. I only detected positive N_2O fluxes on November 8, 2009 and August 30, 2010 in ambient collars. On other dates N_2O flux rates were either negative, suggesting consumption in soil, or not statistically different from zero (Table 2.1).

Artificial soil wetting did not strongly increase N_2O concentrations. However, I did measure higher fluxes following wetting on three occasions (Table 2.1). The largest response to wetting was on November 8, 2009 in which N_2O fluxes were increased by about three times the measured background flux (Table 2.1).

NO fluxes along an elevation gradient

During September 2010, ambient soil NO fluxes in dry soils were highest in chaparral (mean flux = 2.7 ng NO-N m^{-2} s^{-1}) when compared to the mixed conifer (0.3 ng NO-N m^{-2} s^{-1}) and subalpine sites (0.9 ng NO-N m^{-2} s^{-1}; Fig. 2.4). On average, artificial wetting stimulated a fivefold increase in NO emissions in chaparral soils (mean flux= 12.7 ng NO-N m^{-2} s^{-1}). Wetting of dry soils at the mixed conifer sites produced NO fluxes of 1.4 ng NO-N m^{-2} s^{-1} at north-facing sites with much higher fluxes, 21.9 ng NO-N m^{-2} s^{-1}, measured at dryer sites with south aspect (Fig. 2.4). At the subalpine site, ambient NO fluxes at north-facing sites averaged 0.16 ng NO-N m^{-2} s^{-1} and increased to an average of 0.40 ng NO-N m^{-2} s^{-1} after wetting (Fig. 2.4). In south-facing sites, ambient fluxes averaged 0.84 ng NO-N m^{-2} s^{-1}, and when soils were wetted, NO fluxes increased to an average of 213.7 ng NO-N m^{-2} s^{-1} (Fig. 2.4).

NO flux response to C_2H_2 fumigation

Acetylene was used to inhibit nitrification and gain insights into the relative importance of biotic and abiotic mechanisms controlling gaseous N emissions from chaparral soils. In non-fumigated collars, the NO flux in unwetted soil was 1.7 ± 0.75 ng NO-N m^{-2} s^{-1} and after artificial wetting the flux rate increased to 2.4 ± 1.1 ng NO-N m^{-2} s^{-1}, but this change was not statistically significant (p = 0.271; Fig. 2.5). In C_2H_2-fumigated collars, the NO flux in unwetted soil was 0.26 ± 0.03 ng NO-N m^{-2} s^{-1} and increased to 1.49 ± 0.7 ng NO-N m^{-2} s^{-1} following water addition (p = 0.091; Fig. 2.5). In dry soils, the C_2H_2 treatment reduced the ambient average NO flux by 85% (Fig. 2.5; p = 0.078), while in artificially wetted soil, there was no significant difference between C_2H_2-

treated and non-fumigated collars (Fig. 2.5; $p = 0.317$). Overall, artificial wetting of dry soil increased or did not change soil NO emissions regardless of whether C_2H_2 was added or not added to soil. However, in dry soil, C_2H_2 appeared to significantly reduce soil NO emissions (at the 90% confidence level), suggesting that biologically mediated processes governed soil NO emissions.

Effects of temperature and soil moisture on gaseous N fluxes.

We performed linear and nonlinear regressions among soil NO fluxes and air and soil temperature and soil θ using measurements from the chaparral watershed (Figs. 2.6-2.7). I did not attempt to model N_2O fluxes due to the limited number of non-zero measurements (Table 2.1). The relationships between NO flux and air and soil temperature were best described by a linear model (Fig. 2.6). Fluxes of NO were positively correlated with increases in temperature, however, the relationships were weak, and although significant ($P \leq 0.0062$; Fig. 2.6), I made no attempt to model gaseous N fluxes as a function of temperature.

The relationship between θ and NO soil emissions was "U" shaped; NO fluxes were highest at both high and low θ (Fig. 2.7). In developing a model for NO flux based on θ, I chose to separate periods when dry soils undergo rapid wetting from other periods when soils are consistently wet or consistently dry. The wetting and fumigation experiments suggest that some of the processes producing NO during rapid transitions from dry to wet soils may be different from those controlling NO fluxes under steady soil moisture, thus it is suggested that two models are necessary.

During periods of consistent soil moisture, emissions of NO were best described by an exponential decay function using θ at a 5 cm depth (henceforth denoted the "constant θ model"; $R^2 = 0.60$; $p < 0.0001$; Fig. 2.7). The exponential decay function ignored NO fluxes measured two days after the first precipitation event of the wet season (October 16, 2009), as these measurements likely represent enhanced NO fluxes from wetting of dry soil (gray box; Fig. 2.7). Although the relationship between θ at a 30 cm depth and NO flux was significant, it was weaker, and was not used to model NO emissions ($R^2 = 0.2052$; $p < 0.0001$). For periods of rapid soil wetting (increasing soil moisture), I developed a model that related the average maximum NO flux in artificially wetted soils to the average soil water content following rainfall events at the onset of the wet season. That is, the model related how NO fluxes decreased after the initial NO pulse in response to wetting to the average decrease in soil moisture following a rainfall event (Fig. 2.8). The model was developed by fitting an exponential function (henceforth denoted the "dry-to-wet θ model"; $R^2 = 0.90$; $p = 0.03$) to data points obtained by plotting estimates of θ at a 5 cm depth to a corresponding NO flux made on artificially wetted collars between October 11 and November 8, 2009 (Fig. 2.8). The estimates for θ at a 5 cm depth were obtained by averaging θ content of days 0, 1, 5, and 28 of rainfall events recorded on October 14 and December 11, 2009 (Fig. 2.1). Corresponding estimates of NO flux were obtained from the average of all artificially wetted collars on October 11 (day 0), the average of all post-wetting collars on October 12 (day 1), and the average of all pre-wetting collars on October 16 (day 5) and November 8 (day 28) (Fig. 2.2). Next, the constant θ model and dry-to-wet θ model models were run using in situ

measurements of θ at the chaparral site to compute a daily record of NO flux for water year 2010.

Annual gaseous N flux for chaparral ecosystems

We estimated annual gaseous N loss from the chaparral watershed by: (i) interpolating ambient field measurements (Fig. 2.3), (ii) using the constant θ model developed (Fig. 2.7) and continuous measurements of θ at 5 cm depth (Fig. 2.1) and (iii) combining the constant θ and dry-to-wet θ models to include Hot Moments of NO production (Figs. 2.7-2.8).

Based on interpolation of the NO and N_2O fluxes measured in ambient collars in chaparral (i.e., the area under the line shown in Fig. 2.3), I estimate an annual gaseous N flux of 0.23 kg ha^{-1} yr^{-1} (Table 2.2). Using only the constant θ model and continuously recorded measurement of θ, I estimated annual NO flux of 0.27 kg ha^{-1} yr^{-1}. Both of these estimates likely underestimate annual gaseous N fluxes since they disregard the magnitude of the NO pulse following soil wetting. To incorporate the pulse of NO observed following the wetting of dry soil, I combined the constant θ model with the dry-to-wet θ model (combined model), and estimated an annual flux from chaparral of 1.4 ± 1.2 kg N ha^{-1}. For the calculations, I applied the constant θ model ($NO = 0.33 + 39.8\ e^{(-1.2053\times\theta)}$) to periods when soil moisture was consistently dry or wet and used the dry-to-wet θ model ($NO = 0.0013\ e^{(0.4794\times\theta)}$) for two periods based on rapid changes observed in soil moisture shown in Figure 2.1: October 14 and December 11, 2009. Application of the dry-to-wet θ model was confined to a 6-day period beginning on the day of the rain event (5 days post-wetting) since the field data suggest that NO fluxes return back to

ambient levels within 5 days following wetting of dry soil (Fig. 2.2). Although N_2O fluxes were measured, they were not included in the model calculations, as the few data available impeded the development of a regression model (Table 2.1).

Discussion

Processes regulating gaseous N emissions from chaparral ecosystems

Soil gaseous N emissions are regulated by the production and consumption of gases and depend on the diffusivity of gas through soil (Conrad, 1994; Davidson and Schimel, 1995). The biological processes that control the production and consumption of gaseous N emissions are relatively well studied and understood (Davidson et al., 2000). However, our understanding of abiotic processes such as those that operate in soils subjected to high temperature, exposure to intense solar radiation (McCalley and Sparks, 2009), and rapid changes in soil moisture is incomplete. For example, paradoxically, this study suggests that in ambient collars, NO fluxes increase as soil θ decreases, and that nitrification appears to control this flux (i.e., C_2H_2 fumigation inhibited NO emissions only in dry soils; Fig. 2.5) during a period inauspicious to microbial activity. In contrast, when dry soils are wetted, NO fluxes increase rapidly (within 20 seconds) even in the presence of C_2H_2 (Fig. 2.5), suggesting that microbial nitrification may not be the only mechanism controlling NO emissions. However, it is well known that microbial activity is favored in moist soils, since diffusion of soluble substrates facilitates microbial access to resources (Voroney, 2007) and increases in NO production following soil wetting are largely attributed to microbial nitrification (Davidson, 1992; Firestone and Davidson,

1989; Gelfand et al., 2009). Thus, this study raises two important questions: (i) if nitrification controls N emissions from chaparral soils, why do ambient NO fluxes increase during a period that should limit microbial activity (drying soil)? and (ii) why is the NO flux response to artificial soil wetting so rapid and unresponsive to C_2H_2 treatment? I attempt to answer these questions by integrating a conceptual model developed for soil microbial responses to drought in semiarid ecosystems (Parker and Schimel, 2011), with the gaseous N flux measurements.

In moist soils, hydrologically connected microsites and diffusion of resources facilitates microbial growth (Schimel et al., 2007). As soils dry and θ decreases, limited diffusion of soluble substrates typically results in decreased microbial activity (Schimel and Bennett, 2004; Voroney, 2007). Decreases in θ can also cause sites within soil to segregate, and as a consequence, form hydrologically disconnected sites in which resources are plentiful and microbes may be isolated from predators or viruses promoting increases in microbial biomass (Parker and Schimel, 2011). Thus, in chaparral ecosystems, as soils dry, nitrification may be favored in hydrologically disconnected sites, explaining the increase in NO emissions measured towards the end of the dry season. Such observations are consistent with increases in N availability and microbial biomass in dryland soils (Parker and Schimel, 2011), and with the C_2H_2 fumigation experiment, which suggests that microbial nitrification is associated with NO emissions in dry soil.

An important consequence of forming hydrologically disconnected sites in dry soil is the accumulation of NO_2^- and H^+ in microsites derived from nitrification (Davidson

et al., 1993; Gelfand and Yakir, 2008). At the onset of the wet season, soil wetting reestablishes hydrological connectivity, which may favor the reaction between accumulated NO_2^- and H^+ to produce HNO_2 followed by aqueous disproportionation to NO (Hall et al., 1996; Venterea et al., 2005). Production of NO through this abiotic mechanism can explain the very fast rates of NO flux I detected following wetting and are consistent with the lack of a significant inhibitory effect from C_2H_2 fumigation in artificially wetted soils (Fig. 2.5). Thus, during the dry-to-wet seasonal transition in chaparral, chemodenitrification is likely to co-occur with microbial nitrification during soil wetting episodes. It is acknowledged that these suppositions rely on the results of C_2H_2 fumigation experiments that are of low replication and statistical power, and it must be considered that these experiments were performed in the field, where diffusion could have minimized the well-known inhibitory effect of C_2H_2 on microbial nitrification, yet patterns consistent with the interpretations presented emerged. I contend that the patterns observed along with the rapid fluxes of NO following wetting are intriguing and worthy of further research, as they suggest abiotic control in soils undergoing marked changes from dry to wet conditions.

The chemodinitrification hypothesis during soil wetting is also consistent with NO fluxes measured at the chaparral site during winter and spring. The relatively low or negative rates of NO flux observed can be explained by several conditions: (i) when $\theta >$ 0.2, NO diffusion through the soil is reduced (Conrad, 1996) and consumptive processes may be intensified due to the presence of hydrologically connected sites (Chapuis-Lardy et al., 2007), (ii) lower soil temperature reduces microbial nitrification (Ludwig et al.,

2001), and (iii) when grasses and forbs start to grow, increased competition for soluble substrates between microbes and plants may limit nitrification (Parker and Schimel, 2011). Furthermore, as diffusion of substrates is prevalent in moist soils, NO_2^- does not typically accumulate and chemodenitrification rates should be low during the winter and spring in chaparral soils.

NO and N_2O emissions from chaparral soils

Out of the three approaches used to estimate the annual gaseous N flux from chaparral, I contend that the combined model (constant θ + dry-to-wet θ models) best approximates gaseous N emissions in chaparral ecosystems, since it incorporates enhanced NO flux caused by rapid wetting of dry soils (Table 2.2). However, given the large uncertainty associated with the measurements and models (Fig. 2.2, Table 2.2), gaseous N emissions could be significantly higher or lower than 1.4 kg N ha^{-1} yr^{-1}. Because both the annual estimate based on interpolation of N fluxes from ambient collars and the constant θ model likely underestimate N fluxes (they do not properly account for the "hot moment"), they may be used to confine the lower boundary of expected N emissions from chaparral. To estimate an upper boundary to annual gaseous N flux I applied the same approach (Fig. 2.3) to N fluxes from artificially wetted collars which yields a flux rate of 4.1 ± 4.2 kg N ha^{-1} yr^{-1}. Although this approach is likely to grossly overestimate N emissions, it serves to confine an upper boundary to the expected gaseous N flux from chaparral and adds validity to the estimate of 1.4 kg N ha^{-1} yr^{-1} from the combined model (Table 2.2).

From this study it is evident that NO dominates N losses in chaparral and that N_2O plays a minor role. Although I did not measure volatilization of ammonia, I suspect it is not important at the site as this process is favored in alkaline soils (pH>9) (McCalley and Sparks, 2008), and the pH of soil at the site is 6.2. The range of instantaneous fluxes of NO detected in ambient collars in chaparral (<0.06 to 16 ng NO-N m^{-2} s^{-1}) generally span the flux rates measured in other arid and semiarid ecosystems. In a chaparral site in the San Gabriel Mountains (southern California), fluxes of NO in July averaged 2.1 ng NO-N m^{-2} s^{-1} (Anderson and Poth, 1989), while in a pine forest in the San Bernardino Mountains NO fluxes ranged from 1 to 7.5 ng NO-N m^{-2} s^{-1} (Fenn et al., 1996). In other arid and semiarid sites, NO fluxes ranged from 0.14 to 2.5 ng NO-N m^{-2} s^{-1} in the Mojave Desert (McCalley and Sparks, 2008), 1.4 to 4.4 ng NO-N m^{-2} s^{-1} in the Phoenix Arizona urban core (Hall et al., 2008), 1.8 to 3.8 ng NO-N m^{-2} s^{-1} in a dry tropical forest (Davidson et al., 1993), 0.2 to 2.8 ng NO-N m^{-2} s^{-1} in semiarid grassland and shrubland (Smart et al., 1999), 0.3to 21.9 ng NO-N m^{-2} s^{-1} in South African savannas (Parsons et al., 1996), and 0 to 2.9 ng NO-N m^{-2} s^{-1} in a Mediterranean shrubland in Israel (Gelfand et al., 2009).

During artificial wetting of dry soil, the maximum instantaneous rate of NO emission in this study reached 550 ng NO-N m^{-2} s^{-1} in chaparral, and is among the highest NO fluxes recorded. In other ecosystems, soil wetting produced 140 ng NO-N m^{-2} s^{-1} in a seasonally dry tropical forest in Mexico (Davidson et al., 1993; Davidson et al., 1991), 150-250 ng NO-N m^{-2} s^{-1} in a tropical savanna , and 160 ng NO-N m^{-2} s^{-1} in an urban desert in Phoenix, AZ (Hall et al., 2008).

Our work highlights the sensitivity of NO flux to soil moisture, and the availability of substrates for nitrification, and suggests that changes in climate (intensification of drought and rainstorms; Meehl et al., 2007) and increased rates of atmospheric N deposition (Galloway et al., 2004) may interact synergistically to affect ecosystem N losses via gaseous pathways. Along the Sierra Nevada foothills, rates of atmospheric N deposition vary from <3 to about 15 kg N ha^{-1} yr^{-1} with critical loads estimated at 10 to 14 Kg N ha^{-1} yr^{-1} (Fenn et al., 2010), while climate models forecast increases in the length of the dry season with potential increases in the number of dry-wetting episodes during the wet season (Meehl et al., et al., 2007). Because rapid drying-wetting cycles (two week intervals) have been shown to increase both soil N mineralization and nitrification at the study site (Miller et al., 2005), and increased N availability is known to stimulate gaseous N production (Hall and Matson, 2003; Venterea et al., 2003), current rates of atmospheric N deposition coupled with changes in precipitation patterns may enhance NO emissions from soils. Enhanced soil NO emissions can pollute downwind ecosystems underscoring the importance of including gaseous N fluxes in N critical load estimates; a measurement typically ignored despite being an indicator of N-saturation status (Aber et al., 1989).

Nitrous oxide has been shown to be a minor component of N emissions in arid ecosystems (Billings et al., 2002; Fenn et al., 1996). At the studied site, fluxes of N_2O were low, presumably due to the development of favorable saturated soil conditions coinciding with the plant growing season, in which roots would be better competitors for N than microbes (Robertson and Groffman, 2007), and to coarse-textured soils that favor

O_2 diffusion. However, denitrification enzyme activity has been shown to increase as soils dry in California grasslands (Parker and Schimel, 2011), and aerobic denitrification can occur in well-aerated soils (Robertson and Kuenen, 1984). It may also be possible that because the clay content in the chaparral soil increases with depth, finer soil texture limits O_2 diffusion while favoring denitrification (Goldberg et al., 2008).

Although the negative annual N_2O flux calculated for chaparral is based on a limited number of measurements, it suggests that chaparral soils may temporarily be a sink for N_2O. Many studies have reported N_2O uptake in soil (Blackmer and Bremner, 1976; Minami, 1997), and it has been increasingly recognized that soils can be a net N_2O sink (Chapuis-Lardy et al., 2007). At the site, I speculate that denitrification and nitrifier denitrification, in which NO_2^- is used as the electron acceptor in the absence of O_2, could have resulted in net N_2O consumption in soil (Schmidt et al., 2004). Moreover, because during denitrification, NO_3^- is preferred as an electron acceptor over N_2O (Chapuis-Lardy et al., 2007), and chaparral ecosystems are thought to be N-limited (Padgett and Allen, 1999), net consumption of N_2O could have occurred.

Fluxes of NO along altitudinal gradient

The observed patterns in NO emissions from the altitudinal measurements suggest that: (i) wetting of dry soil produces large pulses of NO in all dominant ecosystems of the Sierra Nevada; (ii) the greatest stimulation of NO following wetting is observed in drier soils (i.e., those with south-facing aspect) of the mixed conifer and subalpine sites; and (iii) chemodenitrification appears to be a common process in soils that undergo prolonged drought and abrupt transitions from dry to wet conditions.

Although ambient fluxes of NO along the altitudinal gradient were generally higher in chaparral and lowest at the subalpine and mixed conifer site, the pattern was reversed following artificial wetting. Laboratory incubations of soils from a montane ecosystem in China demonstrated that NO emissions were lowest in soils from higher elevations (Yu et al., 2010). Lower temperatures and lower rates of atmospheric N deposition in high-elevation sites, can explain the patterns observed, as it is well known that both low temperature and reduced soil N availability limit NO production (Meixner and Yang, 2006). During rewetting, however, I measured NO pulses at high elevation sites larger than in chaparral (Fig. 2.4). Presumably, the availability of NO_2^- at higher elevations was greater than in chaparral or the rates of reaction between NO_2^- and H^+ to generate HNO_2 increased along the elevational gradient; soil pH decreases with elevation at the studied sites (Huntington and Akeson, 1987), which facilitates chemodenitrification (Allison, 1963; Su et al., 2011). Although I only took a small number of measurements and did not perform C_2H_2 fumigation experiments at all sites along the elevational gradient, high rates of NO fluxes occurred within 20 seconds of water addition, suggesting that a common process controls gaseous N fluxes from soils within Mediterranean-type ecosystems.

The relatively high rates of NO flux measured in subalpine catchments during the end of the dry season, emphasize the importance of incorporating gaseous N fluxes in the N-budget of high-elevation ecosystems. In high-elevation catchments, the majority of gaseous N flux studies focus on emissions during winter months, since snow insulates soils from freezing allowing for microbial processes to occur (Miller et al., 2009).

However, NO fluxes during summer have been largely overlooked, presumably due to the very low NO emissions observed during winter months when compared to N_2O (Filippa et al., 2009). Because climate models for the Sierra Nevada forecast shifts in precipitation patterns with reductions in snow and increases in rainfall (Knowles et al., 2006), soil drying-wetting episodes, along with reductions in snow cover, may reduce the importance of N_2O during winter while increasing the contribution of NO during snow-free periods.

Summary and conclusions

This study shows that gaseous N emissions are an important route for N losses from chaparral ecosystems of California and that NO is the dominant form of gaseous N export. Microbial nitrification is the main mechanism responsible for gaseous N emissions during dry soil conditions in the summer and early autumn. However, abiotic processes, including chemodenitrification may explain large NO pulses measured in artificially and naturally wetted soils at the onset of the rainy season in chaparral, mixed conifer forests, and subalpine ecosystems of the Sierra Nevada. I hypothesize that climate change and elevated N deposition may work synergistically to increase NO emissions from soils in semiarid environments and those experiencing a Mediterranean climate. This research highlights the importance of incorporating gaseous N fluxes in semiarid ecosystem N budgets, and the sensitivity of these fluxes to soil moisture and availability of substrates for nitrification.

Tables and figures

Table 2.1. Average fluxes of N_2O (ng N m^{-2} s^{-1}) measured at the Stream and Chamise collars in the chaparral study site. n=2 for all values in which a standard deviation is reported in parenthesis. N/A indicates measurements are not available.

	Measurement date								
Treatment	11/8/09	11/25/09	12/19/09	1/24/10	3/16/10	5/7/10	7/2/10	8/30/10	10/22/10
Ambient	2.47 (3.50)	0	-3.18 (4.50)	0	-0.92 (0.02)	0	0	0.19 (3.53)	0
Artificial wetting	10.41 (1.57)	0	2.14 (3.02)	N/A	0.70 (0.99)	0	0	N/A	0

Table 2.2. Annual gaseous N flux estimates for chaparral (± Std. error). Modeled NO emissions from θ_{5cm} are based on NO flux measurements in ambient collars.

Method	NO	N_2O	Total
		(kg N ha^{-1} yr^{-1})	
Field measurements			
Ambient collars	0.35 ± 0.48	-0.08 ± 0.14	0.27 ± 0.51
Model Estimates			
Constant θ	0.23 ± 0.75	-----	0.23 ± 0.75
Combined (Constant θ + dry-to-wet θ)	1.41 ± 1.20	-----	1.41 ± 1.20

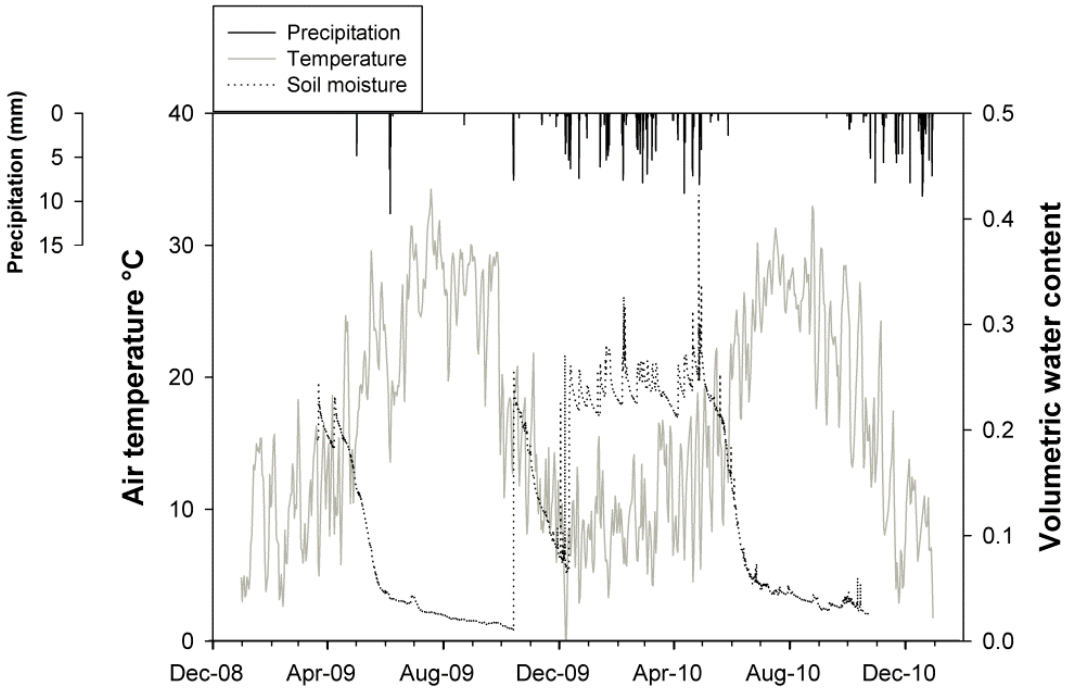

Fig. 2.1. Soil volumetric water content measured at the chaparral site at a 5 cm depth along with air temperature and precipitation measurements from the nearby Ash Mountain meteorological station.

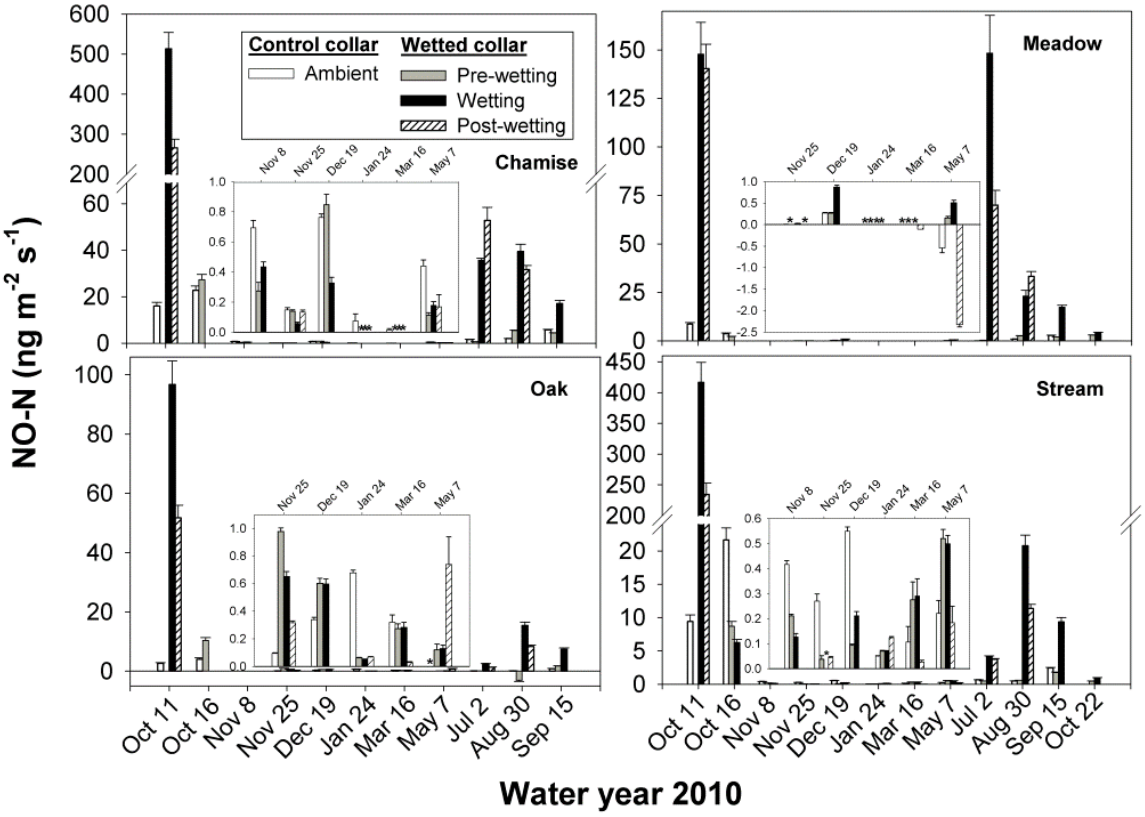

Fig. 2.2. Fluxes of NO measured from the Chamise, Stream, Oak, and Meadow collars at the chaparral study site. Measurements were made in unwetted collars (Ambient) and at three time points in artificially wetted collars: prior to artificial wetting (Pre-wetting), immediately following wetting (Wetting), and approximately 16 hours post-wetting (Post-wetting). Error bars represent the uncertainty associated with each measurement based on the error of the instrument and the error from the calibration slope. * denotes fluxes below detection limit (0.05 ng NO-N m^{-2} s^{-1}).

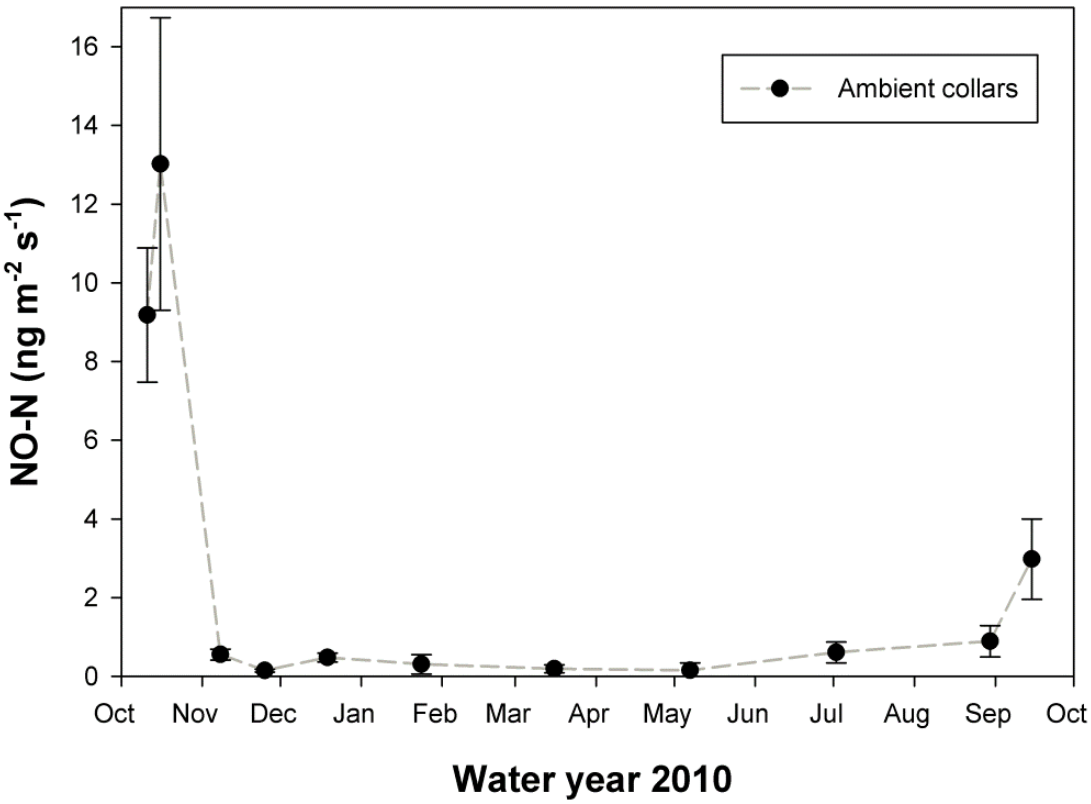

Fig. 2.3. Arithmetic mean flux of NO measured from ambient collars at the chaparral study site. Error bars represent 1 standard error (n=4).

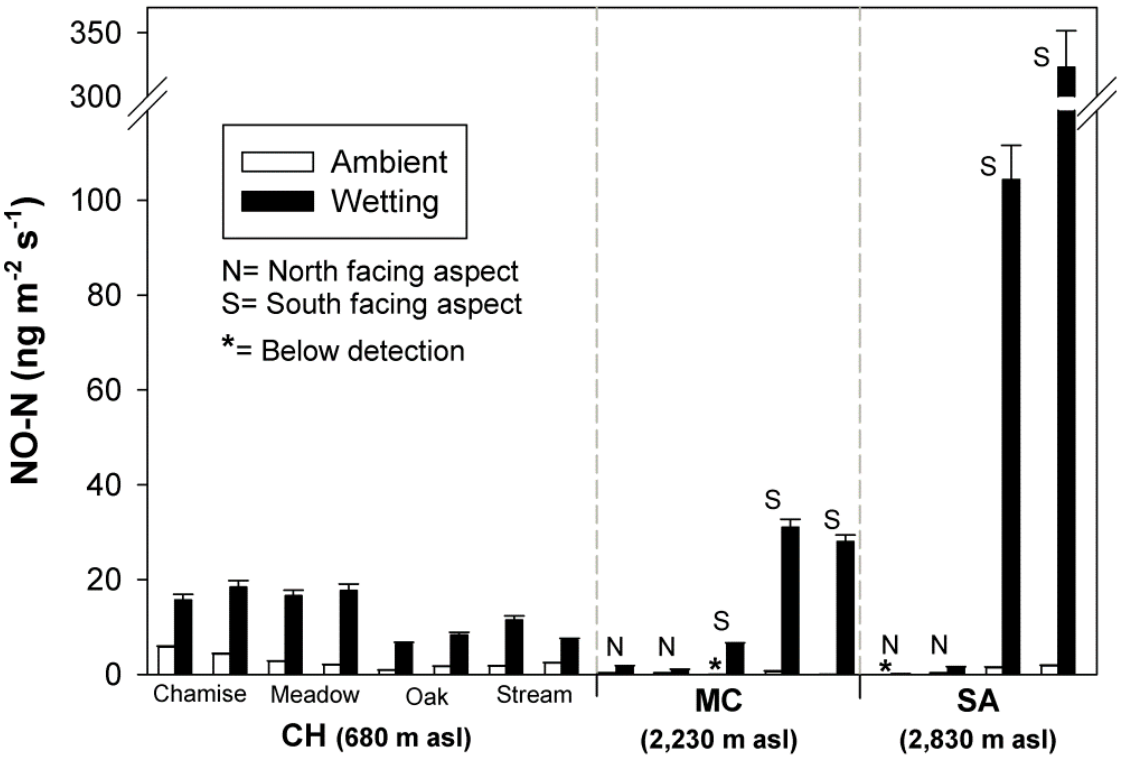

Fig. 2.4. Fluxes of NO measured along an altitudinal gradient in the Sierra Nevada, CA during September 2010. Measurements were made under dry soil conditions and immediately following artificial wetting. Error bars represent the uncertainty associated with each measurement based on the error of the instrument and the error from the calibration slope.

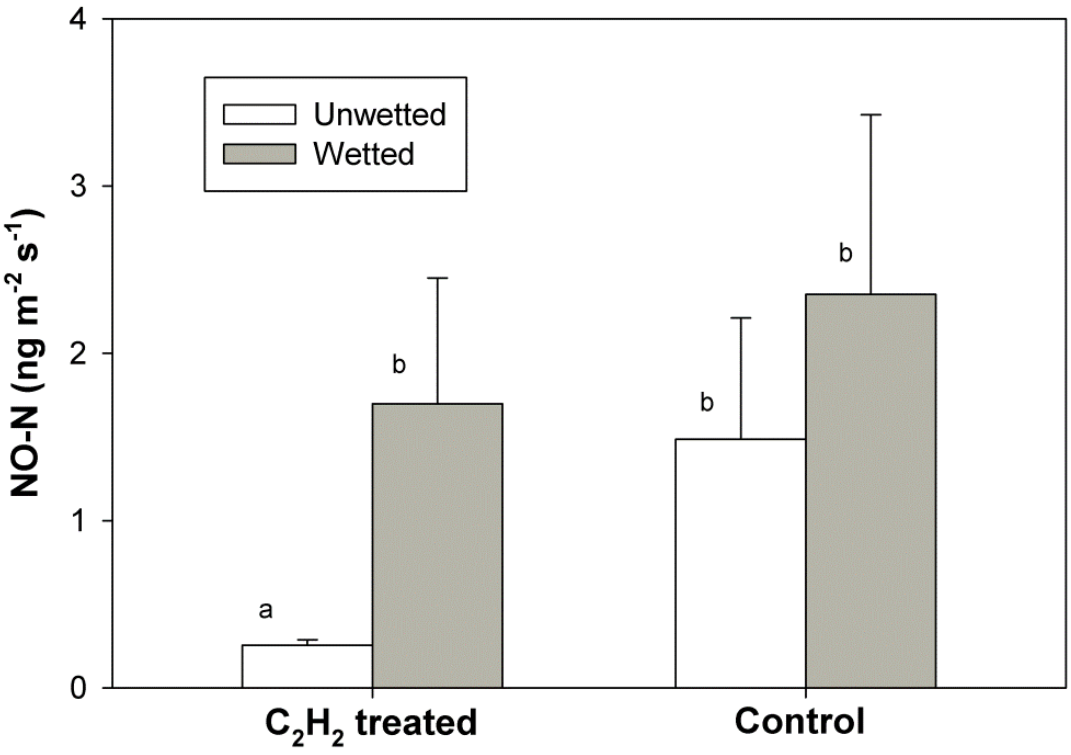

Fig. 2.5. Average flux of NO measured in chaparral under C_2H_2-treated and unfumigated controls during late summer 2010. Both C_2H_2-treated and control collars were measured under ambient conditions and immediately following artificial wetting of dry soil. Error bars represent 1 standard error (n=4). Letters represent statistical significant differences between measured fluxes (α=0.10).

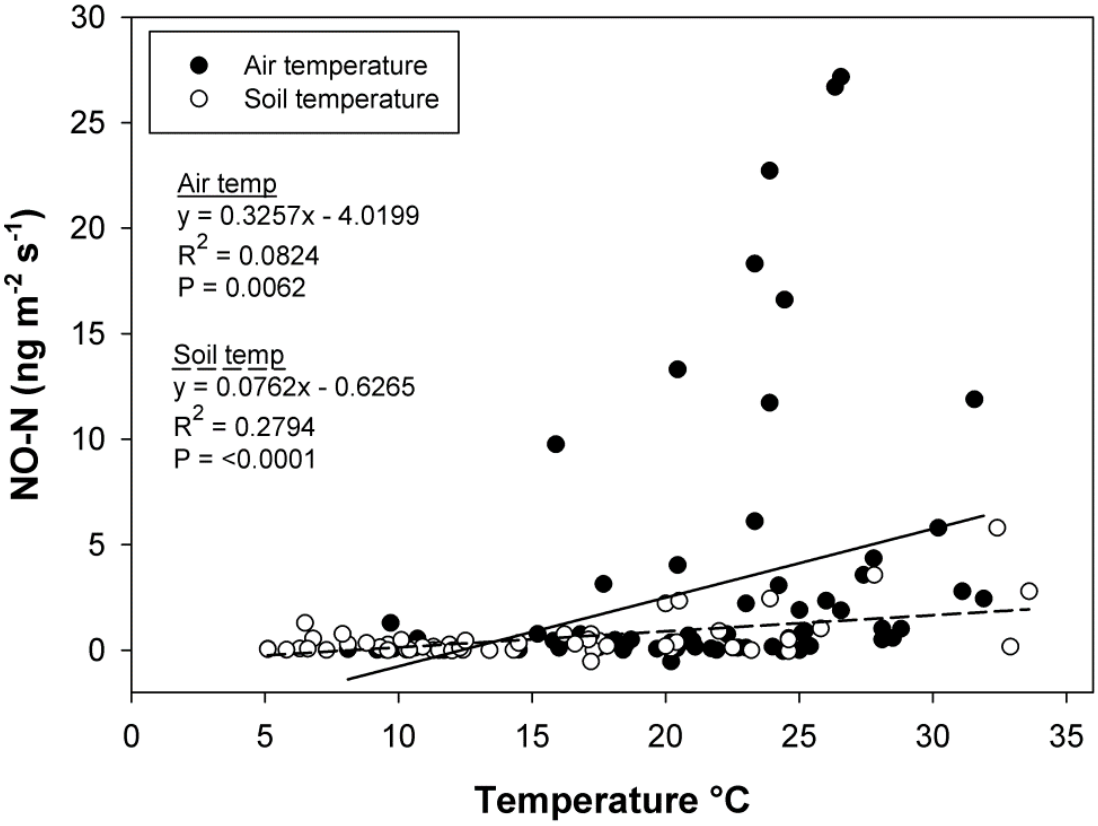

Fig. 2.6. Relationship between chaparral NO fluxes and air and soil temperature.

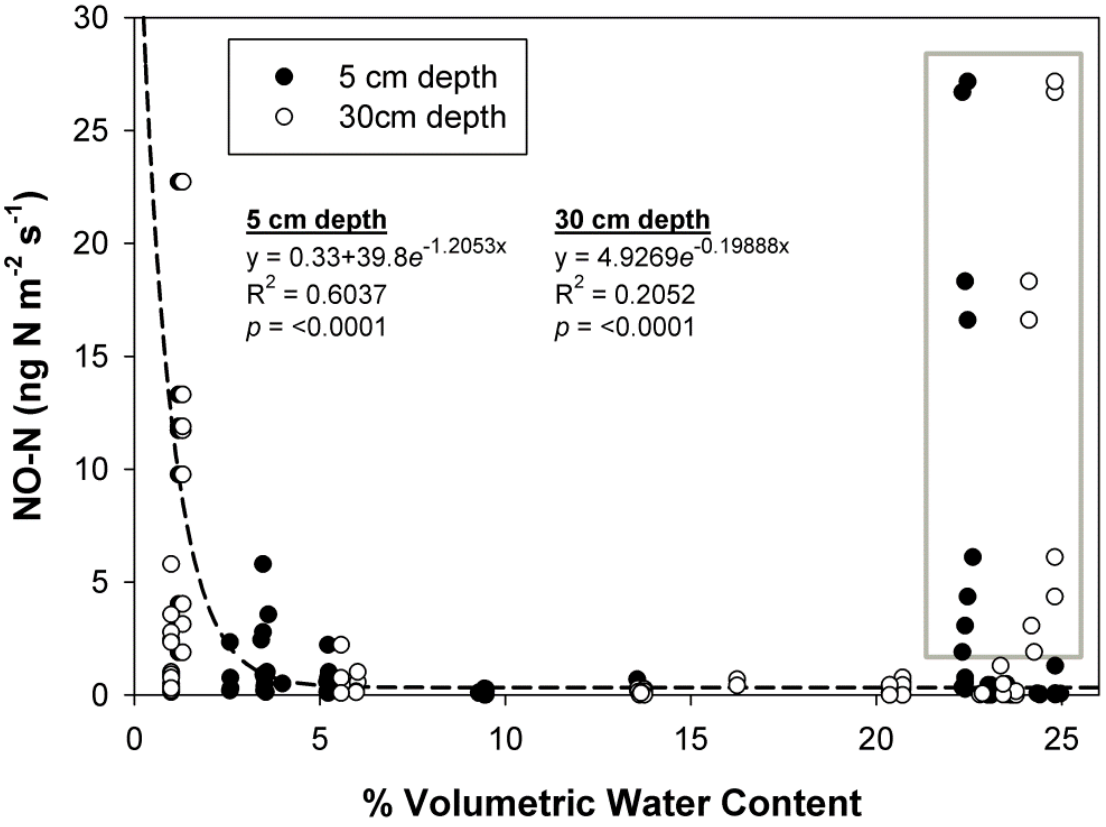

Fig. 2.7. Relationship between chaparral NO fluxes and soil moisture at both a 5 and 30 cm depth, from which the constant θ model is derived. Values inside the gray box represent fluxes of NO measured within two days following the first precipitation event of the wet season and are not included in regression models.

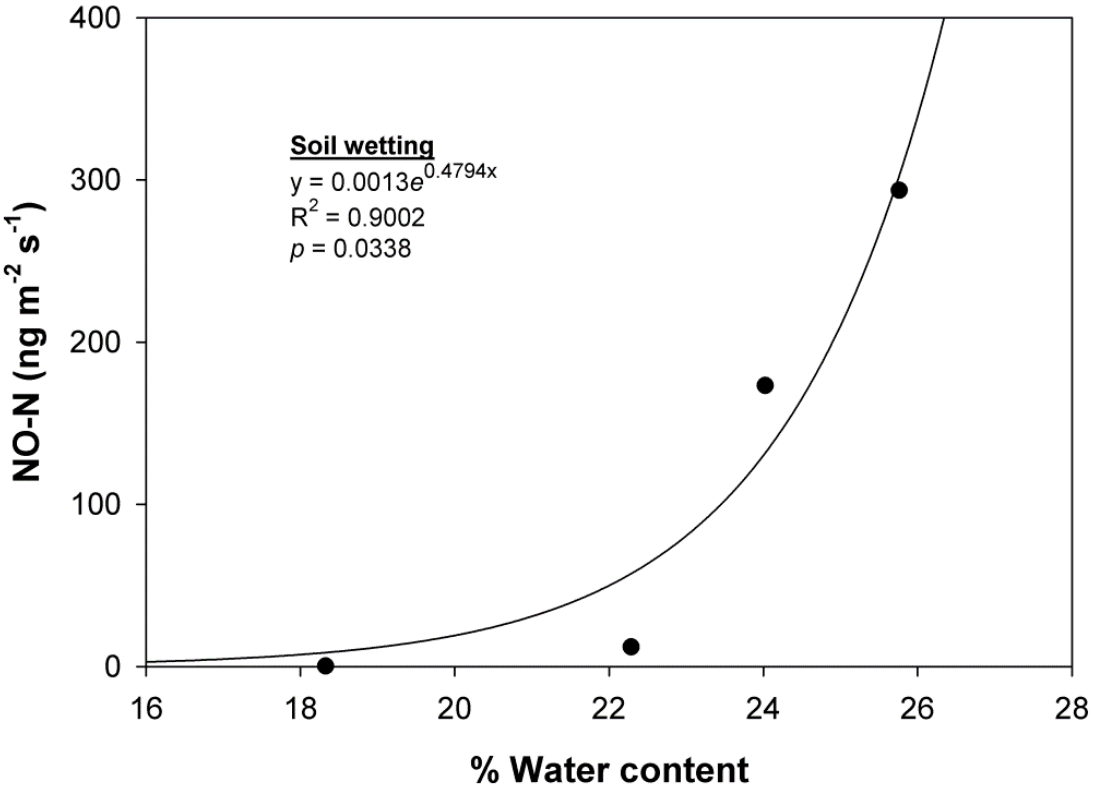

Fig. 2.8. Development of dry-to-wet θ model by plotting the relationship between chaparral NO fluxes measured in artificially wetted collars and average $\theta_{5\text{-cm}}$ from rainfall events measured on October 14 and December 11, 2009.

3. THE N BUDGET FOR A CHAMISE-DOMINATED CHAPARRAL WATERSHED: LIMITATIONS TO THE USE OF N BUDGETS AND N SATURATION INDICATORS

Abstract

Chaparral ecosystems in California can receive some of the highest rates of N deposition in the US (<3 to over 70 kg N ha^{-1} yr^{-1}), yet studies on N pollution in semiarid environments remain limited, bringing into question the application of hypotheses developed in mesic sites to describe xeric environments. To understand the effects of chronic N fertilization on chaparral ecosystems, this study develops a comprehensive N budget for a 4.3 ha chamise-dominated watershed located on the foothills of the Sierra Nevada; an area experiencing rapid increases in N deposition (ca., 9 kg N ha^{-1} yr^{-1}) from the San Joaquin Valley. Atmospheric N inputs and hydrologic N outputs were measured for a two-year period, as well as belowground N dynamics, N concentrations in the soil solution, and overland surface water runoff. N fixation and aboveground N dynamics were obtained from published values. Gaseous N emissions ($NO+N_2O$) were obtained from in-situ measurements at the studied site (Chapter 2). Lastly, isotopic separation of $\delta^{15}N$ and $\delta^{18}O$ was used to trace sources of NO_3^- in streamwater. At the onset of the wet season, during plant senescence, streamwater NO_3^--N concentrations reached 520 µmol L^{-1}, despite ca. 80 % of atmospheric N inputs as NH_4^+, but concomitant with the period of highest gaseous N emissions (ca. 300 ng N m^{-2} s^{-1}). Streamwater $\delta^{15}N$ and $\delta^{18}O$ and belowground N dynamics strongly suggest that nitrification controls the export of N

rather than direct leaching of atmospherically derived NO_3^-. During late winter and spring, hydrologic N fluxes decreased to values no longer indicative of excessive N inputs (< 2 μmol L^{-1} NO_3^--N), in agreement with significant decreases in gaseous N emissions presumably due to increased plant N demand. An N mass balance indicates that ca. 0.5 ± 1.3 kg N ha^{-1} yr^{-1} are retained in the catchment, suggesting that the watershed may be nearing its capacity for N assimilation. However, due to the intrinsic seasonality of semiarid catchments and propensity for N leaching, N saturation indicators and N budgets may have limited application. That is, the intense N losses observed during the dry to wet seasonal transition and early spring may balance N budgets along a wide gradient of N deposition, as well as suggest N saturation in ecosystems where the vegetation remains N limited. It is concluded that chaparral ecosystems exposed to 9 kg N ha^{-1} yr^{-1} of atmospheric deposition exhibit signs of kinetic N saturation, calling for the evaluation of N critical loads in order to minimize N leaching to surface waters and downwind pollution of sensitive ecosystems.

Introduction

Anthropogenic activities have dramatically altered the terrestrial N cycle by intensifying the amount of reactive N supplied to ecosystems, with N additions projected to increase as human populations and agriculture continue to expand (Galloway et al., 2004; Vitousek et al., 1997). The eastern US region is heavily impacted by atmospheric N pollution (NADP, 2010), but in western states, rates of atmospheric N deposition are the highest in the country, in which some of the most N polluted sites receive in excess of 90 kg N ha^{-1} yr^{-1} primarily as dry deposition (Fenn et al., 2003b). Due to the arid climate typical of most western states, N can accumulate on surfaces (e.g., foliage, litter, and soil) during the dry season, and quickly become bioavailable as large pulses during rainfall events (Meixner and Fenn, 2004; Michalski et al., 2004; Padgett et al., 1999). However, because N pollution in the western US is not yet a regional problem, that is, N pollution is concentrated near major metropolitan and agricultural areas (Fenn et al., 2003b), it is not surprising that the majority of studies on ecosystem response to chronic N fertilization have been conducted in the east coast (mesic sites). Nevertheless, much has been learned from N pollution studies in mesic watersheds, including the development of N saturation theory (Aber et al., 1998; Aber et al., 1989), although it remains somewhat unclear how these concepts apply to other ecosystems, in particular, to semiarid chaparral ecosystems with pronounced seasonal transitions from dry to wet soil conditions.

Elevated rates of atmospheric N deposition can negatively affect ecosystems in multiple ways, resulting in a general interest to develop management strategies for the

abatement of N pollution in affected landscapes, as well as limits to the amount of N reaching sensitive ecosystems (Fenn et al., 2010; Pardo et al., 2011). Some of the most commonly documented effects of chronic N fertilization on ecosystems include changes in soil physical and biological properties as well as both direct and indirect effects on vegetation including soil acidification, depletion of soil base cations, plant nutrient imbalances, and toxic effects on plants (Bobbink et al., 2010; Pardo et al., 2011). However, the effects of N pollution vary by ecosystem, with some effects being more important than others depending on the characteristics of soil, climate, and vegetation of the affected landscapes (Pardo et al., 2011).

Chaparral ecosystems in California cover approximately 2.5 million ha, of which a large portion is found on the foothills of the Sierra Nevada mountain range (Keeley and Davis, 2007); an area experiencing rapid increases in atmospheric N deposition due to intense urban and agricultural activities in the San Joaquin valley (Cisneros et al., 2010). In the Sierra Nevada foothills, chaparral communities are dominated by chamise (*Adenostoma fasciculatum*), an evergreen shrub that can be found in over 70% of chaparral stands (Hanes, 1971). A chamise stand reaches maturity in approximately 25 years (Hanes, 1971) and can rapidly regrow following fire by sprouting and seeding (Stohlgren et al., 1984). Chronic N fertilization can threaten chaparral ecosystems through soil acidification (Wood et al., 1992), elevated NO_3^- leaching and NO emissions, and decreased species richness, productivity, and diversity in arbuscular mycorrhizal and epiphytic lichen communities (Bobbink et al., 2010; Fenn et al., 2011). Although chaparral stands are considered resistant to invasion by exotic species (Keeley et al.,

2003), when exposed to frequent fire, exotic grasses have maintained dominance and have slowed the recovery of chaparral (Dickens, 2011; Zedler et al., 1983). Moreover, chronic N fertilization has promoted the invasion of exotic grasslands in coastal sage scrub and desert plant communities in southern California, through changes in the accumulation of fine fuel biomass and alterations in the intensity and frequency of fires (Allen et al., 1998; Rao et al., 2010). Thus, it is not inconceivable that a combination of frequent and intense fire cycles, as altered by synergistic effects between elevated N deposition and increases in fine fuel biomass, can adversely affect chaparral communities.

The concept of N saturation, as developed in mesic sites (Aber et al., 1998; Aber et al., 1989), has been important in framing our understanding of how N pollution can affect ecosystems (Fenn et al., 1996; Pardo et al., 2011; Stoddard, 1994). Nitrogen saturation is defined as the availability of N in excess of soil and plant demand, in which N accumulates uniformly through a progression initiating with the enrichment of plants, followed by litter, and ultimately soil (Aber et al., 1998). The progression of N accumulation in an ecosystem is described through a series of changes (Aber et al., 1998; Stoddard, 1994), in which stage 0 is representative of N-limited systems where NO_3^- losses are low or unmeasurable during the growing season, but may increase during periods in which plants and microbes are senesced (the non-growing season). In stage 1, increasing N inputs alleviate some aspects of N limitation, but N continues to be cycled efficiently, such that the major difference between stage 0 and 1 is a minor increase in N exported during the non-growing season (Stoddard, 1994). At stage 2, an ecosystem is

considered N saturated and the effects of N fertilization are observed through indicators of N saturation, such as elevated hydrologic and gaseous N losses during both growing and non-growing seasons, high rates of nitrification, and foliar N enrichment. Finally, at stage 3, ecosystem N sinks have exceeded their capacity to sequester N, resulting in large N losses through both growing and non-growing seasons ultimately resulting in ecosystem decline.

Although the concept of N saturation has been helpful in understanding how chronic N additions have affected ecosystems in some of the most N polluted catchments in the western US (Fenn et al., 1996), the application of hypotheses developed in mesic sites as well as indicators of N saturation may have limitations when applied to xeric systems. For example, in semiarid catchments, significant N losses have been observed in systems that remain N limited (Vourlitis et al., 2009), suggesting that considerable N leaching can occur without following a strict progression from plants to litter to soil (Lovett and Goodale, 2011). Limits to the use of N saturation theory in xeric environments likely stem from the intrinsic differences between mesic and xeric landscapes; mesic sites are generally consistently wet and have relatively high C content that can support N storage (Taylor and Townsend, 2010), while xeric soils are typically poorly developed, have relatively low C contents (low SOM), and can experience droughts lasting up to several months. Thus, in the context of N deposition, the dry season represents a period during which N inputs are hydrologically disconnected from ecosystem processes (Meixner and Fenn, 2004; Riggan et al., 1985), limiting diffusion, and resulting in the accumulation of N with minimal interaction with physical and

biological soil components (i.e., SOM, roots, and microbes) (Michalski et al., 2004; Padgett et al., 1999). Unlike xeric sites, N deposition in mesic sites has greater hydrological connectivity with soil physical and biologic components, even during winter (Judd et al., 2007), resulting in relatively consistent N inputs without periods of extensive N accumulation. As a result of these differences, indicators of N saturation in xeric sites must be cautiously evaluated, as they may be representative of partial saturation of a sink, rather than ecosystem N saturation.

Because the application of N saturation indicators may have limitations in semiarid ecosystems, comprehensive N budgets should provide a better understanding for the capacity of xeric ecosystems to sequester N; thus, providing an opportunity to better estimate the N saturation status of semiarid landscapes. However, to date, comprehensive N budgets for chaparral ecosystems have not been published, giving rise to several questions: what is the capacity for N assimilation and the N saturation status of chaparral watersheds along the Sierra Nevada foothills? Is the hydrologic flushing of unprocessed atmospherically deposited N, the major pathway for N loss in semiarid ecosystems? What processes control the export of N and how do chaparral ecosystems maintain N limitation under elevated N deposition? In this study, a comprehensive N budget is developed for a chaparral watershed located on the western foothills of the Sierra Nevada, considered at stage 2 (Fenn et al., 2011) of Stoddard's watershed N saturation model (Stoddard, 1994). Atmospheric N inputs, hydrologic N export, and belowground microbial processes were measured for two water years in 2003 and 2004 and unmeasured parameters such as N fixation, aboveground N cycling, and gaseous N

export were obtained from studies at the site (Chapter 2) as well as other chaparral ecosystems in California (Kummerow et al., 1978; Li et al., 2006; Mooney and Rundel, 1979). It is hypothesized that 1) although significant N losses are observed in this catchment, the watershed has not exceeded its capacity to assimilate N; 2) due to the accumulation of atmospherically derived N over the course of the dry season, a significant portion of the N lost, is the result of direct atmospheric N deposition that bypasses watershed biogeochemical processes; and 3) intense hydrologic and gaseous N losses dominate semiarid catchments during the dry to wet seasonal transition, during which N is flushed from catchments, resulting in N limitation during the growing season.

Materials and methods

Site descriptions

We studied a 4.2 ha chamise-dominated watershed located on the southwestern foothills of the Sierra Nevada Mountains (680-700 m a.s.l.), within the Kaweah River drainage, in Sequoia and Kings Canyon National Park (338170 m E ,4042382 m N). The climate at the site is typical of Mediterranean regions with hot dry summers and cool wet winters. The average annual rainfall is approximately 670 mm, of which the majority falls during the wet winter growing season (November to April). The average maximum air temperature is 36.4 °C and the average minimum is 2.2 °C. The watershed drains into a single channel (Chamise Creek) which remains predominantly dry during the hot summer and can reach flows of ~200 L s^{-1} during the wet winter (this study).

Soils at the site are classified as Ultic Haploxeralfs, are well drained, have a sandy clay loam texture, a well-developed argillic horizon, and are derived from gabbro-dioritic parent material (Huntington and Akeson, 1987). The soil pH is ~6, the C content is 2.3 % and 0.1 % for N (Miller et al., 2005). Thick stands of chamise (*Adenostoma fasciculatum*) with annual grasses (*Bromus* species) in between shrubs represent the majority of the aboveground biomass, but California mountain mahogany (*Cercocarpus betuloides*), California scrub oak (*Quercus berberidifolia*), buckbrush (*Ceanothus cuneatus*), and mountain balm (*Eriodictyon californicum*) are also present to a lesser extent. The watershed has not burned since 1960 (Li et al., 2006) and is therefore representative of a fully mature chaparral ecosystem (Rundel and Parsons, 1979).

Atmospheric N deposition and N_2 fixation

Bulk atmospheric N deposition (dry+wet) was measured from July 2002 through July 2004 using ion-exchange resin collectors (Fenn and Poth, 2004). Resin collectors were placed in open meadows (n=4) to capture direct atmospheric N deposition, as well as under chamise cover (n=5) to measure N throughfall. Resin collectors were constructed by attaching a funnel (10 cm diameter) to a 1.27 cm × 35.6 cm polyvinyl chloride (PVC) tube containing 60 mL of a mixed-bed H^+/OH^- polystyrene ion-exchange resin (Amberlite MB150, Rohm and Hass, Philadelphia, PA). Following collection, resin extracts were analyzed for NO_3^--N and NH_4^+-N using a Lachat autoanalyzer (Lachat Instruments, Milwaukee, WI); determination of NH_4^+-N used the diffusion method (Lachat method 31-107-06-5-A), and NO_3^--N was analyzed using the Griess-Ilovsay reaction after Cd reduction (Lachat method 12-107-04-1-B). The average annual N

deposition for water years 2003 and 2004 was estimated by calculating a monthly deposition rate from which the annual rate was derived. An average annual deposition rate from July 2002 through July 2004 was also calculated. Standard errors from the average N concentration in resin collectors for each sampling time were carried through all calculations and reported as a measure of uncertainty.

Nitrogen fixation was not measured at the site, but a rate of 0.01 g N m^{-2} yr^{-1} was reported for a 25-year-old chaparral stand with 30% cover of *Ceanothus greggii* (Kummerow et al., 1978). Although N-fixation rates as high as 0.2-4 g N m^{-2} yr^{-1} have been measured in chaparral communities, they occur as a result of N-fixing plants and shrubs that re-colonize following fire (Ellis and Kummerow, 1989; Poth, 1982). Since the studied watershed has not burned since 1960 and *Ceanothus* species comprise much less than 30% of the plant community, it is presumed that the N_2 fixation is below 0.01 g N m^{-2} yr^{-1} as measured by Kummerow et al. (1978).

Plant N content and dynamics

Vegetation N content, N uptake, N transferred in litterfall, and N translocation to aboveground biomass was not measured in this study. However, past research on chaparral communities have documented N dynamics at a chamise stand in Echo Valley near San Diego, California (Mooney and Rundel, 1979), as well as through modeling (DAYCENT) at Chamise Creek (Li et al., 2006).

Soil net N mineralization, nitrification, nitrification potentials, and C and N content

Net N mineralization was measured using the intact soil core method (DiStefano and Gholz, 1986). In June 2002, two 50 m transects were established from which six sets of duplicate cores were collected at random at six different locations along each transect. Cores were collected by driving 4 cm diameter PVC cylinders to a 10 cm depth below the ground surface. Within 48 hours following collection, gravimetric soil moisture and initial (T_0) exchangeable NH_4^+-N and NO_3^--N was determined in one set of cores. On a second set of cores (n=8), a mixed bed ion-exchange resin (J.T. Baker, IONAC NM-60 H^+/OH^-; Phillipsburg, NJ, USA) held in a fine mesh nylon bag was placed at the base of the PVC cylinder to capture throughfall N, and then returned to their original holes along the transect for a 2-6 week incubation. Replicate sets of soil cores were harvested in 2002 on July 15, September 22, October 14, October 27, November 9, and December 14; for 2003 on January 13, February 8, March 12, April 7, May 20, June 29, July 24, August 29, October 6, November 5, November 19, and December 18; and for 2004 on January 28.

For the determination of net N mineralization, harvested cores were hand sorted to remove roots and particles greater than 2 mm, homogenized, and followed by extraction of a 10 g subsample in 0.5 M K_2SO_4 for 2 h. Ion-exchange resin used to collect throughfall N from cores was first rinsed with deionized water and extracted with 2 M KCl for 2 h. A subset of resin bags that had not been deployed in the field were used as blanks for each harvesting time. All soil and resin extracts were filtered through pre-rinsed 11 µm filters (Whatman #1) and analyzed for inorganic N on a Lachat

autoanalyzer as previously described. Net N mineralization was calculated by subtracting total N at T_0 (exchangeable N) from total N at the end of the incubation (T_1) (exchangeable N + leachate resin N), for each sampling time. Net nitrification was calculated by subtracting NO_3^- measured at T_0 from T_1. A bulk density of 1.5 g cm^{-3} (Huntington and Akeson, 1987) and a depth of 10 cm were used to estimate soil N pools on an aerial basis.

The annual rate for Net N mineralization and nitrification was estimated from core incubations between September 22, 2002 and October 6, 2003 (water year 2003). To estimate a total mass of mineralized or nitrified N, the daily net mineralization or nitrification rate measured in core incubations at day 1 (September 22, 2002) was multiplied by the number of days until the next measurement was made (October 14, 2002), sequentially repeating this calculation for a total of 365 days. The standard error from the average rate of N mineralization and nitrification measured in cores was carried through all calculations and reported as a measure of uncertainty.

The total soil C and N content was estimated from ten 10 cm cores as well as from three pits dug down to 100 cm under chamise cover, California scrub oak, and open meadow. Total C and N was measured on dry finely ground soil subsamples on a Thermo Flash EA 1112 soil combustion CN analyzer.

Nitrification potentials were determined on a second subsample of soils (n=4) collected on July and September 2002 and May and November 2003 using the chlorate-slurry method (Belser and Mays, 1980).

Microbial biomass C and N

Microbial biomass C and N were determined on a third subsample of soils (n=8) using the chloroform fumigation method (Vance et al., 1987) over a three-day fumigation period. Extracts generated from the fumigation were analyzed for total C and N using a persulfate digestion technique (Doyle et al., 2004), and biomass C and N calculated as the difference between fumigated and unfumigated C and N concentrations. In addition, a correction was applied to chloroform-labile C (K_{EC} = 0.4 (Tessier et al., 1998)) and chloroform-labile N (K_{EN} = 0.54 (Brookes et al., 1985)) to calculate microbial biomass.

Soil solution

Six soil lysimeters were installed at a 30 cm depth below the surface under chamise cover. The soil solution was sampled on November 12, 2002; March 24, April 18, April 20, May 3, 2003; and January 8, February 6, February 25, February 29, March 25-26, 2004. Samples were analyzed for NO_3^--N and NH_4^+-N on a Lachat autoanalyzer as previously described. The annual N content in the soil solution was estimated by summing averages for each monthly interval (excluding summer months). The standard error resulting from averaging the six lysimeters for each sampling time was carried through the annual N content calculation and reported as a measure of uncertainty.

Hydrologic and gaseous N losses

The export of N in streamwater was estimated for water years 2003 and 2004 using volume weighted mean concentrations. Estimates of stream flow were obtained at 15 minute time intervals from an H flume installed at the watershed outlet. Stream

chemistry (NO_3^--N, NH_4^+-N, dissolved organic N (DON), dissolved organic C (DOC), Ca^{2+}, and Cl^-) was measured at approximately 30 minute intervals during rainfall events and sporadically during periods of low flow (daily-monthly). During precipitation events, stream water samples were collected by an ISCO auto-sampler as well as by grab samples at the stream outlet. The total hydrologic export of N from the catchment was estimated using a "worked record" approach (Cohn, 1995), in which periods without stream chemistry were interpolated from periods in which measurements were made. As a measure of uncertainty, a 5% error was assigned to both discharge and stream chemistry measurements and a "jackknife" approach (Sokal and Rohlf, 1981) used to estimate the error associated with conducting the worked record. The total error (E_t) was calculated according to the equation:

$$E_t = (E_A^2 + E_B^2 + E_C^2)^{1/2} \qquad \text{Equation 3.1}$$

where E_A is the uncertainty in discharge, E_B the uncertainty in stream chemistry, and E_C the uncertainty introduced by the worked record.

In addition to stream chemistry, runoff water collectors (n=3) were used to measure N concentrations in surface soil water during large precipitation events between November 17, 2003 and March 26, 2004. Runoff water collectors consisted of a trough (20 cm wide) laid flat against the ground surface on a downhill slope, such that water was funneled into plastic bottles for sample collection and storage. Runoff water collectors were placed under chamise cover and DIN concentrations measured on a Lachat autoanalyzer as previously described.

Gaseous N fluxes ($NO+N_2O$) were not measured during water years 2003-2004, but measurements conducted at the site during the 2010 water year suggest an annual gaseous N loss rate of 0.14 ± 0.12 g N m^{-2} (Chapter 2). Although this number is lower than that reported from DAYCENT modeling for the Chamise Creek watershed (0.4 g N m^{-2}) (Li et al., 2006), DAYCENT values presumably overestimate gaseous N fluxes, as NO production increases during winter and spring months (Li et al., 2006); a period during which field measurements of gaseous N fluxes are lowest (Chapter 2).

^{15}N and ^{18}O natural abundance

To understand the direct contribution of atmospheric N deposition and biological processes to the hydrologic export of N, $\delta^{18}O$ and $\delta^{15}N$ of NO_3^- were measured in atmospheric resin column collectors (bulk deposition and throughfall), rainfall, soil solution, runoff water, stream water, and soils. Measurements for $\delta^{15}N$ and $\delta^{18}O$ were performed by isotope ratio mass spectrometry following the bacterial denitrifier method (Sigman et al., 2001), with *P. chlororaphis* used for the determination of $\delta^{15}N$ in atmospheric samples, as *P. aureofaciens* can overestimate $\delta^{15}N$ (Coplen et al., 2004). A two-component mixing model was used to estimate the contribution of atmospheric NO_3^- deposition to stream water (f_{atm}), and elaborate on the mechanisms controlling the export of N through hydrologic pathways. The two-component mixing model used the $\delta^{18}O$-NO_3^- from stream water ($\delta^{18}O_{stream}$) and soil solution ($\delta^{18}O_{soil}$) samples to calculate f_{atm}:

$$f_{atm} = \frac{\delta^{18}O_{stream} - \delta^{18}O_{soil}}{\delta^{18}O_{throughfall} - \delta^{18}O_{soil}} \times 100 \qquad \text{Equation 3.2}$$

once f_{atm} was determined, it was used to estimate the fraction of atmospherically deposited NO_3^- that exits the watershed unprocessed ($f_{unprocessed}$) as:

$$f_{unprocessed} = \frac{f_{atm} \times NF_{stream}}{NF_{atm}} \qquad \text{Equation 3.3}$$

where, NF denotes the N flux from the atmosphere and flux in stream water (Table 3.1).

Results

Atmospheric N deposition

Atmospheric N deposition was highest in 2003 when compared to the 2004 water year (Table 3.1). Much of the difference in N deposition between the two sampled years can be explained by differences in throughfall; approximately 613 mm of rain fell in 2003 compared to 487 mm in 2004. Differences in precipitation between the two years presumably limited the amount of N washed-off from vegetation surfaces yielding lower rates of atmospheric N inputs. Of the total N deposition measured at the site, NH_4^+ was the dominant form, accounting for approximately (average ± Std. Error) 71 ± 0.02 % of the total N deposition in 2003 and 83 ± 0.02 % in 2004.

Hydrologic outputs

The export of N in stream water was larger for the 2003 water year than for 2004; 2003 was a wetter year than 2004 (Table 3.1). Stream water DIN concentrations showed dramatic increases during the dry-wet seasonal transition, of which the majority of the exported N was in the form of NO_3^- (Fig. 3.1). During the first precipitation event of the

2003 water year, NO_3^--N concentrations rose to as high as 520 µM; NH_4^+-N concentrations remained low and did not rise above 7 µM (Fig. 3.1). Although the magnitude of the initial NO_3^- pulse declined over the length of the wet season, a pulse in stream water NO_3^- concentrations was always observed with increases in discharge following a dry period (Fig. 3.1). However, during consecutive rainfall events, NO_3^- concentrations peaked only once, resulting in relatively constant NO_3^- concentrations regardless of variations in stream flow (Fig. 3.2). By May 2003, pulses in NO_3^--N concentrations in response to discharge did not increase beyond 32 µM (Fig. 3.1). For the 2004 water year, similar patterns observed in 2003 emerged, with stream water NO_3^--N concentrations peaking at 442 µM and 4.7 µM for NH_4^+-N (Fig. 3.1).

During early stages of the 2003 wet season, the dramatic response in streamwater NO_3^--N concentrations to increases in discharge formed clockwise hysteresis loops (Fig. 3.3); NO_3^--N concentrations rose quickly during the rising limb of the hydrograph and were higher than NO_3^--N concentrations measured during the falling limb. As soil moisture increased in soils, towards the end of the wet season, counterclockwise hysteresis loops were developed in response to increases in discharge following periods of little to no rainfall, in which measured NO_3^--N concentrations were higher during the falling limb of the hydrograph than during the start (Fig. 3.3, loop a). However, with continued rainfall and concomitant increases in discharge, clockwise hysteresis loops were once again observed (Fig. 3.3, loops b-c), but the difference in NO_3^--N concentrations between the rising limb and falling limb of the hydrograph were substantially smaller than during the clockwise loops observed for the first precipitation

events of the wet season (Fig. 3.3). It is possible that counterclockwise hysteresis loops developed in response to short rainfall events that did not contribute significantly to discharge, but that nonetheless transported NO_3^- to streamwater or promoted in-stream nitrification during reductions in discharge.

Consistent with DIN measurements in stream chemistry, soil lysimeters and runoff water collectors showed increases in DIN concentrations during rainfall events (Figs. 3.4-3.5). Although a pulse in soil solution NO_3^--N was detected in response to the first precipitation event of the wet season in both 2003 and 2004 water years, NH_4^+ became the dominant form of DIN during subsequent measurements, reaching larger concentrations than those measured in stream water (Fig. 3.4). For runoff water, NH_4^+ was generally the dominant form of DIN with concentrations as high as 1,100 µM during the first rainfall event of the wet season (Fig. 3.5). Consistent with the patterns observed for DIN in stream chemistry, NH_4^+ concentrations in runoff water collectors decreased with increased frequency of rainfall events, but continued to be the dominant form of DIN over NO_3^- (Fig. 3.5).

Although the response of stream water DOC and DON to the first precipitation event of the wet season was not as distinct as for DIN, fairly similar patterns emerged, in which generally higher concentrations were measured at the onset of the wet season with decreasing concentrations over time (Fig. 3.6). Due to similarities between DIN and DON export patterns, increases in DON concentrations were related to increases in NO_3^-; however, the relationship was poor but significant (Fig. 3.7). Similarly, during consecutive rainfall events, DOC and DON concentrations were generally characterized

by an initial pulse in response to increased discharge, but concentrations did not respond to subsequent rainfall events and concomitant increases in stream flow (Fig. 3.2). In general, DON was closely related to DOC, such that increases in DON were accompanied by a stoichiometric increase in DOC (Fig. 3.6 insert). However, on few occasions in which DON concentrations were above 100 µM, a proportional stoichiometric increase in DOC was not observed; these isolated events occurred during high discharge events following a dry period (Fig. 3.6; gray oval). In general, the ratio of DOC:DON ranged from 5.3 to 50.5 with an average (± Std. Error) of 24.8 ± 0.69 (n=135).

Net N mineralization, nitrification, nitrification potentials, and C and N content

The average (± Std. error; n=131) rate of net N mineralization in all cores from July 15 2002 through January 28 2004 was -0.04 ± 0.04 µg N g^{-1} d^{-1}, and generally fluctuated between 0.15 and -0.12 µg N g^{-1} d^{-1}, except during November 9 2002, in which a large net N immobilization event was measured at the onset of the wet season (-0.88 µg N g^{-1} d^{-1}; Fig. 3.8). Prior to November 9 2002, during the dry season, net rates of N mineralization were positive, and were also generally positive during the wet season of 2003, except during April, in which N immobilization was once again detected, presumably in response to an increase in soil moisture (Fig. 3.8). As the volumetric water content in soil decreased during the wet-dry seasonal transition, so did the rates of net N mineralization, resulting in a second net N immobilization event on July 24 2003 corresponding to a continued decline in soil moisture (Fig. 3.8). On August 29 2003, however, a small rise in soil moisture resulted in a positive short-lived pulse in net N

mineralization, which returned once again to net negative (immobilization) by October 6, 2003. At the onset of the wet season of 2004, rates of net N mineralization became positive and remained relatively constant through the last measurement on January 28, 2004 (Fig. 3.8).

The large net N immobilization event observed on November 9 2002 (Fig. 3.8) heavily influenced the estimated annual rate for net N mineralization (0.03 ± 3.5 g N m^{-2} yr^{-1}). However, because the large N immobilization event observed in 2002 did not occur in 2003 in response to wetting, an annual rate for net N mineralization was also calculated excluding this event (2.3 ± 2.2 g N m^{-2}), which may be representative of the N mineralization rate for the 2004 water year. This rate was calculated by extending the rate of N mineralization measured on October 27 and December 14 2002 for an additional 13 days (6.5 days each).

The average (± Std. error; n=131) rate of net nitrification in all cores from July 15 2002 through January 28 2004 was -0.02 ± 0.03 µg N g^{-1} d^{-1}, and generally fluctuated between 0.13 and -0.09 µg N g^{-1} d^{-1}, except during the November 9 2002 net N immobilization event (-0.59 µg N g^{-1} d^{-1}; Fig. 3.8). Similar to rates of net N mineralization, net nitrification rates were positive during the dry season of 2002, but contrary to net N mineralization, the first rainfall event of the 2002-2003 wet season resulted in an increase in net nitrification (Fig. 3.8). During the remainder of the incubations, nitrification rates showed similar patterns and were comparable to those of net N mineralization (Fig. 3.7). Nitrification potentials increased as soils dried during the summer of 2002 and were lowest when measured in late spring 2003 (Fig. 3.9). By the

end of the dry season of 2003 nitrification potentials had increased to values comparable to the dry season of 2002 (Fig. 3.9). As with net N mineralization, the N immobilization event of November 2002 heavily influenced the annual estimate for nitrification, yielding an average rate of 0.6 ± 2.5 g N m^{-2} yr^{-1}; exclusion of the November 9 2002 N immobilization event yielded an average net nitrification rate of 2.3 ± 1.5 g N m^{-2} yr^{-1}.

The average C content in the upper 10 cm of soil was 2 % and 0.14 % for N. Both C and N content decreased with soil depth to 0.06 % C and < 0.01 % N at a 90-100 cm depth.

Extractable soil N pools

Extractable soil NO_3^--N and NH_4^+-N concentrations exhibited contrasting patterns during the dry season of 2002, in which NH_4^+-N concentrations increased as soils dried while NO_3^--N concentrations declined or remained low (Fig. 3.10). At the onset of the dry-wet seasonal transition (2002), increases in soil moisture generally corresponded with a pulse in soil NO_3^--N concentrations and a decline in soil NH_4^+-N, until the large rainfall event in November 2002, during which both soil NO_3^--N and NH_4^+-N concentrations precipitously declined (Fig. 3.10). During the wet season of 2002-2003, soil DIN concentrations generally followed the patterns observed in soil moisture; increases in soil moisture corresponded with increases in DIN and DIN concentrations declined as soils dried. However, as soils began to dry, past April 7 2003, both soil DIN concentrations increased until June 29 2003 (Fig. 3.10). Past this point, a pattern somewhat similar to that observed during the dry season of 2002 had presumably started to emerge, in which soil NH_4^+-N concentrations were greater than NO_3^--N (Fig. 3.10). However, a small

precipitation event during August 2003, slightly increased soil moisture, resulting in a sudden increase in NO_3^--N with concomitant reductions in NH_4^+-N (Fig. 3.10). When extractable soil N pools were measured again on October 6 2003, soil moisture had declined to levels prior to the August rainfall event and NH_4^+-N concentrations were once again greater than NO_3^--N (Fig. 3.10). Increases in soil moisture during the 2003 dry-wet seasonal corresponded with slight increases in soil NO_3^--N and decreases in soil NH_4^+-N. In the wet season (2003-2004), similar patterns to those of the 2002-2003 wet season emerged; soil NH_4^+-N concentrations were generally greater than NO_3^--N and appeared to follow fluctuations in soil moisture (Fig. 3.9).

Microbial biomass C and N

Average microbial biomass C and N generally decreased during the 2002 dry season (Fig. 3.11). While microbial biomass C continued to decrease after small increments in soil moisture, microbial biomass N increased in response to the first rainfall event of the 2002-2003 wet season (Fig. 3.11), resulting in opposing patterns through January 13 2003; microbial biomass N increased while microbial biomass C decreased or stayed relatively constant (Fig. 3.10). Estimates of both microbial biomass C and N following January 2003, were well synchronized through the onset of the 2003 dry season, resulting in simultaneous increases or decreases in both microbial biomass C and N (Fig. 3.11). As soils dried during the summer of 2003, both microbial biomass C and N generally increased until a peak in soil moisture on December 18, 2003, after which both microbial biomass C and N declined (Fig. 3.11).

Atmospheric and terrestrial $\delta^{15}N$ and $\delta^{18}O$ of NO_3^-

The distribution of $\delta^{15}N$ among measured components ranged between -2.69 and -6.87 ‰ (Fig. 3.12); on average, soils were the most enriched in ^{15}N and water from runoff collectors the most depleted (Table 3.2). For $\delta^{18}O$, the separation between measured components was greater (Fig. 3.12), with average values ranging from 1.31 ‰ for terrestrial components to 81.06 ‰ for atmospheric end-members (Table 3.2). In agreement with observed $\delta^{18}O$ values, the $\delta^{18}O$ composition of runoff water was intermediate to both atmospheric and terrestrial components (21.26 ‰), highlighting the mixed composition of runoff water. For stream water, $\delta^{18}O$ values were well confined (Table 3.2), and remained relatively constant through both 2003 and 2004 water years (Fig. 3.13). However, during the first precipitation event in November 2002, a $\delta^{18}O$ value of 53 ‰ was recorded in stream water (Fig. 3.13). Of the NO_3^- measured in the stream, approximately 0.9 % is directly from atmospheric sources (equation 3.2), signifying that approximately 0.6 % of the atmospheric NO_3^- inputs are unaltered by watershed biogeochemical processes for the 2003 water year and 0.2 % for 2004 (equation 3.3). Isotopic separation of NO_3^- in streamwater provided some indication that denitrification occurred in Chamise Creek, as the slope of the $\delta^{18}O$ vs. $\delta^{15}N$ value for NO_3^- in stream water (0.84 ± 0.30; dashed line Fig. 3.12) was within range of the expected slope of 0.5 characteristic of denitrification (Kendall, 1998).

N budget

Nitrogen pools and fluxes for Chamise Creek are presented in figure 3.14. A mass balance between N inputs (atmospheric deposition and N_2 fixation) and outputs

(hydrologic and gaseous) suggests that the watershed retains 0.05 ± 0.13 g N m^{-2}. However, if N fixation is reduced by half of that reported by Kummerow (1989) — a reasonable assumption since *Ceanothus* species are not dominant at the site, and N losses to ground water are presumed to be equivalent to the annual N content in the soil solution (Fig. 3.14; 0.03 ± 0.005 g N m^{-2}), the net retention of N in the watershed is reduced to 0.015 ± 0.13 g N m^{-2}.

The average annual plant N demand (3.42 to 6.9 g N m^{-2}; Fig. 3.14) is higher than the average annual net N mineralization, but certainly within the measurement error for both estimates reported in this study (Fig. 3.14). Thus, soil net N mineralization can satisfy the average annual plant demand for N, resulting in the export of atmospherically deposited N through hydrologic and gaseous pathways as suggested by the near balance between N inputs and outputs.

Discussion

N export from semiarid catchments

The episodic hydrology and biogeochemistry of semiarid systems is a well documented phenomenon controlled by pronounced shifts in dry to wet soil conditions (Fenn et al., 1996; Miller et al., 2005; Parker and Schimel, 2011), in which large pulses of NO_3^- (Fenn and Poth, 1999; Meixner and Fenn, 2004; Riggan et al., 1985), and NO, and to a much lesser extent N_2O, are observed following the wetting of dry soil (Chapter 2; Gelfand et al., 2009; McCalley and Sparks, 2009). The results from this study are consistent with our understanding of N dynamics in semiarid catchments suggesting that

the seasonal transition period from dry to wet soil conditions, is in fact, an important mechanism maintaining N limitation in these ecosystems (Vitousek and Field, 2001; Vourlitis et al., 2009).

The hydrologic export of N from semiarid catchments is strongly dominated by NO_3^- (Fenn et al., 1998; Meixner and Fenn, 2004). Because it has been shown that atmospheric NO_3^- can accumulate on land surfaces followed by quick flushing from catchments with minimal biogeochemical processing (Michalski et al., 2004), it was hypothesized that the export of N in this study could be controlled by similar mechanisms. However, little evidence from water runoff collectors, soil solution, and stream chemistry supported this case. Although clockwise hysteresis loops developed during early storm flow events suggest that new event water flushed large quantities of NO_3^- (Evans and Davies, 1998), presumably indicating rapid flushing of atmospherically deposited NO_3^-, it is clear from surface runoff collectors and the composition of atmospherically deposited N (ca. 80 % NH_4^+), that NH_4^+, not NO_3^-, was the major form of N washed-off from land surfaces. Thus, since the majority of the N measured in streamwater occurred as NO_3^-, rapid nitrification of NH_4^+ rather than flushing of atmospheric NO_3^- must have controlled N losses from Chamise Creek; a pattern consistent with observations in other chaparral ecosystems (Fenn et al., 1993; Vourlitis et al., 2007b) as well as in mesic catchments (Curtis et al., 2011).

Nitrification is strongly influenced by soil moisture, such that at low soil water content, the slow diffusion of NH_4^+ to nitrifiers can limit nitrification (Stark and Firestone, 1995). In chaparral, the characteristic low soil water content limit nitrification

(as low as 1% gravimetric water content; upper 10 cm), but soil microbes can be well adapted to drought-induced stress and remain active in thin water films during summer (Schimel et al., 2007), such that NH_4^+ accumulation in soil can be quickly diffused to active nitrifiers following wetting (Parker and Schimel, 2011). In this study, DIN concentrations in surface runoff collectors and soil solution are supportive of rapid nitrification of NH_4^+. Although higher NH_4^+-N than NO_3^--N concentrations were detected in surface runoff collectors, the opposite was true in the soil solution at the onset of the wet season, suggesting that as water percolated through shallow surface flowpaths (Swarowsky et al., 2012), rapid nitrification occurred (Vourlitis and Zorba, 2007). It is also possible that in-stream nitrification accounted for the large NO_3^- losses (Curtis et al., 2011). The rapid nitrification of NH_4^+, either in shallow surface flowpaths or in the stream, is further supported by isotopic analysis of streamwater NO_3^--$\delta^{18}O$ and NO_3^--$\delta^{15}N$ (Fig. 3.12, Table 3.2), strongly suggesting that nitrification controls hydrologic N losses in Chamise Creek (Kendall, 1998); a two-component end member analysis suggests that 99 % of the NO_3^- in streamwater results from nitrification. It is acknowledged, however, that a few high NO_3^--$\delta^{18}O$ values were recorded in streamwater samples gathered at the onset of the wet season (2003 water year), suggesting a higher contribution of unprocessed atmospherically derived NO_3^- (Fig. 3.13). Nevertheless, the overwhelming majority of data in this study is strongly indicative of biologically controlled export of NO_3^-.

Despite the dominance of NO_3^- as the major pathway for the export of N in semiarid catchments (Meixner and Fenn, 2004), N losses through DON accounted for 13

% of the watershed N export in the 2003 water year and 29 % in 2004 (2004 was drier than 2003). The export of DON is important in unpolluted catchments (Hedin et al., 1995; Perakis and Hedin, 2002), and can be used as an indicator of shifting N dynamics (Goodale et al., 2000). In unpolluted catchments, where concentrations of DIN in stream water are low, the slow turnover of soil organic matter (SOM) controls the export of N through DON (Perakis and Hedin, 2002), such that DON is in strict stoichiometric proportion with DOC, and is independent of N demand and cycling as described by the "Passive Carbon Vehicle Hypothesis" (Brookshire et al., 2007). In this study, DON concentrations were generally proportional to DOC (Fig. 3.6), indicating that the slow turnover of SOM regulates DON losses regardless of whether rapid nitrification controls DIN. However, higher concentrations of DOC and DON were observed following the wetting of dry soil than when soils were consistently wet (Fig. 3.6, spring), suggesting that different mechanisms may regulate the turnover of SOM. In Chamise Creek, increased export of DON can result from the microbial stress response to changes in soil water potential (Fang et al., 2009), as well as through the exposure of previously protected SOM to microbes during drying-wetting cycles (Miller et al., 2005; Navarro-Garcia et al., 2012) and increased decomposition and mineralization of SOM (no change in SOM C:N; Fang et al., 2009).

In southern California, the dry season can extend for 5-6 months during which chaparral ecosystems receive little to no rain, compelling soil microbes to accumulate intracellular osmoregulatory solutes to avoid dehydration (Fierer and Schimel, 2003). At the time of wetting, however, microbes must quickly dispose accumulated osmolytes or

their cells may be ruptured due to increases in soil water potential (Kieft et al., 1987). Thus, it is possible that the release of intracellular material (amino acids and other organic monomers) from microbial stress response (Schimel and Bennett, 2004), as well as microbial access to previously protected SOM through multiple dry/wet cycles (Navarro-Garcia et al., 2012), may explain the increase in DOC and DON export following wetting of dry soil. However, it is worth noting that a few exceptions to the strict stoichiometry between DOC and DON were observed, and that these "irregularities" occurred strictly during pulses in DON after soil wet-up (Fig. 3.6, gray oval).

As an alternative to the passive C vehicle hypothesis, the "Stoichiometric Enrichment Hypothesis" proposes that in N polluted systems, DON leaching from soil is not stoichiometrically fixed to DOC, such that the ratio of DOC:DON decreases as DON is enriched through two potential mechanisms: by altering the stoichiometry of the SOM pool or by direct enrichment of dissolved organic matter (DOM) (Brookshire et al., 2007). Although stream water NO_3^- and DON concentrations were poorly related in this study, the relationship was significant (Fig. 3.7), suggesting that DIN may enrich the DON pool (Fang et al., 2009; Goodale et al., 2000) at the time of wet-up. In soils that undergo marked changes from dry to wet conditions, shifts in soil moisture can significantly influence N dynamics (Fierer and Schimel, 2002; Miller et al., 2005), such that as soils dry, and hydrologic connectivity decreases, microsites become disconnected forming pockets in which resources can accumulate due to limited diffusion (Parker and Schimel, 2011). Thus, over the course of a dry season, semiarid systems can accumulate

NH_4^+ (Parker and Schimel, 2011), but more importantly, nitrite (NO_2^-) (Gelfand and Yakir, 2008). During the wet season, however, hydrologic connectivity is reestablished and diffusion of soluble substrates accumulated during the dry season can be accessed by the surviving microbial biomass resulting in rapid nitrification of the accumulated NH_4^+ and NO_2^- pool as well as production of more NO_2^-; NO_2^- is an obligate intermediate in the nitrification pathway. Because NO_2^- has been shown to readily react with SOM (Dail et al., 2001; Fitzhugh et al., 2003), it may explain the enrichment of the DOM pool at the time of soil wet-up, effectively enriching DON with a concomitant decrease in the ratio of DOC:DON (Fang et al., 2009).

N retention in chaparral

The substantial N loss through hydrologic pathways measured in this study, in conjunction with significant gaseous N emissions (Chapter 2) during transitions from dry to wet soil conditions, provide further evidence of the limited capacity for chaparral ecosystems to retain N, as well as highlight the avenues by which N-limitation is maintained. In arid and semiarid ecosystems, soils are typically of relatively low C content (Garcia et al., 1994). Because the long-term storage of atmospherically deposited N requires a stable organic matter pool (Curtis et al., 2011), N retention in chaparral soils is understandably low. Thus, excess N deposition in predominantly C-poor soils can induce C limitation, and promote the export of NO_3^- from ecosystems (Taylor and Townsend, 2010). DOC:NO_3^- ratios between 2.2 and 2.5 have been found to mark the threshold for C limitation at which elevated NO_3^- losses are observed among earth's ecosystems (Taylor and Townsend, 2010). In Chamise Creek, DOC:NO_3^- ratios were as

low as 2.7 during early stages of the dry to wet seasonal transition and as high as 970 during late spring, consistent with the explanation that C limitation exerts control on the export of NO_3^- from chaparral soils.

The retention of N in chaparral catchments depends on the season in which N additions are made. In a four-year fertilization study of chaparral (50 kg ^{15}N ha^{-1} yr^{-1}), in which N was applied yearly in October (end of dry season), N additions failed to stimulate ecosystem N storage in soils and plant biomass, with the majority of the added N being exported through hydrologic and presumably gaseous pathways (Vourlitis et al., 2007a; Vourlitis et al., 2009); gaseous N emissions were not measured but should have been important (Chapter 2). Because of the significant export of NO_3^- observed at Chamise Creek in this study, and significant gaseous N losses (Chapter 2), it is not surprising that N additions during the dry season would have escaped from fertilized plots with minimal retention in soils and plant biomass (Vourlitis et al., 2007a; Vourlitis et al., 2009). However, because the magnitude of the exported N in stream chemistry in this study decreased as the wet season progressed—a pattern consistent with gaseous N emissions from soils at this site, it may suggest that fertilization during the spring (growing season), would have resulted in greater N retention. Indeed, N fertilization studies in which 50 kg N ha^{-1} yr^{-1} are applied as slow release urea to N polluted watersheds (background deposition >30 kg N ha^{-1} yr^{-1}), relive N-limitation (Grulke et al., 2005). Therefore, the capacity for N assimilation in chaparral ecosystems may not only depend on soil C-limitation but also on plant N uptake (ca. 3.4 to 6.9 g N m^{-2} yr^{-1}; Fig. 3.14).

The observed decreases in the export of N in chaparral watersheds as the wet season progresses are thus presumably due to two principal mechanisms—a physical and a biological: 1) substrate limitation as the atmospherically deposited (mainly NH_4^+ in this study) or mineralizable soil N pool is nitrified and exported from the catchment and/or 2) N immobilization on stable soil organic matter pools and increased plant N uptake. Because the concentration of NO_3^--N in streamwater steadily decreased into the growing season (Fig. 3.1), it is possible that both substrate limitation and N immobilization could have occurred. Indeed, net N immobilization was observed, presumably as microbes degraded C from previously protected SOM (Navarro-Garcia et al., 2012) or litter high in C:N, but it was temporary (Fig. 3.8). Seemingly, a reduction in the export of N due to substrate limitation of atmospherically deposited N is consistent with the observed decrease in NH_4^+ concentrations in runoff collectors and soils, which precipitously declined after wet-up. However, because the average annual rate of net N mineralization was positive (Fig. 3.14), and net N mineralization was observed during spring (Fig. 3.8), neither net N immobilization in soil nor substrate limitation can fully explain the observed reductions in hydrologic and gaseous N losses as the wet season progressed. In chaparral ecosystems, plant N demand does not peak until the spring, during which annual grasses are first to tap into soil N pools followed by woody plants (in this case chamise; March-April) (Mooney and Rundel, 1979). Although net N immobilization and substrate limitation may have accounted for some reductions in the export of N during early stages of the wet season, when plants were still dormant, plant N uptake during spring likely accounted for the increased retention of N. Thus, in chaparral ecosystems,

large N loses through hydrologic and gaseous pathways are likely regulated by the asynchrony between N availability and plant N demand (Meixner and Fenn, 2004), constituting an important mechanism by which N limitation is maintained in ecosystems that may receive in excess of 50 kg N ha^{-1} yr^{-1} (Vourlitis et al., 2009).

The role of plant N uptake regulating N losses in chaparral ecosystems during the dry-wet seasonal transition is analogous to N losses in mesic sites following major disturbance. In northern hardwoods, forest harvesting can temporarily disrupt the N cycle (Aber et al., 2002; Bormann et al., 1974; Burns and Murdoch, 2005), elevating exchangeable soil N (Homyak et al., 2008), and increasing NO_3^- concentrations in streamwater to values in excess of 1,400 µM (Burns and Murdoch, 2005; Likens et al., 1970). Most importantly, the enhanced export of N through hydrologic pathways is not due to enhanced rates of N mineralization or nitrification, but to the lack of plant N uptake (Burns and Murdoch, 2005). Similarly, in semiarid systems, the onset of the wet season may be viewed as a temporary "disturbance", during which plants are senesced and unable to consume mineralized N. That is, rates of N mineralization and nitrification generally remain constant, suggesting that the asynchrony between N availability and plant N demand controls hydrologic and gaseous N losses. Of concern, however, is the accumulation of atmospheric dry deposition during summer, which can be rapidly nitrified following soil wetting, resulting in significant gaseous and hydrologic N export that can pollute downwind and downstream ecosystems. Moreover, because nitrification is an acidifying process, it can further lower the pH of soils already impacted by N

deposition (Wood et al., 2007); nitric acid is an important component of N deposition for the western Sierra Nevada (Cisneros et al., 2010).

Belowground N dynamics

Belowground N dynamics explain the observed patterns in hydrologic N export as well as gaseous N emissions measured at Chamise Creek (Chapter 2), and are consistent with other studies in seasonally dry ecosystems (Li et al., 2006; Miller et al., 2005; Parker and Schimel, 2011). At the onset of the 2002 and 2003 wet season, net nitrification rates increased immediately after wet-up, consistent with the isotopic analysis of NO_3^- in stream water that suggest rapid nitrification, as well as with the significant NO_3^- and NO losses (Chapter 2) measured at the site (byproducts of nitrification). As soils dry during summer, extracellular enzyme activity can remain active (Sardans et al., 2008), and transform SOM into a stress-labile C pool that can be quickly mineralized by surviving microbes at the time of wet-up (Miller et al., 2005). It is also likely that due to the large proportion of NH_4^+ in atmospherically deposited N, which accumulated on soil surfaces during the dry season, rapid nitrification could have occurred as increases in soil moisture allowed diffusion of NH_4^+ to nitrifiers.

As soils dry, solutes such as NH_4^+ and NO_2^- may not only accumulate in hydrologically disconnected sites, but can also form microsites within the soil matrix, in which microbes have access to nutrients, and may remain hydrologically disconnected from predators or viruses that cause their death (Parker and Schimel, 2011). Thus, over the course of a dry season, soils can show both accumulation of nutrients and increases in nitrification potentials (index of nitrifying population size) and microbial biomass (Parker

and Schimel, 2011). During the wet season, however, hydrologic connectivity is reestablished, and accumulated substrates are diffused to the surviving microbial biomass (Miller et al., 2005). Consistent with this explanation, nitrification potentials in this study increased as soils dried, suggesting that nitrifier populations remained active through the summer, and supporting observed increases in NO emissions from soils as water content decreased during the wet to dry seasonal transition (NO is a byproduct of nitrification; Chapter 2). At the time of wetting, however, reestablishment of hydrological connectivity would have allowed microbes access to the stress-labile C pool made available by extracellular enzyme activity during summer (Miller et al., 2005), previously protected SOM made available through physical disruption of soil aggregates (Navarro-Garcia et al., 2012), as well as to atmospherically deposited NH_4^+, explaining the considerable export of NO_3^- and elevated NO emissions during the dry to wet seasonal transition.

Except for a strong net N immobilization period observed at the onset of the wet season during November 2002, rates of N mineralization and nitrification did not vary greatly and generally responded to increases in soil moisture through an initial pulse in net nitrification followed by a pulse in net N immobilization, likely indicative of the slower cycling of a heavy fraction C pool (Miller et al., 2005). Because wetting can physically disrupt soil aggregates through slaking (Le Bissonnais, 1996), it can expose previously protected SOM to microbial attack (Navarro-Garcia et al., 2012), resulting in a pool of C that through exoenzyme activity may slowly become available to soil microbes, lessening C limitation, and promoting N immobilization (Miller et al., 2005; Navarro-

Garcia et al., 2012). It is also possible that microbial access to material high in C:N (litterfall) at the time of wetting would have promoted net N immobilization (Homyak et al., 2008; Miller et al., 2005).

During the 2002 dry season, NH_4^+ accumulated in soil, but both microbial biomass C and N generally decreased. In contrast, NH_4^+ accumulation in soil during the dry season of 2003 was not as clear as in 2002, but there was an increase in both microbial biomass C and N (Figs. 3.10-3.11). Given the dominance of nitrifying bacteria in chaparral soils (Vourlitis et al., 2007b), the observed soil N and C dynamics may be due to the sensitivity of nitrifiers to limited diffusion (Stark and Firestone, 1995). In the same way in which microbes may successfully grow in hydrologically disconnected sites during soil drying (Parker and Schimel, 2011), microbes may also exhaust available resources over the length of the dry season, explaining the concomitant decrease in microbial biomass C and N and accumulation of NH_4^+ in 2002. In the dry season of 2003, NH_4^+-N concentrations in soils were initially higher than NO_3^--N, and presumably would have continued to increase as nitrifiers consumed available resources in hydrologically disconnected sites. However, hydrologic connectivity was temporarily reestablished in late August, during which substrates were presumably resupplied, through diffusion, to nitrifiers (increase in NO_3^- and decrease in NH_4^+; Fig. 3.10).

Reassessment of N saturation in semiarid ecosystems

The concept of N saturation has been critical in advancing our understanding of how ecosystems respond to chronic N pollution, as well as in the development of N critical loads to prevent negative effects on ecosystems (Fenn et al., 2010). However, it

has been increasingly recognized that the hypotheses developed by Aber and others (1998) are in need of revision (Lovett and Goodale, 2011). In some instances, it has been argued that the application of hypotheses developed for N-polluted sites may have limitations when applied to ecosystems that are naturally N-rich (Perakis and Sinkhorn, 2011); net N mineralization should decline when N availability is above soil and plant demand, but it does not. In other ecosystems, elevated N inputs do not always result in increased rates of N mineralization and nitrification or foliar N content (Lovett and Goodale, 2011), and in semiarid systems, significant N losses occur through hydrologic and gaseous pathways (Chapter 2) before the capacity for N assimilation in plants has been exceeded (Vourlitis et al., 2009); a pattern contrary to that originally hypothesized by Aber et al. (1998). In an attempt to best represent the progression of N saturation in xeric systems, the conceptual model for forest ecosystem response to chronic N additions as originally postulated by Aber and others (1998) was modified (see Fig. 1 in Fenn et al., 1998), better reflecting increased N losses prior to a peak in net primary productivity as observed in N-polluted catchments downwind of the Los Angeles basin. However, this study underscores the need for additional refinement: specifically, the use of indicators of N saturation and N budgets as tools to assess the N status of semiarid watersheds. Because the application of N saturation theory to naturally N-rich ecosystems can have limitations (Perakis and Sinkhorn, 2011), the use of N saturation indicators can be misinformative in ecosystems that naturally export considerable quantities of N as a mechanism to maintain N limitation.

In semiarid catchments, the use NO_3^- leaching as a symptom of N saturation can lead to inaccuracies, and may result in the evaluation of watersheds as N-saturated when they are not, or as N-limited when they receive N inputs in excess of 50 kg N ha^{-1} yr^{-1} (Vourlitis et al., 2009). For instance, if streamwater NO_3^- concentrations in this study would have been evaluated either during the dry-wet seasonal transition or during spring, a different stage of N saturation would have been assigned to each period; likely stage 1 during spring and stage 2 or 3 during the dry to wet transition. Although Stoddard's model for watershed N saturation differentiates between N export during the growing and non-growing season (Stoddard, 1994), it predicts that N export during the non-growing season should be minimal for watersheds at stage 0 or 1. However, because in chaparral catchments the soil C content is relatively low and the vegetation is senesced during the dry-wet seasonal transition, a period of intense N cycling (Miller et al., 2005; Parker and Schimel, 2011; Riggan et al., 1985), unpolluted catchments can also express elevated streamwater NO_3^- concentrations as controlled by C-limitation and lack of plant N uptake (Bernal et al., 2005; Vourlitis et al., 2009). Although limited evidence suggests that the magnitude of the hydrologic N loss decreases in N-unpolluted catchments (Riggan et al., 1985), somewhat contradicting what is being proposed, it is not surprising that watersheds with lower N inputs would export less N. The proposed argument contends that wetting a dry soil temporarily and significantly alters the N cycle (Miller et al., 2005; Navarro-Garcia et al., 2012; Parker and Schimel, 2011; Xiang et al., 2008), suggesting that even N-unpolluted semiarid catchments can exhibit elevated NO_3^- losses at the onset of the wet season (Bernal et al., 2005), and inappropriately be described as N saturated.

Because Riggan and others (1985) did not measure N fluxes during the dry-wet transition (measurements were conducted in spring), it is understandable why N losses were low—plants were actively consuming N. In support of the proposed argument, in a relatively N unpolluted semiarid catchment (bulk N deposition = 4.1 kg N ha^{-1} yr^{-1}), NO_3^- concentrations at the onset of the wet season were approximately 230 µM (Bernal et al., 2005); a concentrations suggestive of N saturation (Stoddard, 1994). Furthermore, rates of N mineralization and nitrification in semiarid grasslands receiving 3-5 kg N ha^{-1} yr^{-1} are similar to those reported in this study (Parker and Schimel, 2011), suggesting that elevated N losses would have also been measured at the onset of the wet season assuming favorable hydrology.

As an alternative to using indicators to assess the N saturation status of a catchment, N input-output budgets can be more informative, as N saturation can be estimated by mass balance. In an N-limited system, N inputs should be greater than N outputs such that the watershed exhibits net N retention. As the watershed approaches N saturation, however, N outputs should begin to balance N inputs, eventually shifting to greater N outputs than inputs during ecosystem decline (Stoddard, 1994). In this study, N inputs are nearly balanced by N outputs suggesting that at 9 kg N ha^{-1} yr^{-1}, the Chamise Creek watershed has about exceeded its capacity to assimilate N. However, similar to the use of streamwater NO_3^- as an indicator of N saturation, the use of N budgets can also be problematic, as budgets may be nearly balanced in systems that naturally leak N. Since semiarid catchments export large quantities of N during early stages of the wet season (Bernal et al., 2005; Meixner and Fenn, 2004; Riggan et al., 1985), and the majority of N

deposition occurs during summer (Cisneros et al., 2010), when plants are senesced, it is likely that outputs can frequently balance N inputs across a wide range of N loading assuming favorable hydrology. That is, whether a chaparral watershed receives N inputs in excess of 50 kg N ha^{-1} yr^{-1} or lower, the majority of N is nitrified and lost during the dry to wet seasonal transition with minimal storage in plants or soils (Vourlitis et al., 2009), likely resulting in nearly balanced N budgets that suggest an ecosystem has nearly reached its capacity for N assimilation when the vegetation component remains N limited.

In an effort to refine the concept of N saturation and incorporate the growing number of observations displaying inconsistencies with the hypotheses developed by Aber and others (1989, 1998), Lovett and Goodale (2011) introduce the concept of kinetic and capacity N saturation and introduce a new conceptual model of N saturation. Kinetic N saturation occurs when the rate of N inputs exceeds the soil and vegetation N net sink rates, and capacity N saturation, when N accumulation in soils and vegetation no longer occurs irrespective of the rate at which N is being added (Lovett and Goodale, 2011). The new conceptual model proposes that rather than expecting a sequential passage of N from vegetation to litter to soil, to eventually elevated N losses, the concept of N saturation should be expressed as a simultaneous flow of N to all four possible fates: vegetation, detritus and SOM, leaching, or gaseous loss (Lovett and Goodale, 2011), such that elevated N losses, as those observed in this study and other xeric ecosystems, can be explained while the vegetation component remains N-limited. Although expressing N saturation through this new concept is consistent with the observations in this study and

other semiarid ecosystems, there is need for minor modification: the introduction of C-limitation and asynchrony between N availability and plant N demand as a controlling factor determining the flow of N to leaching and gaseous N loss fates (predominantly NO) (see Fig. 6 in Lovett and Goodale (2011)).

The use of this new model is helpful for managing semiarid ecosystems, as it allows research to focus on kinetic N saturation rather than on capacity N saturation; capacity N saturation is not likely to occur in ecosystems that naturally leak N. Based on this new model, it can be concluded that at N deposition rates of 9 kg N ha^{-1} yr^{-1}, chaparral ecosystems are kinetically N saturated, but that challenges still remain in setting benchmarks for understanding how much N is too much N in kinetically N saturated watersheds. Specifically, because chaparral ecosystems naturally leak N and capacity N saturation may be difficult to reach, it is difficult to set limits to N critical loads, resulting in efforts that may do little to protect ecosystems from chronic N fertilization. Some of these gaps in knowledge can be filled by studies across N deposition gradients that capture the transition from dry to wet soil conditions and develop response curves for streamwater NO_3^- export as a function of precipitation over time. Although the initial response to wetting should be elevated, even in unpolluted catchments, streamwater NO_3^- concentrations in N unpolluted catchments should decline at faster rates than in N polluted watersheds (Riggan et al., 1985), aiding in the development of criteria to define stages of kinetic N saturation. Because the majority of N deposition occurs during summer (Cisneros et al., 2010), where it accumulates on surfaces, kinetic N saturation is expected to continue to occur at the recommended N

critical load of 10-14 kg N ha^{-1} yr^{-1} for chaparral ecosystems (Fenn et al., 2010). Thus, it is recommended that a lower critical load be implemented—presumably 3-6 kg N ha^{-1} yr^{-1} as recently suggested by Fenn and others (2011). By adhering to this new concept, management plans can be developed to address the negative impacts of chronic N pollution as well as aid in the development of critical loads consistent with the distinction between kinetic and capacity N saturation. For example, management plans should focus on the summer period to reduce atmospheric N inputs to semiarid ecosystems. If critical loads are to protect semiarid drylands from the negative impacts of N pollution, their development must consider the disproportional export of N that occurs at the onset of the wet season during which chaparral ecosystems exhibit kinetic N saturation.

Summary and conclusions

Atmospheric N inputs to chaparral ecosystems of southern California can be quickly exported through hydrologic and gaseous pathways, such that chaparral vegetation can remain N-limited even under elevated rates of N deposition. Belowground N dynamics are consistent with observations in other dryland ecosystems suggesting that the transition from dry to wet soil conditions significantly affects microbial N processing and regulates N loss. That is, the strong dominance of nitrifying bacteria in chaparral soils imposes limits on the amount of N that can be sequestered in these ecosystems during plant senescence. This study further contributes to our understanding of N cycling and N saturation in xeric ecosystems by considering C-limitation and the asynchrony between N availability and plant N demand, as an

important controlling factor regulating kinetic N saturation in semiarid catchments. Based on this study, chaparral ecosystems receiving 9 kg N ha^{-1} yr^{-1} are kinetically N saturated, but that capacity N saturation has not been reached as evidenced by low hydrologic and gaseous N export during the growing season, and generally strict stoichiometry between DOC and DON. It is proposed that capacity N saturation may be difficult to observe in semiarid catchments, not due to the capacity of these ecosystems to assimilate N, but to their predisposition to quickly export N prior to the start of the growing season; explicitly, C-limitation and the asynchrony between N availability and plant demand as controlling factors maintaining N-limitation. Finally, it is suggested that the calculation of critical loads for chaparral ecosystems incorporates the concept of kinetic N saturation to reevaluate the proposed critical load of 10-14 kg N ha^{-1} yr^{-1} to a more recent estimate of 3-6 kg N ha^{-1} yr^{-1} (Fenn et al., 2011; Fenn et al., 2010) aimed at minimizing the export of N, soil acidification, and reestablishing mycorrhizal and lichen communities. Future studies that examine N export from N unpolluted catchments would be important for developing criteria aimed at identifying different stages of kinetic N saturation and development of N critical loads.

Tables and figures

Table 3.1. Average (± std. error) atmospheric N inputs as measured in bulk deposition and throughfall collectors and hydrologic N export during water years 2003 and 2004.

	Atmospheric N deposition (kg ha^{-1})		Hydrologic N export
Water year	Throughfall	Direct	
2003	10.3 ± 1.5	5.5 ± 0.6	7 ± 0.5
2004	5.3 ± 0.4	4.1 ± 0.1	1 ± 0.07
Average	8.8 ± 0.1	5.1 ± 0.4	--

Table 3.2. Average $\delta^{15}N$ and $\delta^{18}O$ (± standard error) of NO_3^- from soils, precipitation, atmospheric bulk deposition, throughfall, streamwater, surface runoff water, and soil solution during water years 2003-2004.

		$\delta^{15}N$ (‰)		$\delta^{18}O$ (‰)	
Component	n	Average	Std. error	Average	Std. error
Soil	2	-2.70	± 0.15	12.19	± 0.11
Precipitation	20	-2.75	± 0.42	76.93	± 1.71
Bulk deposition	47	-4.76	± 0.50	60.92	± 2.51
Throughfall	16	-2.69	± 0.70	81.06	± 1.70
Stream water	66	-3.02	± 0.41	2.06	± 1.03
Runoff water	11	-6.87	± 1.50	21.26	± 6.65
Soil solution	18	-3.92	± 1.33	1.31	± 1.27

.

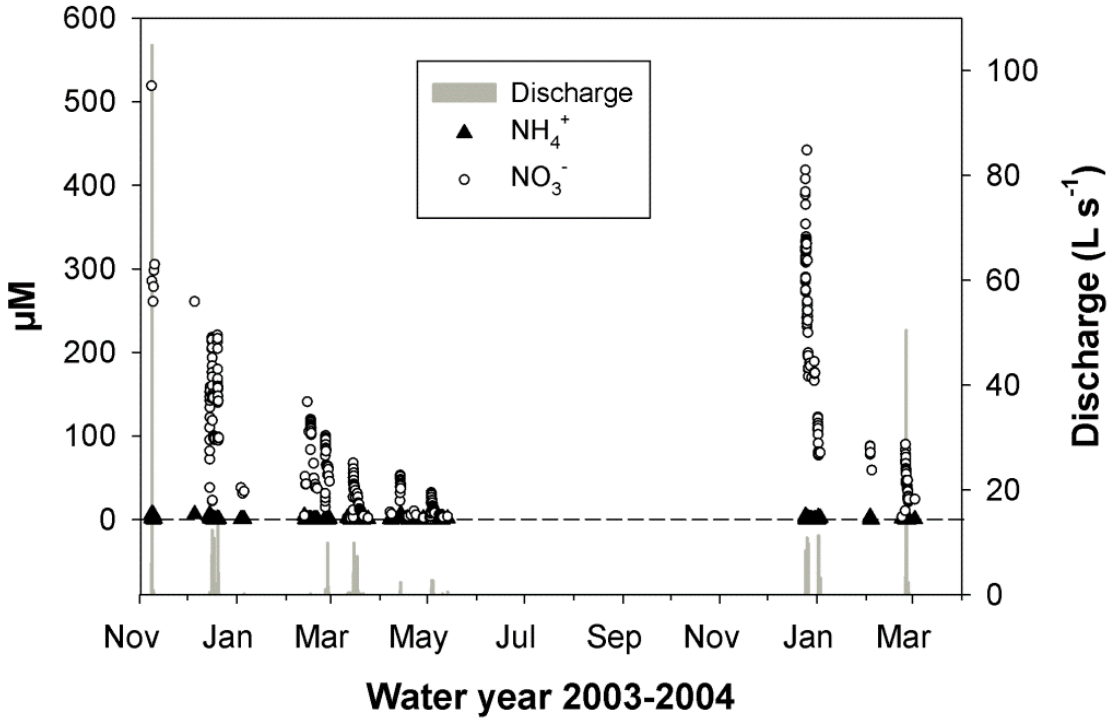

Fig. 3.1. Streamwater NO_3^--N and NH_4^+-N concentrations and discharge during water years 2003-2004.

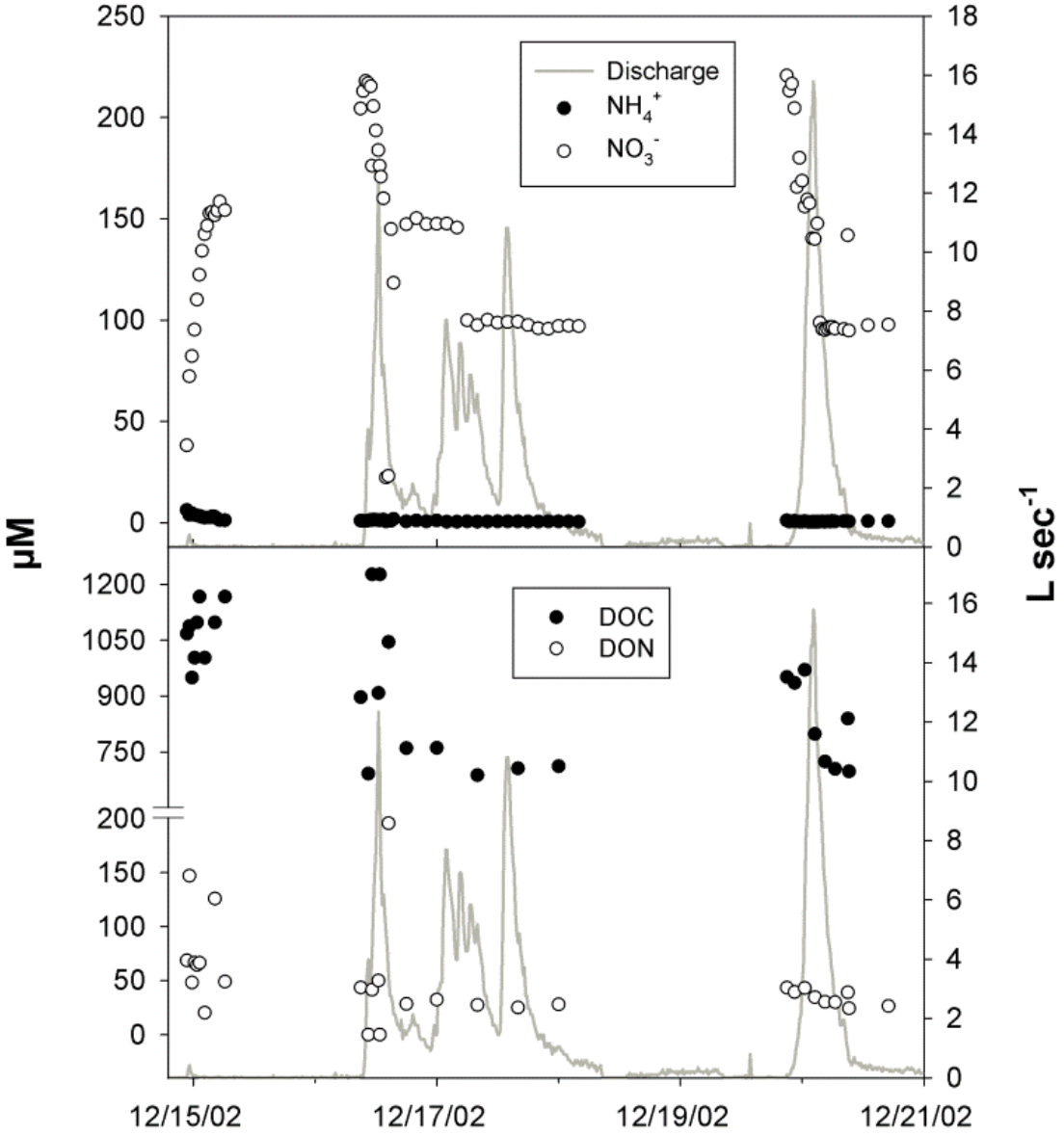

Fig. 3.2. Streamwater NO_3^--N, NH_4^+-N, DOC, DON concentrations and discharge during an early wet season rainfall event recorded on December 15-21, 2002.

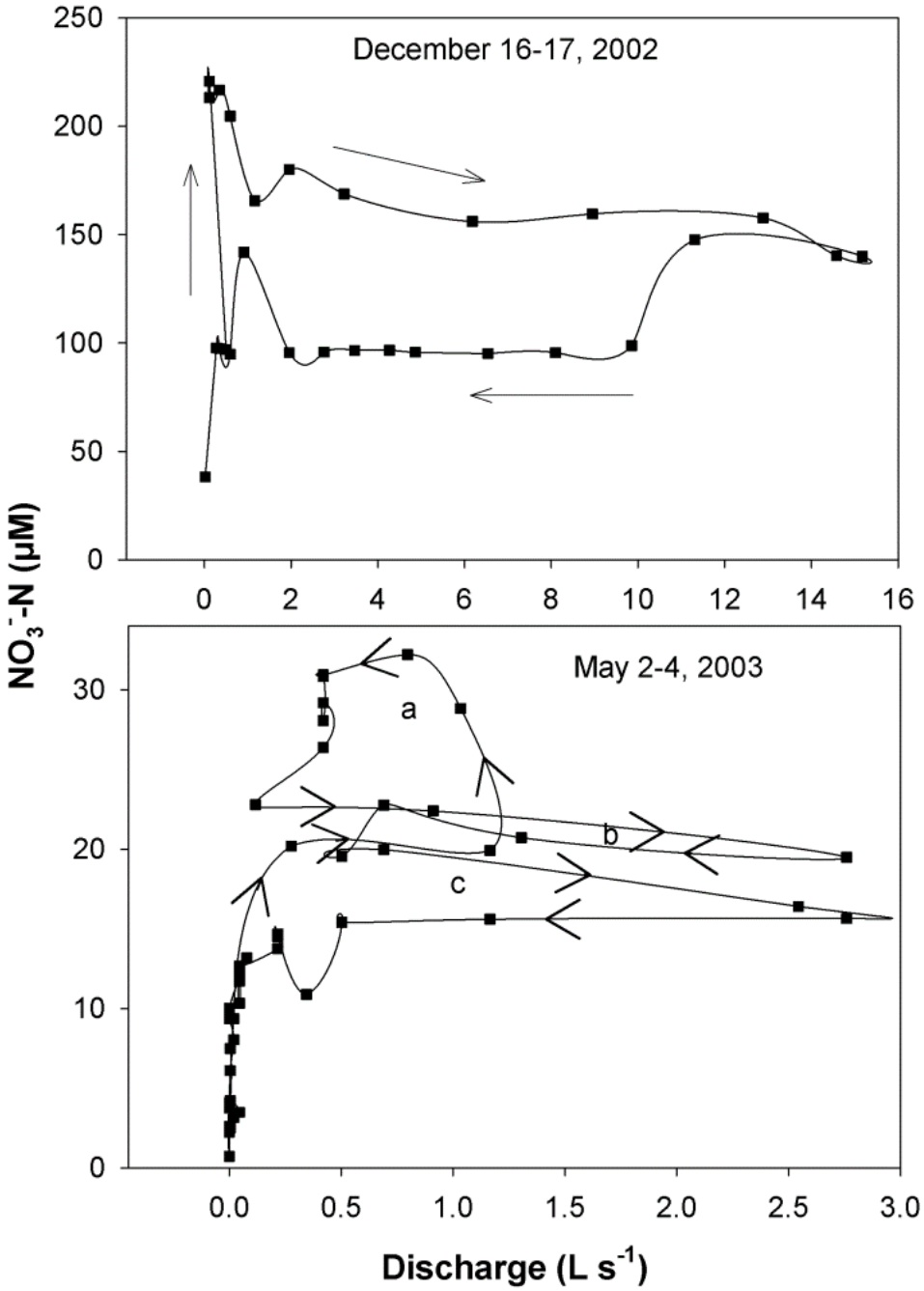

Fig. 3.3. Relationship between streamwater NO_3^--N concentrations and discharge and the formation of clockwise and counterclockwise hysteresis loops.

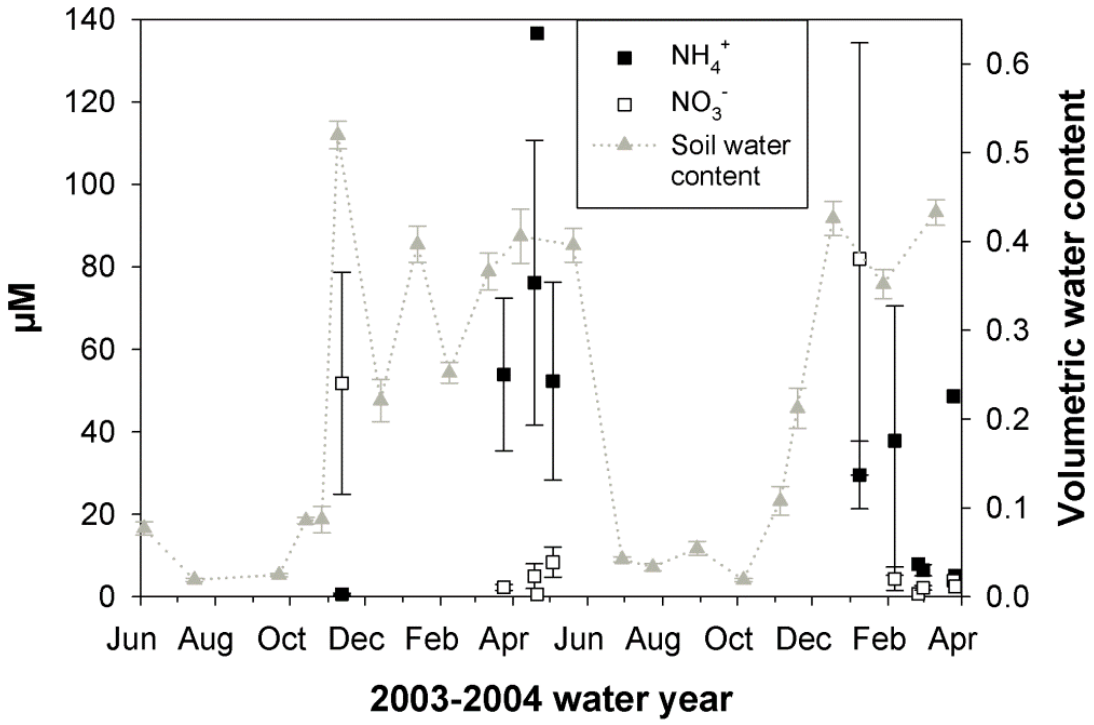

Fig. 3.4. Average soil solution NO_3^--N and NH_4^+-N concentrations extracted from soil lysimeters (30 cm depth) during water years 2003-2004. Error bars represent standard errors.

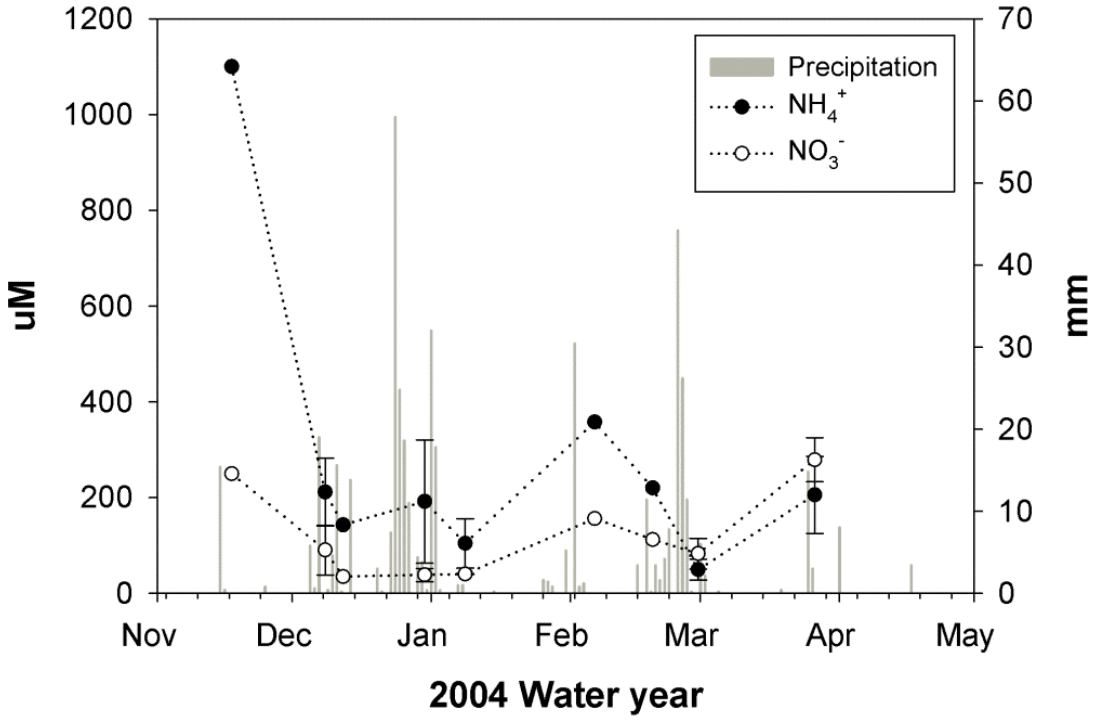

Fig. 3.5. Average NO_3^--N and NH_4^+-N concentrations in surface water runoff collectors during the 2004 water year. Error bars represent standard errors.

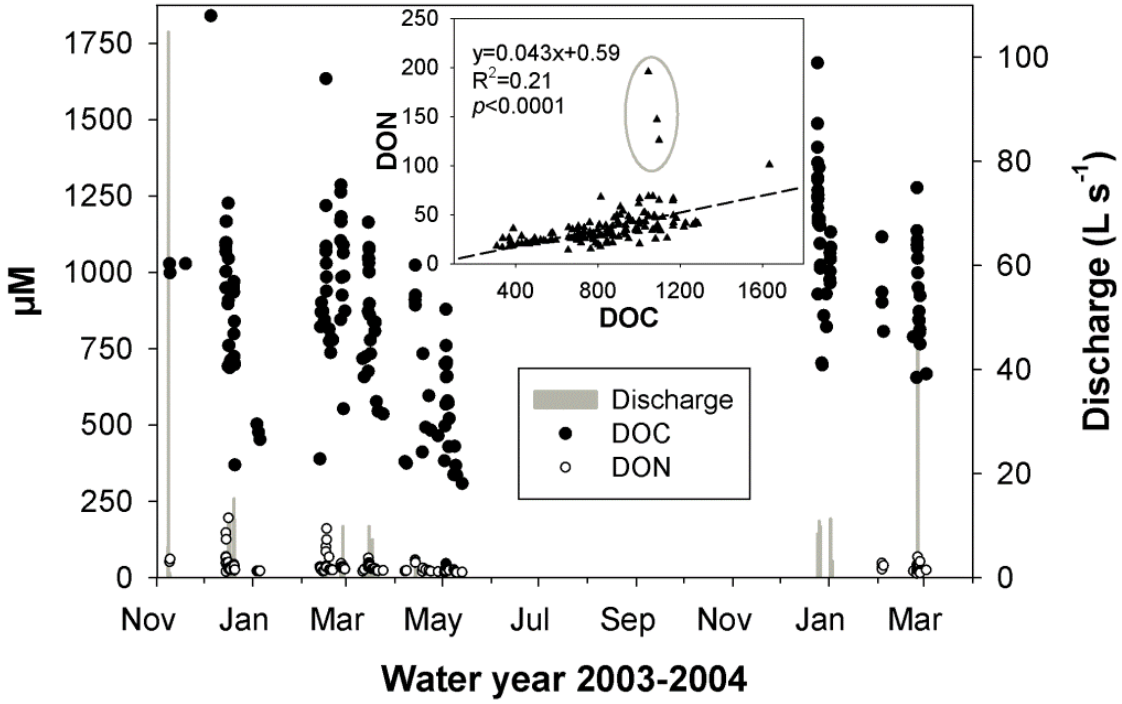

Fig. 3.6. Streamwater DOC and DON concentrations and discharge during water years 2003-2004. Inset: relationship of DON as a function of DOC for water years 2003-2004. The gray oval encloses samples collected during the dry-wet seasonal transition following soil rewetting.

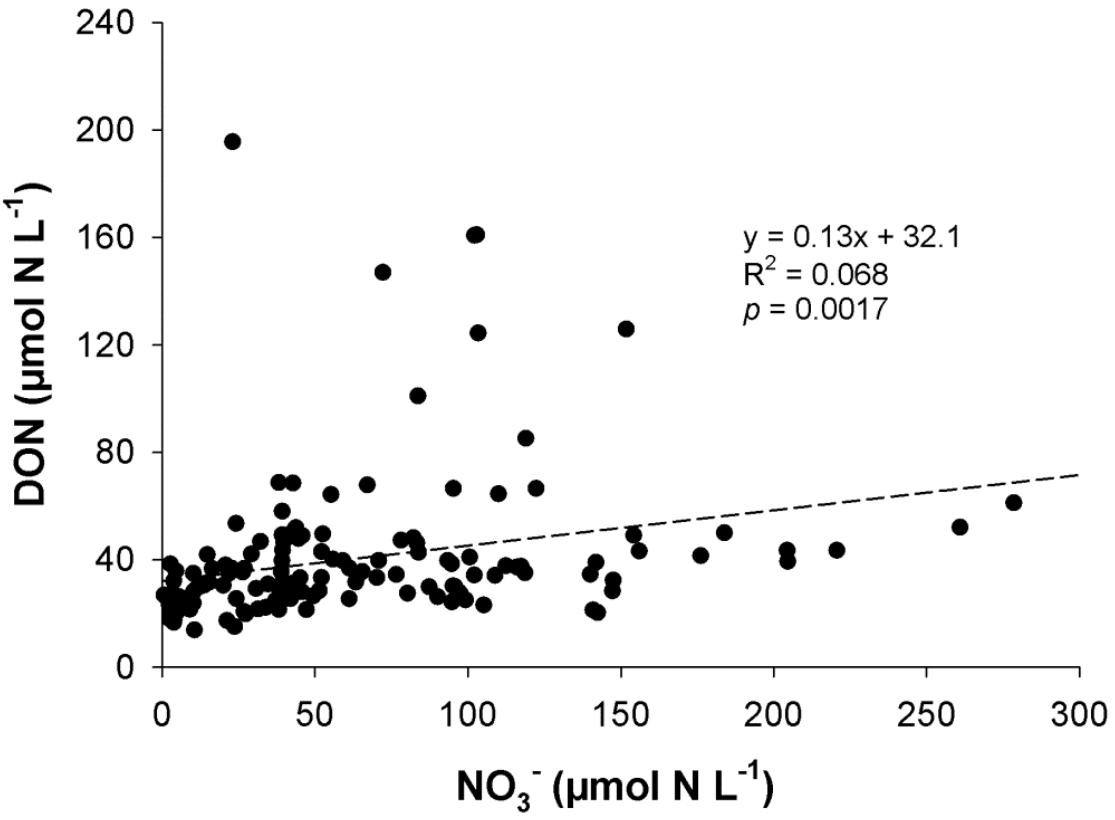

Fig. 3.7. Relationship between streamwater DON and NO_3^--N concentrations for water years 2003-2004.

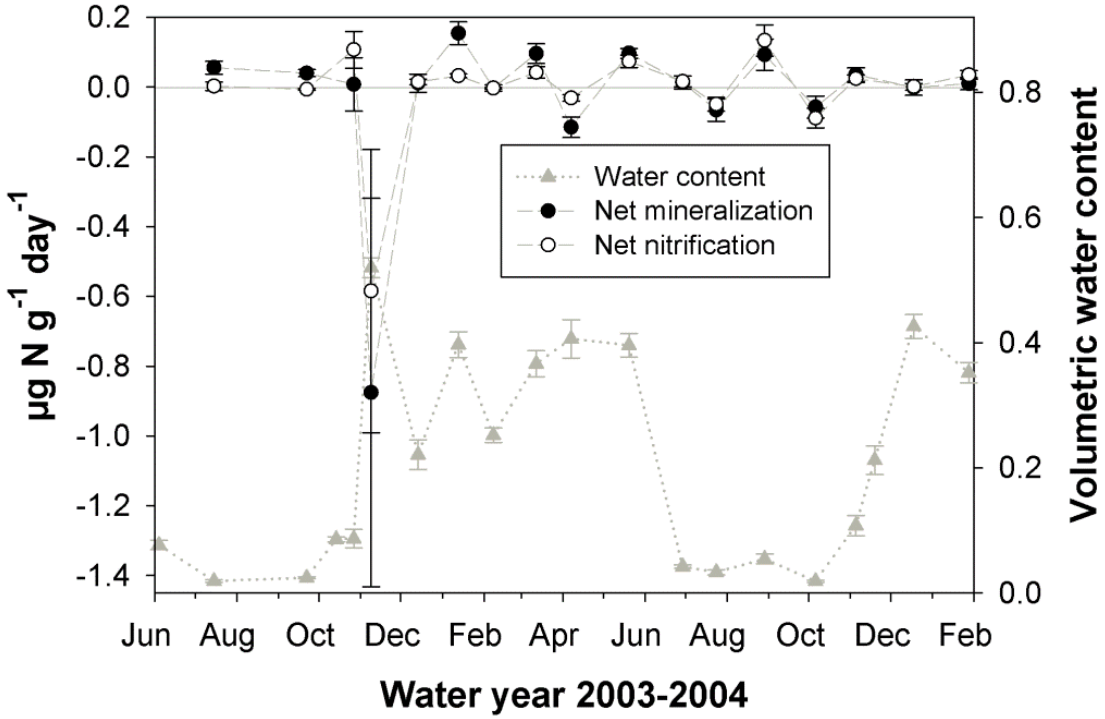

Fig. 3.8. Average net N mineralization (NO_3^--N + NH_4^+-N) and nitrification (NO_3^--N) for 3-4 week incubations and volumetric water content in soil cores collected during water years 2003-2004. Error bars represent standard errors.

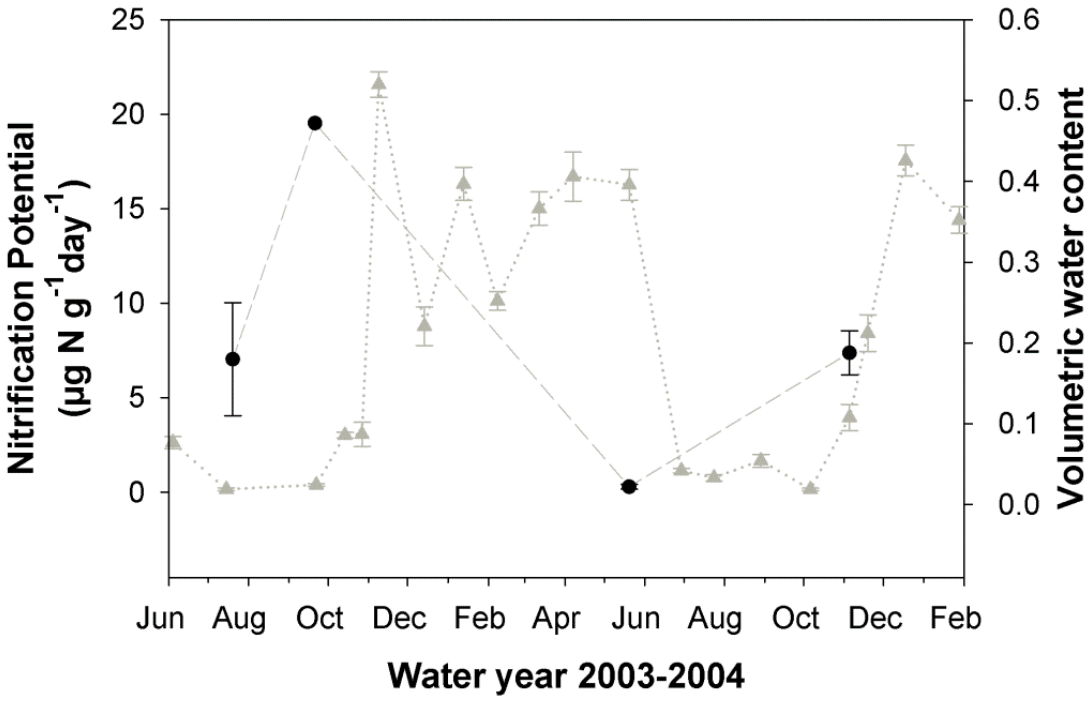

Fig. 3.9. Average nitrification potentials and volumetric water content from soil cores collected during water years 2003-2004. Error bars represent standard errors.

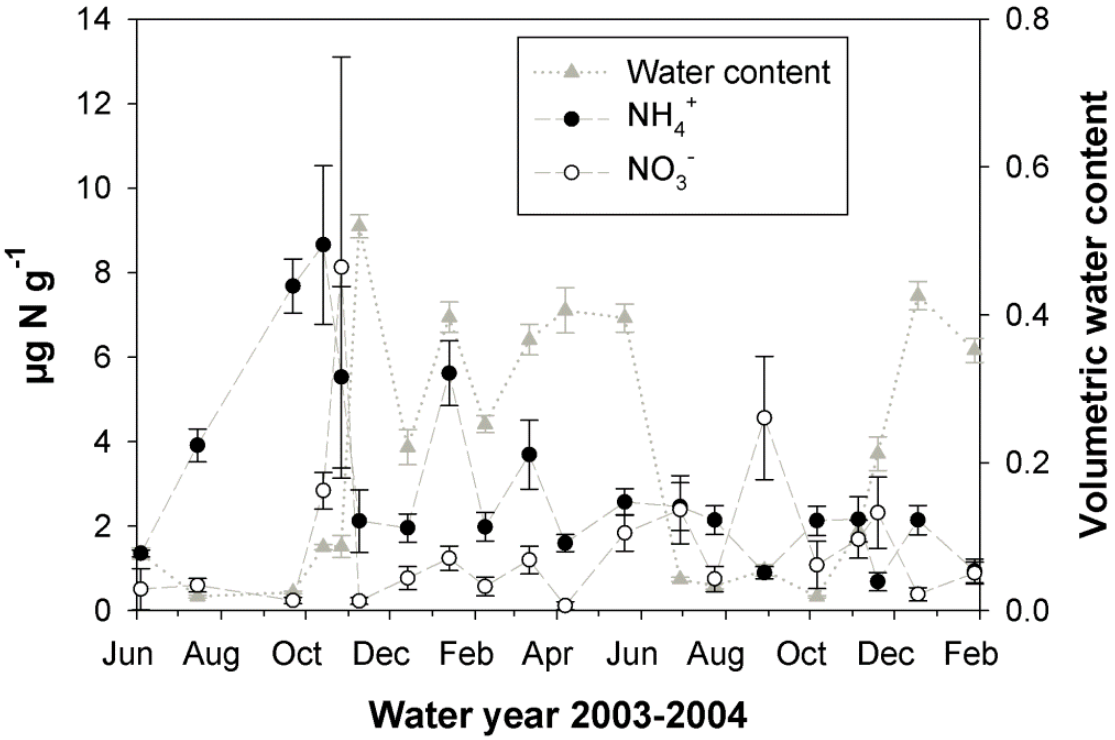

Fig. 3.10. Average soil NO_3^--N and NH_4^+-N concentrations and volumetric water content from soil cores collected during water years 2003-2004. Error bars represent standard errors.

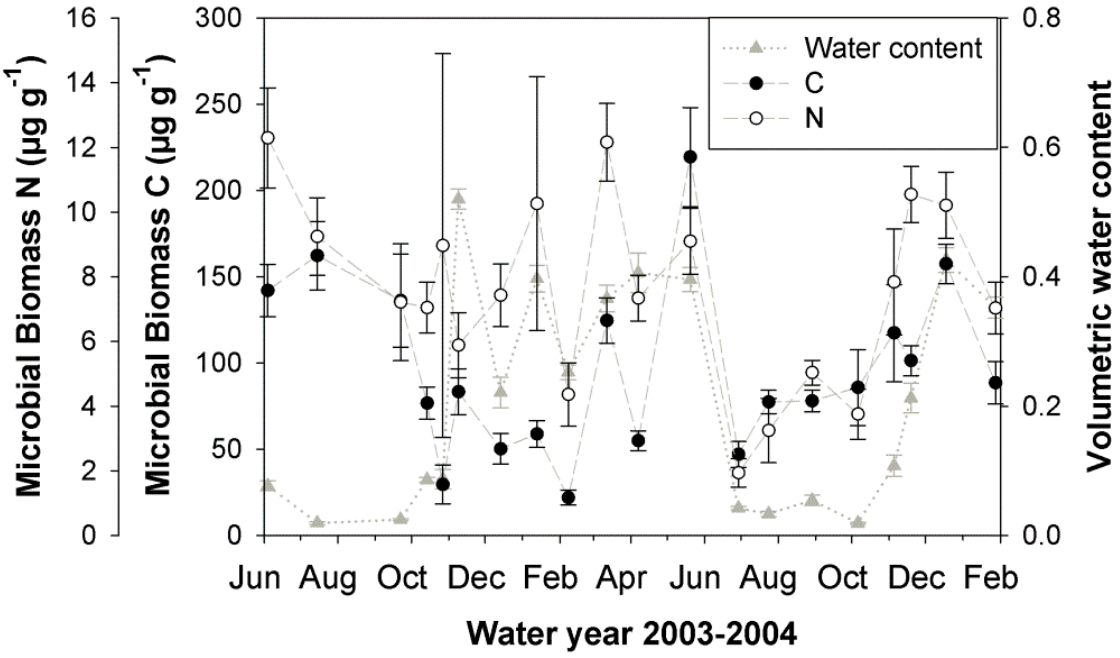

Fig. 3.11. Average microbial biomass C and N and volumetric water content from soil cores collected during water years 2003-2004. Error bars represent standard errors.

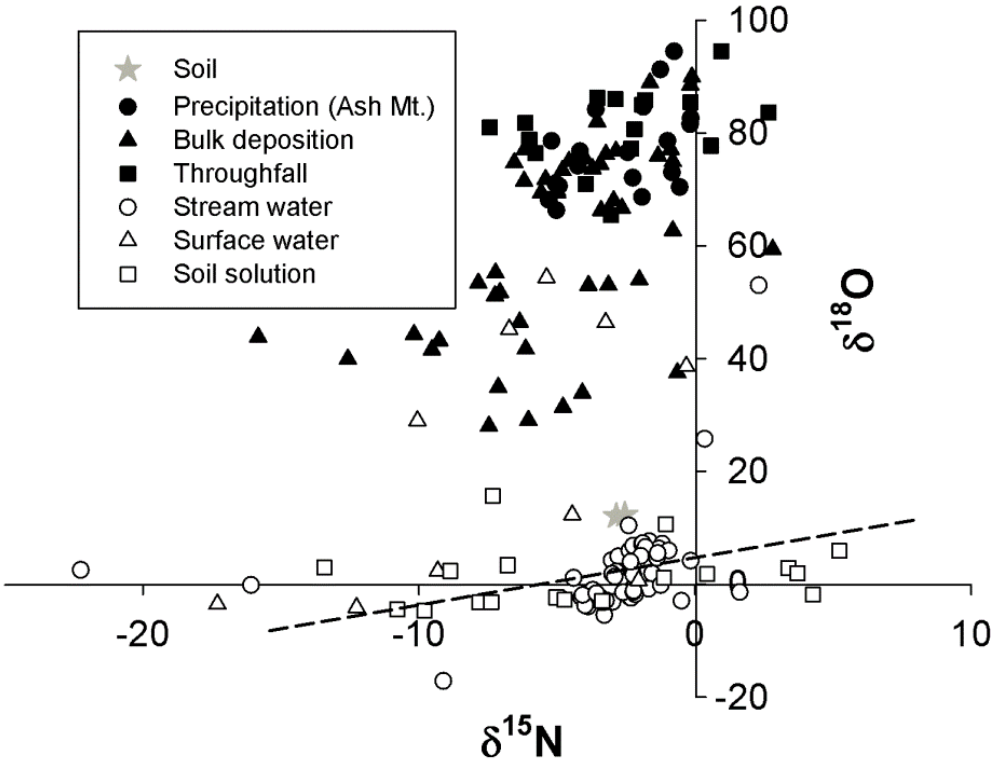

Fig. 3.12. $\delta^{15}N$ and $\delta^{18}O$ of NO_3^- from soils, precipitation, atmospheric bulk deposition, throughfall, streamwater, surface runoff water, and soil solution during water years 2003-2004. The dashed line represents the best fit line using linear regression for streamwater NO_3^- ($y = 0.84x + 4.6$; $R^2 = 0.11$; $p = 0.0063$).

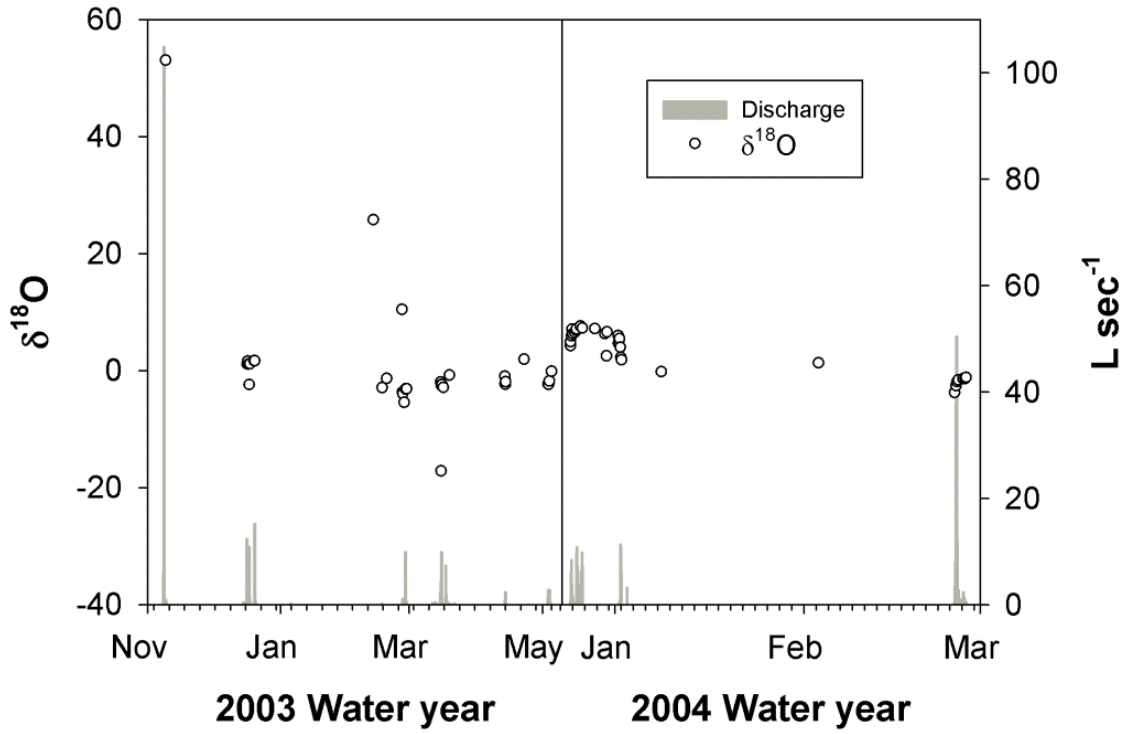

Fig. 3.13. Streamwater NO_3^--N-$\delta^{18}O$ and discharge during the wet season of water year 2003 (left panel) and 2004 (right panel).

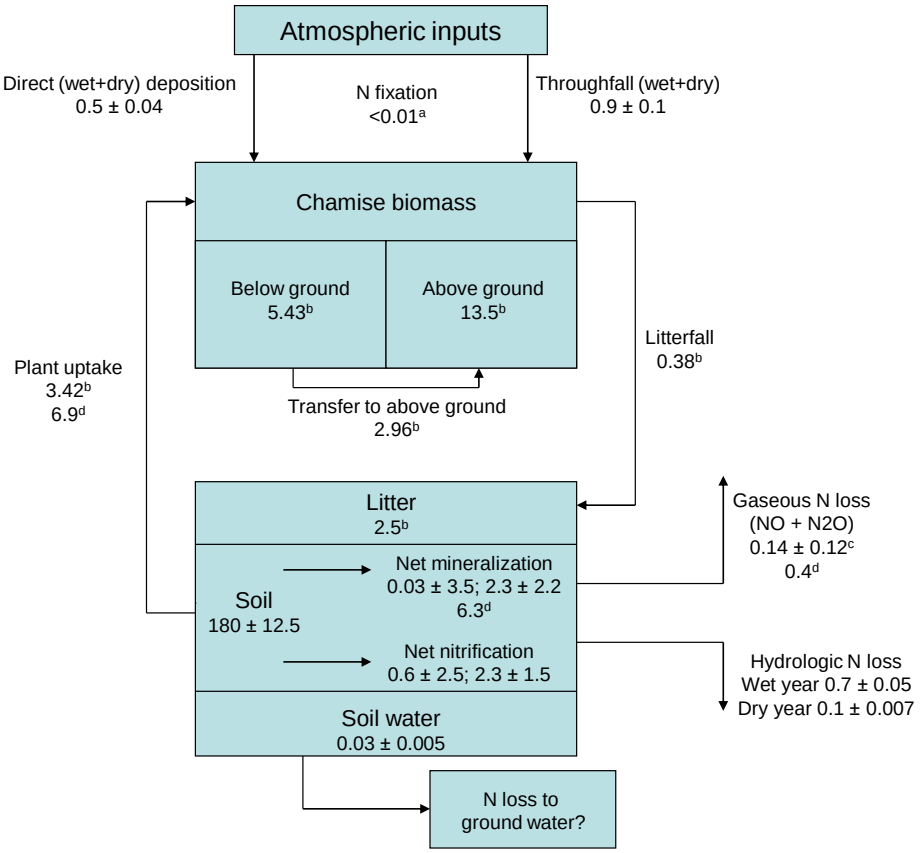

Fig. 3.14. Watershed N budget (average ± standard error; g N m^{-2}) for chaparral ecosystems as calculated from this study, [a]Kummerow et al. (1978), [b]Mooney and Rundel (1979), [c]Chapter 2, and [d]Li et al. (2006).

4. PHOSPHORUS CONCENTRATIONS IN HIGH-ELEVATION SOILS OF THE SIERRA NEVADA, CALIFORNIA: IMPLICATIONS FOR TRANSFER OF P TO HIGH-ELEVATION LAKES

Abstract

High-elevation lakes in the Sierra Nevada are experiencing changing nutrient loading with concomitant shifts between P to N limitation of phytoplankton growth. Because N inputs have remained relatively constant, increases in P supply are presumably driving changes. Since temperature, runoff patterns, and the timing of snowmelt influence N biogeochemistry in high-elevation ecosystems, I hypothesize that these processes, and atmospheric P deposition, regulate P transport from soils to surface waters. I analyzed soils in the Emerald Lake watershed to estimate the contribution of atmospheric processes to soil P pools and to understand how P varied seasonally. Approximately 69 % of the total mass of P found in soil has been atmospherically deposited over the past 10,000 years. Total P averaged 692 µg P g^{-1} in the top 10 cm of soil (O and A horizons) and 547 µg P g^{-1} in the 10-60 cm depth (B and C horizons), of which 70% in A horizons and 60% in B horizons was freely exchangeable or associated with Fe and Al. Approximately 27 % of the total P is efficiently transferred between organic and inorganic pools from winter to spring to summer, in which on average inorganic P pools decrease by 232 µg P g^{-1} but organic P pools increase by 242 µg P g^{-1}. Microbial biomass P was highest during winter (369 µg P g^{-1}) and decreased six-fold over time to a minimum in the fall. Because climate change scenarios predict earlier

snowmelt and increased rainfall, the loss of snowpack insulating properties and hydrologic flushing may synergistically act to enhance the transport of P from soils to aquatic environments.

Introduction

Phosphorus is an essential nutrient in biological processes and is a reactant in the synthesis of DNA, RNA, and ATP (Schlesinger, 1997). However, P is typically found in short supply relative to ecosystem demand as P forms stable associations with soil minerals and is tightly biocycled within ecosystems minimizing losses (Smeck, 1973; Walker and Syers, 1976; Yanai, 1992). Thus, increased P supply to ecosystems commonly enhances net primary productivity (Schindler, 1977), but can also lead to negative effects when available in excess (Caraco, 1993). In aquatic environments, increases in P availability are of concern since P can cause the eutrophication of surface waters and lead to reductions in dissolved O_2 and changes in trophic conditions (Correll, 1998; Edmondson et al., 1956).

In high-elevation lakes of the Sierra Nevada, California, increases in P supply over the past 30 years have resulted in mild eutrophication events and increased incidence of N limitation of phytoplankton productivity (Sickman and Melack, 1998; Sickman et al., 2003b). While the source of P remains undetermined, since soil temperature, depth, and duration of the snowpack, and timing and magnitude of snowmelt have been shown to control the release of nitrate from high elevation soils (Brooks et al., 1998; Sickman et al., 2003a) I hypothesize that these same mechanisms regulate P transport to high-elevation lakes. Thus, climate-driven changes in soil and snowpack conditions, therefore, may underlie the observed patterns of P supply to Sierra Nevada lakes. However, little is known about the P content and biogeochemistry of high-elevation Sierran soils or how soil P pools respond to interannual climate variability. In

particular, information on the size and distribution of the soil P pool and how its availability changes seasonally is lacking. Because catchment hydrology can alter soil physicochemical conditions, P can be alternatively sequestered or mobilized from redox-sensitive pools (Miller et al., 2001), potentially controlling the rate of P-loading to high-elevation lakes.

Although soils may have a high P content, the lability of P (i.e., plant or microbial available P) is strongly influenced by pedogenic processes (Parton et al., 2005; Walker and Syers, 1976). In young unweathered soils, the majority of P is typically associated with stable primary calcium phosphate minerals, which are unlikely to be heavily influenced, over short timescales (seasons), by changes in soil physicochemical conditions (Walker and Syers, 1976). However, as soils age, geochemical weathering processes affect mineral surfaces releasing P to the soil solution where it can be taken up by plants, transferred to surface waters, sorbed to secondary minerals, or become occluded in soil aggregates by agglomeration processes (Smeck, 1985). Because of the high sorption capacity of Fe- and Al-oxides, most of the P weathered from primary minerals is bound to secondary minerals (e.g., calcite or Fe and Al oxyhydroxides), which can be sensitive to changes in soil redox or pH (Miller et al., 2001). Thus, changes in physicochemical soil conditions during seasonal transitions (summer to fall, spring to summer), can potentially influence the lability of P, from the dissolution of secondary minerals within relatively short timescales, facilitating P transport from terrestrial to aquatic ecosystems (Kana and Kopacek, 2006).

Soils in high-elevation catchments of the Sierra Nevada are relatively young (ca. 10,000 years old). Because weathering processes control P release from soil parent material (Smeck, 1973), the lability of soil P is presumably low, and likely associated with primary minerals in stable pools (Cross and Schlesinger, 1995). However, atmospheric P inputs can be important to P budgets (Chadwick et al., 1999; Vicars et al., 2010), and due to the acidity of alpine Sierran soils (Lund et al., 1987), enhanced weathering processes could promote the formation of secondary minerals which, over relatively short time scales, can be sensitive to changes in soil physicochemical conditions (Walker and Syers, 1976). Thus, atmospheric P deposition, weathering of P-bearing primary minerals, and sorption onto secondary soil minerals can potentially increase the lability of P, facilitating the transport of P from soils to surface waters during favorable hydrologic conditions.

Although soil weathering processes can increase the lability of P, formation of secondary minerals can also favor the stabilization of P on oxide surfaces (Walker and Syers, 1976). In studies of P dynamics in lake sediments, Kopacek et al. (2005), found that P was effectively bound by Al when the ratio of $Al:Fe_{(H2O+NaHCO3+NaOH)}$ was >3 or the ratio of $Al_{NaOH}:P_{(H2O+NaHCO3)}$ >25. Unlike Fe, Al is insensitive to reducing environments, and can irreversibly adsorb P liberated during the reduction of Fe-phosphates (Kopacek et al., 2005). More recently, research on P dynamics in acidic forest soils, has demonstrated that Al can play an important role in the stabilization of P (SanClements et al., 2009, 2010). Because soils in the EML catchment are acidic (Lund et al., 1987), and weathering processes in alpine ecosystems of the Sierra Nevada favor the formation Al-

dominated clay minerals (Dahlgren et al., 1997), P may be effectively stabilized in secondary minerals reducing leaching and potential mobilization to high-elevation lakes.

Our study was designed to address fundamental questions regarding P cycling and lability in high-elevation soils of the Sierra Nevada. Specifically, I sought to answer the following questions: i) What is the contribution of atmospheric processes to alpine soils, what are the major pools of P, and how do these pools change seasonally? ii) How important are microbial processes in regulating P availability in high-elevation soils? iii) What is the P sorption capacity of high-elevation Sierran soils and has it been exhausted? And iv) What mechanisms control the stabilization and transport of P from soils to aquatic environments during seasonal transitions? To answer these questions I employed a sequential fractionation procedure to identify dominant soil P pools and used it to monitor seasonal changes in these pools and their responses to seasonal transition. I also used a chloroform fumigation technique to monitor seasonal changes in soil microbial biomass P and used a P sorption experiment, as well as measurements of soil Ca, Fe, and Al pools, to understand the P retention capacity of EML watershed soils. Finally, I use a P mass balance extending over the past 10,000 years to estimate the relative contribution of atmospheric P deposition and bedrock weathering to P accumulation in soils. I hypothesized that due to the oligotrophic nature of high-elevation lakes, soil P concentrations in Sierran catchments are low, and that P is predominantly found in unweathered primary mineral pools or secondary Al-dominated clay minerals.

Materials and methods

Site descriptions

Our study was conducted in the Emerald Lake (EML) watershed (UTM Zone 11, 350054 m E, 4051454 m N), located along the western slope of the Sierra Nevada within Sequoia and Kings Canyon National Park. The watershed is a glacial cirque of approximately 120 ha, and varies in elevation from 2,813 to 3,493 m a.s.l. Its geology is dominated by fine and medium-grained porphyritic granodiorite and coarse-grained granite. Soils cover approximately 20% of the catchment, are poorly developed, acidic (pH≈ 4.5-5.5), weakly buffered, well to somewhat excessively drained, with a bulk density of 1.0 to 1.2, a C:N ratio of about 17 (Huntington and Akeson, 1987), and are representative of soils throughout the Sierra Nevada (Melack et al., 1998). The most important secondary soil minerals include vermiculite, kaolinite, and gibbsite (Brown et al., 1990), with smectite, chlorite, mica, and hydroxyinterlayered minerals also present (Appendix A). The climate is typical of Mediterranean regions with dry summers and wet winters, a mean annual temperature of 4.6°C (Leydecker A., unpublished data), and average annual precipitation of 1,510 mm, of which approximately 90% falls as snow during the winter (Sickman et al., 2001). Vegetation is sparse and characterized by Lodgepole Pine (*Pinus contorta*), Western White Pine (*Pinus monticola*), and low woody shrubs such as Sierra willow (*Salix orestera*) and grasses (*Calamagrostis canadensis*).

Soil sampling

To quantify the major soil P pools in the EML catchment, in summer 2008, I sampled six dominant soils that represented five soil subgroups as classified and mapped by Huntington and Akeson (1987): Typic Cryofluvents (TCF), Typic Cryorthods (TC), Lithic Cryumbrepts (LC), Rock outcrop-Lithic Cryumbrepts (RLC), Entic Cryumbrepts (EC), and Cryaquepts (C). Based on the soil survey, TCF are not widely abundant in the catchment, but are found along the shore of EML and support dense communities of willow and grasses. They are deep, well-drained, with a fine sandy loam surface underlain by fine gravelly sand and subject to seasonal flooding. TC soils are well to somewhat excessively drained that form in sandy colluviums and on ridge slopes under white pine. The solum is coarse to moderately coarse and acidic. LC soils are representative of meadow areas in the EML basin, which are considered hotspots for biogeochemical cycling (Miller et al., 2009). They are dark colored, well to somewhat excessively drained, coarse to moderately coarse textured, and formed on granitic colluvium. RLC soils are shallower than LC and found on south-facing slopes. They are grayish brown to brown and gravelly to stony. EC soils are found in exposed areas that drain directly into EML, are shallow, grayish brown to brown, well to excessively drained, gravely to stony, coarse-textured, and support mainly forbs and grasses. Lastly, C soils are formed in granitic alluvium-colluvium accumulated in rock basins, are poorly drained, dark colored with coarse to medium textures, strongly acidic and high in organic matter.

At each of the soil sampling sites, I dug shallow pits by hand with a small trowel. Samples were obtained from A horizons (ca. top 10 cm) and B horizons (ca. below 10 cm to a depth of 60 cm) in duplicate. At a few sites it was noted that a thin O horizon was collected along with A horizon samples. Similarly, a few of the B horizon samples contained small amounts of C horizon soil. Soil samples were bagged, homogenized, and temporarily stored in coolers filled with blue ice until stored in the laboratory at 4°C. Prior to elemental analysis, stones and gravel along with roots, twigs, and leaves were removed, but the soil was not air-dried and remained fresh, since drying is known to affect soil P measurements (Blackwell et al., 2009). However, subsamples from each soil were oven-dried at 105°C to estimate gravimetric water content, and express the soil P content from fresh soil samples on an oven-dried basis.

To monitor seasonal changes in soil chemistry, I sampled A and B horizons in the three most common soil subgroups found at EML (EC, LC, and TCF) on a seasonal basis. Samples were collected during peak snow accumulation (April) representative of winter conditions, spring (June), summer (September) and fall (October) 2010. The 2009-2010 water year at EML was characterized by above normal snowpack, which lasted until early July 2010 delaying the onset of summer conditions. At each of the three sampled soils (EC, LC, and TCF), and at each sampling time (winter, spring summer, and fall), I randomly selected three sites in which I dug a small pit and collected a sample from the A horizon and B horizon (i.e., n=6 for A horizons and n=6 for B horizons at each sampling time). However, during winter 2010, only one pit was dug at each of the three sampled soil subgroups (i.e., n=3 for A horizons and n=3 for B horizons).

Elemental and chemical analyses

Fresh soil subsamples (n=2; 0.5 g equivalent dry weight) from samples collected at the two pits dug at each of the six soil subgroups in summer 2008 and the seasonally sampled EC, LC, and TCF soils were used for elemental and chemical analysis. Soil pH was determined in DI water (Hendershot et al., 2008) and soil C and N content were measured using an elemental analyzer (Thermo Flash EA 1112). Soil P content was determined using a slightly modified version of a sequential extraction method of Tiessen & Moir (2008), in which a microwave digestion with HNO_3 and HCl replaced a digestion with $H2SO_4$ and H_2O_2 as the final step in the procedure. Extracted soil P fractions included: 1) extract with resin strip in water for 16 h, at 25°C, considered freely exchangeable inorganic P fraction (Resin–P_i); 2) 0.5 M $NaHCO_3$ extract for 16 h, at 25°C, considered plant available inorganic P ($NaHCO_3$ –P_i) and organic matter P ($NaHCO_3$ –P_o) bound to reducible metal hydroxides (primarily Fe but may include Al) that is easily mineralizable; 3) 0.1 M NaOH extract for 16 h, at 25°C, predominantly inorganic P (NaOH–P_i) associated with amorphous and some crystalline Al oxides, but that may contain Fe-associated P not extracted in the previous step, as well as organic P (NaOH–P_o) associated with humic compounds and polyphosphates that are thought to store P in long-term pools (Tiessen et al., 1983); 4) 1 M HCl extract for 16 h, at 25°C, considered Ca-associated inorganic P (1MHCl–P_i) and not readily available in short timescales; 5) concentrated HCl extract for 1 h, at 80°C, representing inorganic (conc. HCl–P_i) and organic (conc. HCl–P_o) P bound to very stable residual pools; 6) microwave extract with concentrated HNO_3 and HCl (3:1) representing highly

recalcitrant inorganic P (Residual-P). For the seasonally sampled EC, LC, and TCF soils the sequential extractions did not go beyond the NaOH step, since subsequent extractions represent increasingly recalcitrant soil P pools that are not likely to significantly vary with changes in seasonality and associated changes in soil physicochemical conditions (Cross and Schlesinger, 1995). All extracts were analyzed for P colorimetrically (Murphy and Riley, 1962). Seasonal changes in soil C:N:P ratios were calculated using the sum (P_{sum}) of Resin–P_i, $NaHCO_3$–P_T, and NaOH–P_T ($P_T = P_i + P_o$) as the value for P, since total P was not measured directly during seasonal measurements.

Microbial biomass P

Microbial biomass P was measured in A and B horizons in seasonally collected EC, LC, and TCF collected using a chloroform ($CHCl_3$) fumigation method (Voroney et al., 2008). Fresh soil subsamples (10 g equivalent dry weight) from each soil and horizon were fumigated with $CHCl_3$ for 24 h in an evacuated desiccator containing water and soda-lime, and then extracted with 0.5 M $NaHCO_3$ at pH 8.5. Following extraction, the mixtures were shaken at 20°C for 30 min on an orbital shaker and filtered into acid-washed plastic bottles. In order to correct for the sorption of released P onto soil colloids following fumigation, I determined the recovery efficiency for each soil by spiking with a known quantity of P (250 µg P). Microbial biomass P was calculated without using a correction for extraction efficiency, and thus represents $CHCl_3$-labile P pools rather than total microbial biomass. The P concentration in all extracts was determined colorimetrically (Murphy and Riley, 1962).

Ca, Al, and Fe soil pools

Calcium, Fe, and Al concentrations were measured by inductive coupled plasma spectroscopy atomic emission spectroscopy (ICP-AES) in duplicate subsamples from the $NaHCO_3$, NaOH, and acid microwave digestion extracts generated from A and B horizons from the seasonally sampled EC, LC, and TCF soils. I summed Fe and Al concentrations and calculated Al:Fe ratios in the $NaHCO_3$ and NaOH extracts to estimate the likelihood of P transport from soils to aquatic environments (Kopacek et al., 2005; SanClements et al., 2009).

Soil P sorption capacity

The P sorption capacity of EML catchment soils was determined in duplicate samples collected in fall 2010 from A horizons and B horizons in EC, LC, and TCF using methods described by Sharpley et al. (2008). Equilibrating P solutions corresponding to 0, 50, 100, 250, 500, 750, 1000, and 1500 µg P g soil^{-1} were added to fresh soil samples (1 g; equivalent dry weight), shaken, allowed to equilibrate for 24 h, centrifuged (3,000 g) for 10 minutes, and filtered through Whatman No. 42 filter paper (2.5 µm). All extracts were analyzed for P colorimetrically (Murphy and Riley, 1962).

To calculate the P adsorption maximum (S_{max}), I used the linear form of the Langmuir equilibrium-based adsorption model:

$$\frac{C}{q} = \frac{1}{kb} + \frac{C}{b} \qquad \text{Equation 4.1}$$

where C is the equilibrium or final adsorptive concentration after equilibration with soil, q is the mass adsorbed, k is a constant related to the binding strength, and b is the maximum amount of adsorptive that can be adsorbed assuming monolayer coverage. The

adsorption maximum was calculated from the slope (1/*b*) resulting from the plot between *C/q* vs. *C*.

To gain insight into which soil pools were most retentive of P additions, I sequentially extracted P-amended (1500 µg P g soil^{-1}) soils from the previously conducted adsorption procedure and compared their P concentrations with P concentrations from reference soils. Phosphorus concentrations in reference soils were measured in duplicate for A and B horizons from fresh subsamples of EC, LC, and TCF soils sampled in fall and used for the P adsorption procedure. Changes in $NaHCO_3$–$P_{i,o}$, NaOH–$P_{i,o}$, and 1 M HCl–P_i in the P-amended and unamended soils were used to identify which P pools participate in P retention processes over short time scales. Paired t-tests were used to distinguish statistically significant differences between P amended and reference soils (α=0.05).

Results

General soil characteristics

Soil pH, texture, CEC, abundance in the watershed (area), mean depth, and bulk density for the major soil types are contained in Table 4.1. In general, EML soils are shallow, acidic, of sandy texture, with an approximate CEC of 11 mEq 100g^{-1}.

Major element pools in watershed soils

From the measurements of soil P content, and areal soil mapping in the EML catchment (Brown et al., 1990), I estimated a total P mass in soils of 78,600 kg, of which approximately 1% is considered freely exchangeable, 9% plant available or associated

with reducible hydroxides, 58% sorbed to Al oxides and Fe not extracted in the $NaHCO_3$ step, 24% associated with Ca, and 8% considered occluded in recalcitrant soil pools. Because I did not sample Typic Cryorthents (TCT), due to safety precautions (very steep slopes), described as poorly developed soils located on very steep slopes, I use a total P content of 178 μg P g^{-1}, a mean depth of 0.25 m, and an area of 4.5 ha in the calculations (Brown et al., 1990). However, Brown et al. (1990) measured total P only, and did not sequentially extract soils as performed in this study, limiting the calculation of P_i and P_o pools for each extractant in TCT. Because an important aspect of this research is to quantify the total mass of P considered labile and recalcitrant in the watershed, I use the proportion of P extracted:total P for LC as a best approximation for TCT. Of the soils I sampled, LC are most similar to TCT based on their development, vegetative cover, and location within the watershed, and thus are used in this calculation to best represent the distribution of P in labile and recalcitrant P pools.

The average total soil P content in RLC, TCF, TC, C, LC, and EC soil subgroups is 867 μg g^{-1} in A horizons and 597 μg g^{-1} in B horizons (Fig. 4.1). The NaOH-extractable pool contained the highest average P concentration (534 μg g^{-1} in A horizons and 362 μg g^{-1} in B horizons) followed by the 1 M HCl pool (124 μg g^{-1} in A horizons and 119 μg g^{-1} in B horizons), $NaHCO_3$ extractable pool (115 μg g^{-1} in A horizons and 50 μg g^{-1} in B horizons), residual pool (20 μg g^{-1} in A horizons and 14 μg g^{-1} in B horizons), and freely exchangeable pool (7μg g^{-1} in A horizons and 3 μg g^{-1} in B horizons) pool (Fig. 4.1, Table 4.2). The highest total P concentrations were found in EC soils, followed by LC, C, TCF, RLC, and TC soils (Table 4.2). Although P_i and P_o concentrations in

extracts varied across soil types, differences in total P concentrations among the soils sampled were attributable to differences in the NaOH–P_o-extractable pool (Table 4.1).

On average, 14% of the total P in A horizons was labile or considered plant available (Resin–P_i + $NaHCO_3$–P_T), 62% was bound to Al and residual Fe not extracted in the $NaHCO_3$ step (NaOH–P_T), and 24% was considered refractory (1 M HCl–P_i + conc. HCl–P_T + Residual–P). For B horizons, 9% of the total P was labile, 61% was bound to Al and Fe, and 30% was refractory. Biologically controlled soil P pools, defined as the $NaHCO_3$–P_o + NaOH–P_o + conc. HCl–P_o (Cross and Schlesinger, 1995),represented 62% (540 µg g^{-1}) of the total P in A horizons and 53% (314 µg g^{-1}) in B horizons. Soil P pools previously described to be controlled by geochemical processes, Resin–P_i + $NaHCO_3$–P_i + NaOH–P_i + 1 M HCl–P_i + conc. HCl–P_i + Residual–P (Cross and Schlesinger, 1995), accounted for 38% (327 µg g^{-1}) of the total P in A horizons and 48% (283 µg g^{-1}) in B horizons. In EML soils, 66% of the total labile forms of P in A horizons may be readily mineralized through biological processes ($NaHCO_3$ –P_o/Resin–P_i + $NaHCO_3$ –P_i + $NaHCO_3$–P_o)(Cross and Schlesinger, 1995) and 67 % in B horizons.

On average, the C content (average ± Std. Error) of EML soils was 91,180 ± 24,763 µg C g^{-1} in A horizons and 30,708 ± 6,654 µg C g^{-1} in B horizons. The N content was 4,888 ± 1,017 µg N g^{-1} in A horizons and 2,073 ± 521 µg N g^{-1} in B horizons and the P content was 908 ± 100 µg P g^{-1} in A horizons and 542 ± 104 µg P g^{-1} in B horizons. From these values I estimated an average C:N:P ratio of 100:5:1 in A horizons and 57:4:1 in B horizons.

Total Fe concentrations (average ± Std Error) in LC, EC and TCF were highest among Al and Ca, reaching 8588 ± 758 µg g^{-1} in A horizons and 10729 ± 602 µg g^{-1} in B horizons (Fig. 4.3). Total Al concentrations reached 7860 ± 299 µg g^{-1} in A horizons and 9706 ± 540 µg g^{-1} in B horizons, and total Ca concentrations were lowest, averaging 959 ± 174 µg g^{-1} in A horizons and 841 ± 94µg g^{-1} in B horizons (Fig. 4.3). Although total Fe concentrations are highest, over 92% is not extracted by $NaHCO_3$ or NaOH, indicating that Fe is mostly found in recalcitrant soil P pools, and may not actively participate in the cycling of P. In contrast, the majority of Al was extracted by $NaHCO_3$ and NaOH, suggesting that Al dominates soil exchange sites where P may adsorb (Fig. 4.3); the sum of extractable Al ($NaHCO_3$ + NaOH) is five times that of Fe and 12 times that of Ca in A horizons and six times that of Fe and 13 times that of Ca in B horizons (Fig. 4.3).

The ratio of $Al:Fe_{(NaHCO3 +NaOH)}$ in EML soil was 5.2 in A horizons and 5.9 in B horizons and the ratio of $Al_{NaOH}:P_{NaHCO3}$ was 32.5 in A horizons and 51.6 in B horizons. $Al:Fe_{(NaHCO3+NaOH)}$ ratios >3 and an $Al_{NaOH}:P_{NaHCO3}$ >25 are associated with the inactivation of P by Al (Kopacek et al., 2005), and suggest that EML watershed soils are highly retentive of P.

Seasonal changes in soil P pools, pH, and element ratios

Inorganic soil P concentrations (Resin–P_i, $NaHCO_3$–P_i, and NaOH–P_i) were generally highest in winter, during which a thick snowpack insulated soils, and gradually decreased over the summer and into the fall (Fig. 4.2). However, average Resin–P_i concentrations briefly increased during summer, to 19.8 µg P g^{-1} in A horizons and 14.3 µg P g^{-1} in B horizons, as well as NaOH–P_i during fall (105.8 µg P g^{-1} in A and 110.3 µg

P g^{-1} in B horizons; Fig. 4.2). In the seasonally sampled soils, the NaOH–P_i pool contained the largest amount of P in winter (244.5 µg P g^{-1} in A horizons and 224.5 µg P g^{-1} in B horizons), followed by $NaHCO_3$–P_i (81.1 µg P g^{-1} in A horizons and 51.7µg P g^{-1} in B horizons) and resin–P_i (36.6 µg P g^{-1} in A horizons and 15.6 µg P g^{-1} in B horizons). In fall, the relative pools sizes were identical between A horizons and B horizons, with NaOH–P_i having the largest concentrations, followed by $NaHCO_3$–P_i, and resin–P_i (Fig. 4.2). The effect of seasonality on P_o concentrations was opposite to that observed for P_i, in which P_o concentrations generally increased into the summer (Fig. 4.2). Although soil $NaHCO_3$–P_o remained relatively unchanged in both A and B horizons from the start of measurements in winter through the next year's fall, there was an abrupt increase in P during summer (Fig. 4.2). For NaOH–P_o, there was a positive trend in P concentrations in both A and B horizons from winter towards fall (151.1 µg P g^{-1} in A and 187.4 µg P g^{-1} in B horizons in winter and 235.5 µg P g^{-1} in A and 232.4 µg P g^{-1} in B horizons in fall), with also an abrupt increase in P during summer (439.9 µg P g^{-1} in A and 327.1 µg P g^{-1} in B horizons; Fig. 4.2).

Soil C:N:P_{sum} ratios were highest in winter, during which soils were snow-covered, and gradually decreased over the summer and fall (Table 4.3). Soil C:N:P_{sum} ratios were always higher in A horizons relative to B horizons, mostly due to differences in C and N levels of A and B horizon soils rather than differences in P content. The C and N content of A horizons was about 50% greater than in B horizons and P_{sum} in A horizons was only 16% greater than in B horizons (Table 4.3).

P retention capacity of soils

The average S_{max} for EML soils in A horizons was 967 ± 102 µg P g^{-1} and 1187 ± 84 µg P g^{-1} in B horizons (± std. error; Fig. 4.4). Because P sorption measurements were conducted on resin–P_i, $NaHCO_3$–P_T, and NaOH–P_T extracts, I compared the sum of P concentrations in these pools to the calculated S_{max} to quantify how much additional P can be adsorbed by EML soils. A horizon soils have 368 µg P g^{-1} of unmet adsorption capacity (61% of current concentration) and B horizon soils have 586 µg P g^{-1} of unmet P adsorption capacity (98% of current concentration). The LC soils had the highest S_{max} (1171 µg P g^{-1} in A and 1351 µg P g^{-1} in B horizons), followed by TCF soils (871 in A µg P g^{-1} and 1138 µg P g^{-1} in B horizons) and EC soils (857 µg P g^{-1} in A and 1072 µg P g^{-1} in B horizons).

In the P-amended soils, 19% of the added P was recovered in A horizons and 33% in B horizons. Of the recovered P, the majority was found in the NaOH–P_i pool (65% in A horizons and 66% in B horizons) and the $NaHCO_3$–P_i pool (36% in A horizons and 26% in B horizons); P amendment had a statistically significant effect on both NaOH–P_i and $NaHCO_3$–P_i pools ($p < 0.05$). However, The 1 M HCl–P_i pool remained relatively unchanged and significant differences were not detected between P-amended and unamended soils ($p > 0.61$ for both A and B horizons; Fig. 4.5). For organic P pools, I detected smaller P concentrations in P-amended soils compared to unamended soils, but the differences were not statistically significant ($p > 0.15$ for both A and B horizons; Fig. 4.5). For $NaHCO_3$–P_o, however, P concentrations increased in P-amended soils, and

approximately 24% of the recovered P was found in A and B horizons (p = 0.03 in A horizons and p = 0.02 in B horizons; Fig. 4.5).

Soil microbial biomass P

Soil microbial biomass P for EC, LC, and TCF soils (average ± std. error) was highest in winter (369 ± 90 µg P g^{-1} in A horizons and 179 ± 39 µg P g^{-1} in B horizons) and decreased over the summer reaching a minimum in the fall (58 ± 17 µg P g^{-1} in A horizons and 31 ± 11 µg P g^{-1} in B horizons; Fig. 4.6). The greatest change in microbial biomass P occurred during the winter-spring seasonal transition, during which microbial biomass P declined 58% in A horizons and 76% in B horizons (Fig. 4.6). During all seasons, microbial biomass P was higher in A horizons relative to B horizons (Fig. 4.6), and EC soils generally had the greatest microbial biomass P (up to 443 µg P g^{-1}) followed by TCF soils (up to 475 µg P g^{-1}) and LC soils (up to 189 µg P g^{-1}).

Discussion

Phosphorus content of high-elevation Sierran soils

The primary motivation for this study was to quantify the size and distribution of P in high-elevation soils and evaluate whether soils can contribute to the increases in P supply to Sierra Nevada alpine lakes documented by Sickman et al. (2003b). On average, the EML catchment contains a mass of approximately 78,600 kg of P in soil (Table 4.4); a much greater mass than the 2,000 kg previously estimated using soil N concentrations and N:P ratios (Sickman et al., 2003b). I found that soils of the EML catchment are not P-deficient (Fig. 4.1, Table 4.2) and are rather at the high-end range of P concentrations

found in most soils (50-1,000 µg P g^{-1}) (Cross and Schlesinger, 1995; Harrison, 1987), suggesting that mobilization of only the freely exchangeable P pool, can account for 61 times the annual export of P from the catchment (Table 4.4).

In the EML catchment, atmospheric P inputs can more than balance P outputs (Vicars et al., 2010), suggesting that atmospheric processes can influence P dynamics in high-elevation watersheds, and possibly account for a proportion of the P stored in soils (Table 4.4). It is well known that atmospheric processes can supply P to terrestrial ecosystems (Chadwick et al., 1999; Morales-Baquero et al., 2006; Vicars et al., 2010), such that as soils weather and rock-derived elements are depleted (Smeck, 1973), atmospheric inputs can alleviate ecosystem nutrient limitations (Chadwick et al., 1999). Soils in the EML catchment are derived from granitic bedrock (Huntington and Akeson, 1987), an igneous rock of relative low P content, such that atmospheric subsidies can be critical in supplementing the accumulation of P in soils. To understand the contribution of atmospheric inputs to soil P stocks in high-elevation Sierran catchments, the long-term hydrochemical record of EML (1985-1999) and the average (± std. error) Si and P content of granite (n=9; 0.66 mg P g^{-1} ± 0.096 and 297 mg Si g^{-1} ± 6.9453; Sickman and Leydecker, unpublished data; Table 4.4) were used to construct a P mass balance for the catchment over the past 10,000 years of pedogenesis. The mass balance assumes a fixed rate for atmospheric P inputs (Vicars et al., 2010) as well as a fixed rate of P weathering from bedrock (Table 4.4). P weathering was estimated by assuming that the export of Si from EML (336 moles Si ha^{-1} yr^{-1} from 1985-1999; Sickman, unpublished data), corrected for atmospheric Si inputs (0.1 kg ha^{-1} yr^{-1}; (Tegen and Kohfeld, 2006)), is a

direct estimate of the weathering rate of granite, from which the rate of P weathering can be estimated using Si:P ratios. As a result, rock weathering and atmospheric P inputs nearly balance P outputs and P storage in the catchment (Table 4.4), suggesting that weathering of granitic bedrock can explain only 31 % of the P stored in soils, while atmospheric deposition, over the past 10,000 years, presumably account for the remaining 69 % of the P measured in the EML catchment. The significant influence of atmospheric processes on soil P accumulation is consistent with estimates of dust deposition for the western US, indicating that the Sierra Nevada region has experienced significant long-term inputs of dust (Chadwick et al., 1999), in which predominantly westerly winds have and continue to transport P-bearing particles from sources as far away as central Asia across the Pacific (Vicars and Sickman, 2011).

In general, EML soils had higher P concentrations than soils in coniferous forests at Acadia National Park (334 μg P g^{-1}) (SanClements et al., 2009) and at Goliath Peak in Colorado (275-333 μg P g^{-1}) (Shiels and Sanford, 2001), but are similar to soils in other mountain regions where P concentrations ranged between 988-1127 μg P g^{-1} (Parker and Sanford 1999) and 980-1636 μg P g^{-1} (Litaor et al., 2005) at Niwot Ridge, Colorado, 216-1117 μg P g^{-1} in the Pyrenees, France (Cassagne et al., 2000), and 746-1009 μg P g^{-1} in the Minshan Mountains of southwestern China (Zhang et al., 2011). Differences in soil P concentrations are likely due to differences in age and physical characteristics that affect pedogenic processes and therefore the retention capacity of atmospheric P (Parton et al., 2005). For example, soils at Goliath Peak have a limited water holding capacity (Shiels

and Sanford, 2001), resulting in low weathering rates, slow soil development, and low amounts of total and available P (Litaor et al., 2005).

Entisols and inceptisols such as those sampled in the EML basin, can contain P from atmospheric sources as well as from weathering of P-bearing primary minerals with subsequent accumulation in Fe- and Al-dominated inorganic and organic pools (Parton et al., 2005). Soil C:N:P ratios in EML soils (Table 4.3) are substantially lower than the global average of 186:13:1 in soil and to 60:7:1 in microbial biomass (Cleveland and Liptzin, 2007) suggesting that high-elevation soils are relatively replete in P. I measured low P concentrations in 1M HCl and concentrated HCl extracts relative to other pools. Because P extracted with HCl is representative of P held in primary minerals (Cross and Schlesinger, 1995; Walker and Syers, 1976), it is conceivable that 10,000 years of mineral weathering and biological processes has transferred P into soil organic and inorganic pools dominated by Fe and Al hydroxides (Walker and Syers, 1976). However, for RLC, HCl-extractable P accounts for 46-50% of the total P (Table 4.2). The sampled RLCs have similar properties to the soils sampled at Goliath Peak by Shiels and Sanford (2001), are located on steep slopes, are shallow, and lack vegetation cover, suggesting that their low water holding capacity minimizes weathering processes and P transfer to organic P pools (Litaor et al., 2005).

Organic phosphorous constitutes 20-80% of the total P in most soils (Anderson, 1980), and in the EML watershed, P_o accounts for 53-62% of total P (Fig. 4.1). In soil, the P_o pool is generally comprised of mostly inositol phosphates (phosphate monoesters), followed by phospholipids, nucleic acids (DNA and RNA), phosphorylated polymers,

and teichoic acids (Celi and Barberis, 2005), of which phosphate monoesters are considered mobile and most labile (Turner, 2005). The significant proportion of P_o found in EML soils (Fig. 4.1, Table 4.2) is typical of other alpine soils (Cassagne et al., 2000; Litaor et al., 2005; Parker and Sandford, 1999; Zhang et al., 2011) and is consistent with mechanisms of pedogenic P accumulation (Parton et al., 2005), in which phosphatase enzyme activity can be suppressed due to high P availability (Quiquampoix and Mousain, 2005), minimizing P_o degradation, and thereby enriching the P_o pool (Bowman and Cole, 1978b; Condron and Tiessen, 2005). At EML, P_o accumulation in soil may be favored by the relative importance of atmospheric P deposition that may lower phosphatase enzyme activity, the low temperature characteristic of alpine environments limiting P_o decomposition (Conant et al., 2011; Nadelhoffer et al., 1991), and the relatively low weathering rates (weathering is largely constricted to a two-month period during snowmelt (Dahlgren et al., 1997)), and high sorption capacity to Fe and Al oxides (Walker and Syers, 1976). Thus, the cycling of P in an ecosystem over time depends on efficient transfers between P_i and P_o pools (Yanai, 1992), and P supply to ecosystems becomes a function of the capability of biological processes to maintain active P cycling between organic and inorganic forms (Cole et al., 1978) and atmospheric P deposition (Chadwick et al., 1999).

Soil P retention

The lability of P in soil is controlled by the solubility of Ca-, Fe-, and Al-phosphates, which depends on soil pH (Lindsay, 1979); P is most soluble at pH 6.5 at which the solubility of Ca-, Fe-, and Al-phosphates converge (Hesterberg, 2010).

Because soils of the EML catchment are acidic (pH ≈ 5; Fig. 4.2), the solubility of P is predominantly controlled by Fe- and Al-phosphates, which become increasingly stable below pH 6.5 (Hesterberg, 2010). The importance of Fe and Al on P dynamics in EML soils is evident in the high proportion of P measured in both $NaHCO_3$ and NaOH extracts (Fig. 4.1, Table 4.2), the Al-dominated clay mineralogy of the catchment (Appendix A), as well as from the significant recovery of P in $NaHCO_3$- and NaOH-extractable pools following exogenous P amendments (Fig. 4.5). The soil P adsorption measurements at EML suggest that soils can retain an additional 368 µg P g^{-1} in A horizons and 586 µg P g^{-1} in B horizons. However, in acidic soils, the dominance of Al-oxides over Fe-oxides has significant consequences for P retention (Kana and Kopacek, 2006; SanClements et al., 2009, 2010). While P may be liberated from the reduction of Fe-phosphates, under low redox conditions, Al is readily available to adsorb the liberated P and minimize P leaching (Kana and Kopacek, 2006). Because of the high $Al:Fe_{(NaHCO3+NaOH)}$ of approximately 6 and an $Al_{NaOH}:P_{(NaHCO3)}$ in the range of 33-52 measured in EML soils, Al is expected to control the lability of P (Kopacek et al., 2005; SanClements et al., 2009). In lake sediments, $Al:Fe_{(H2O+NaHCO3+NaOH)}$ ratios >3 and an $Al_{NaOH}:P_{(H2O+NaHCO3)}$ >25 effectively inactivated P from active cycling (Kopacek et al., 2005). Although I did not measure Fe and Al concentrations in water extracts from soils, any Al or Fe that would have been released in water would have been measured by $NaHCO_3$ extraction.

In Sierran high-elevation soils, the accumulation of Al clay minerals and oxides are favored by the acidic and intense leaching environments that occur during snowmelt (Burkins et al., 1999; Dahlgren et al., 1997). Because the hydraulic conductivity of EML

catchment soil is on the order of 0.1 to 0.01 mm s^{-1} (Brown et al., 1990), water could percolate through 0.5 m (average soil depth at EML) of soil within minutes, effectively providing a vehicle for Si and Al elluviation. However, soil hydraulic conductivity decreases with depth at the EML catchment (Brown et al., 1990), which favors the accumulation of Si and Al in zones of illuviation and contributes to the formation of Al-dominated clays and oxides found in the watershed, such as hydroxyinterlayered minerals, kaolinite, and gibbsite (Appendix A; Brown et al., 1990). Importantly, the amorphous Al content in EML soil ranges from 9.5 to 30 g kg^{-1} (Brown et al., 1990), which due to its greater surface area when compared to crystalline forms, can significantly influence P retention (Turner, 2007). In EML soils, the relative importance of organic compounds can prevent the crystallization of amorphous oxides and promote further P accumulation (Celi and Barberis, 2005). High-elevation Sierran soils also contain volcanic glass derived from Pleistocene and Holocene volcanic eruptions from the Mono/Inyo Craters region (Wood, 1977). Since volcanic glass is of high reactivity and may play a role in the formation of gibbsite (Burkins et al., 1999), it may constitute an important mechanisms for the retention of P in catchment soils.

The control that Al, and to a lesser extent Fe and Ca, exert on P dynamics in the EML catchment, is not only important for the stabilization of P_i, but also for P_o, which constitutes a significant mechanism for P retention in soil (Walker and Syers, 1976). The accretion of P_o in soil, is enhanced by sorption onto ferric (Anderson and Arlidge, 1962; Celi et al., 1999) and aluminum oxide surfaces (Anderson, 1974), clay minerals (Anderson and Arlidge, 1962), complexation with Al, Fe, and Ca (House and Denison,

2002) and incorporation into organic matter (Pant et al., 1994). Of the organic forms of P in soil, inositol phosphates have a high charge density (Celi and Barberis, 2005), and are most strongly retained on amorphous Al and Fe oxide surfaces in acidic soils (Anderson et al., 1974). However, not all forms of P_o readily bind onto Fe and Al oxides (Turner, 2005), and other biological mechanisms contribute to the stabilization of organic P in EML soils. Phosphatase enzymes, which are generated by soil microbes and roots, can hydrolyze labile P_o into relatively immobile PO_4^{3-}, where it can be readily taken up by plants or microbes, or stabilized in Fe and Al complexes (Turner, 2005).

Nevertheless, this work suggests that P stabilization in soil is not only a function of micro-scale chemical or biological mechanisms, but that large-scale ecosystem processes also influence P retention. In subnivean soils, microbial activity, as measured by microbial biomass P, is at its highest (Fig. 4.6). Although low temperatures limit biological processes (Conant et al., 2011; Nadelhoffer et al., 1991), some microbes remain active well below 0°C (Mikan et al., 2002; Miller et al., 2007), and can survive as long as liquid water films are present (Coxson and Parkinson, 1987); liquid water films have been detected in soil particles at temperatures as low as -10°C (Romanovsky and Osterkamp, 2000). In the EML catchment, winter conditions are typically characterized by deep snowpacks that insulate soils to temperatures near 0°C (Sickman et al., 2003a), and allow for the metabolism of C from senesced biomass and corresponding mineralization and immobilization of nutrients (Taylor and Jones, 1990). Thus, during winter, P may be immobilized in soil microbial biomass effectively minimizing losses during plant senescence (Oberson and Joner, 2005). During spring, however, hydrologic

flushing may export P from soils (Blackwell et al., 2009) as microbial biomass declines due to C limitation (Lipson et al., 2000) or increased competition with plants for available resources (Edwards et al., 2006). In EML soils, however, approximately 27 % of the total P (232 to 242 µg P g^{-1}) is involved in transfers between organic and inorganic pools during the period from winter to summer, in which on average (A+B horizons) P_i pools decrease by 232 µg P g^{-1} with a concomitant increase of 242 µg P g^{-1} in P_o pools (Fig. 4.2). These appreciable transfers between inorganic and organic P pools underscore the importance of ecosystem-scale processes in sequestering P that otherwise could have been flushed during snowmelt. Therefore, the efficient transfer of P from microbial control during winter to plant biomass during summer (Miller et al., 2009; Schmidt and Lipson, 2004), constitutes an important pathway for P stabilization in alpine soils.

Soil P export to aquatic environments

The transfer of solutes from terrestrial to aquatic environments in alpine catchments is regulated by catchment hydrology (Sickman et al., 2003a). In the EML basin, hydrology is predominantly controlled by snowmelt, resulting in approximately a two-month period of intense hydrologic flushing as evidenced in the clay mineralogy of high-elevation Sierran soils (Appendix A; Dahlgren et al., 1997); however, snowmelt can last for six months in the EML basin (Sickman et al., 2003a). Although the high P retention capacity of the Al-dominated clay fraction at EML (Brown et al., 1990), the efficient transfer of P_i to P_o pools from winter to spring to summer (Fig. 4.2), the relatively small exchangeable soil P pool (resin-P_i; Figs. 4.1-4.2), and low hydrochemical export of P during snowmelt (Sickman and Melack, unpublished data) suggest that

transfers of P from soils to surface waters are minimal, over long timescales, snowmelt is presumably the main driver for P supply to alpine lakes. Because EML soils are well drained and have high hydraulic conductivities (Brown et al., 1990), P in equilibrium with the soil solution should be transferred to surface waters. Moreover, because the higher pH of infiltrating snowmelt raises the pH of soil and reducing conditions can occur during winter (Sickman et al., 2003a), I speculate that increased solubility of Fe- and Al-oxides due to higher pH and desorption of P from reduced Fe, may mobilize, at least some P from soils to surface waters during spring flushing.

Importantly, climate change forecasts for the Sierra Nevada predict earlier spring snowmelt and lessening of the snowpack depth (Maurer et al., 2007; Stewart et al., 2005) as well as shifts in precipitation patterns resulting in less snow and more rain (Kim, 2005). Because microbial activity in alpine environments depends on the insulating properties of snow (Brooks et al., 1996; Miller et al., 2007; Miller et al., 2009), reductions in snow cover may affect the efficient transfer of P between inorganic and organic pools during the critical winter-spring seasonal transition observed in this study (Schmidt and Lipson, 2004), potentially enhancing the export of P_i to surface waters. In alpine ecosystems, snow depths of at least 0.3 m are required to keep soils from freezing (Cline, 1995; Williams et al., 1998), preventing freeze-thaw cycles from disrupting soil aggregate stability (Freppaz et al., 2007) and from inducing microbial cell lysis (Ron Vaz et al., 1994) that may enhance P mineralization during periods of low plant demand and high hydrologic transport.

Changes in climate may also enhance the transfer of P_o to surface waters. From measurements at EML, it is clear that the P_o pool is an important component of the P cycle and that biological processes exert control on P dynamics (Fig. 4.1, Table 4.2). Until recently, it was thought that P_o was unavailable to plants or microbes, presumably because P_o forms very stable complexes with Fe- and Al-oxides, and higher-order inositol phosphates are strongly sorbed in soils (Turner, 2005, 2007). However, mycorrhizal fungi can utilize inositol phosphates (Allen et al., 1981), representing a pathway by which stable forms of P_o can be biocycled. Furthermore, the adsorption of organic phosphates on soil colloids can reverse the surface charge to negative, resulting in repulsive forces that increase particle separation facilitating the transport of P from soils to surface waters (Celi and Barberis, 2005). It is also known that sugar phosphates and phosphate diesters are weakly bound to soils (Turner, 2005), and can be rapidly hydrolyzed by phosphatase enzymes followed by biological uptake (Bowman and Cole, 1978a), or leaching to surface waters (Frossard et al., 1989). The seasonal measurements indicate that the P_o pool increases during summer, creating a window of opportunity for P_o mobilization to aquatic environments assuming favorable hydrologic conditions. Thus, changes in climate may alter P dynamics in alpine catchments by 1) enhancing C storage and subsequent P_o accumulation due to warmer temperatures (Dahlgren et al., 1997; Luckman and Kavanagh, 2000) and 2) increased incidence of rainfall (Kim, 2005) providing pathways for P transport to aquatic environments.

At EML, summer rainfall transferred sufficient terrestrial organic material to cause a 20-30 µM increase in surface water concentrations of dissolved organic carbon

(Sadro et al., 2011a), which presumably mobilized P as well. Periodic rainfall can enhance the mobilization of P_o through soil drying-wetting cycles, which can expose previously protected soil organic matter to microbial attack (Navarro-Garcia et al., 2012) and release significant amounts of P to solution (Butterly et al., 2011; Turner et al., 2003; Turner and Haygarth, 2001) that can be quickly mobilized through cracks and other preferential flowpaths typical of dry soils (Simard et al., 2000). In summer of 2009, an intense rainfall event flooded the EML catchment with 15-20 cm of rain within a 24 h period, increasing dissolved organic P concentrations in EML by 50% and TP by 61% (Sadro and Melack, 2012). Thus, shifts in climate that increase the number and intensity of rainfall events can have important consequences on P cycling by enhancing the transport of P from terrestrial to aquatic environments in high elevation catchments.

Summary and conclusions

Atmospheric processes can significantly influence the P content of alpine catchments in the Sierra Nevada accounting for approximately 69 % of the P stored in soils. At EML, the P content of soils is typical of other alpine ecosystems, in which concentrations are not indicative of P deficiency, and the majority of P is found in Fe- and Al-associated pools. Of the soils sampled, P_o accounts for the majority of P, which coupled with favorable hydrology, may represent an important pathway for P supply to alpine lakes. I speculate that transfers of P from soils to high-elevation lakes occur primarily during snowmelt and summer rainfall events. However, I dismiss P export during snowmelt as a significant contributor to the eutrophication of high-elevation lakes,

as it occurs during a period asynchronous with biological demand (Sadro et al., 2011b). Because climate change models forecast reductions in snow and increases in rainfall, loss of the insulating properties of snow coupled with repeated soil freeze-thaw and drying-rewetting episodes, can contribute to the destabilization of soil P pools and increased transfer to sensitive aquatic ecosystems.

.

Tables and Figures

Table 4.1. Soil characteristics for Entic Cryumbrepts (EC), Lithic Cryumbrepts (LC), Cryaquepts (C), Typic Cryofluvents (TCF), Rock outcrop-Lithic Cryumbrepts (RLC), and Typic Cryorthods (TC). Values for area, depth, bulk density, soil texture for EC, TC, and LC, and CEC for TC are summarized from Brown et al. (1990). Soil texture for C and CEC for LC, C, and EC are summarized from Lund et al. (1987).

Soil	Horizon	pH	Texture (%)			CEC	Area	Mean depth	Bulk density
			Sand	Silt	Clay	(mEq 100 g^{-1})	(ha)	(m)	(Mg m^{-3})
Entic Cryumbrepts							4.4	0.37	1.35
	A	4.9	62	34	4	10.30			
	B	---	72	26	2	11.74			
Lithic Cryumbrepts							6.2	0.24	1.41
	A	4.45	51	33	16	7.84			
	B	4.68	51	36	13	11.26			
Cryaquepts							0.26	0.5	1.02
	A	4.59	42	39	19	52.06			
	B	4.93	63	25	12	20.63			
Typic Cryofluvents							0.07	1.5	1.35
	A	4.72	---	---	---	---			
	B	4.79	---	---	---	---			
Rock outcrop-Lithic Cryumbrepts							9.315	0.34	1.41
	A	5.27	---	---	---	---			
	B	5.11	---	---	---	---			
Typic Cryorthods							2.085	0.33	1.35
	A	4.26	74	20	6	11.18			
	B	4.78	78	18	4	10.66			

Table 4.2. Average P concentrations (± standard deviation) for all sampled soils in the EML watershed (n=4; EC n=6).

Horizon	Resin–P_i	$NaHCO_3$ – P_i	$NaHCO_3$ – P_o	NaOH–P_i	NaOH–P_o	1M HCl	Conc. HCl–P_i	Conc. HCl–P_o	Residual P	Total P
Entic Cryumbrepts										
A+B	9.46	77.93	34.83	202.39	498.23	206.94	44.61	18.36	22.01	1114.76
	(5.11)	(53.37)	(11.64)	(87.94)	(123.52)	(123.15)	(7.71)	(8.17)	(6.84)	(203.32)
Lithic Cryumbrepts										
A	6.78	11.74	112.01	32.54	767.23	56.46	48.32	31.19	23.52	1089.8
	(2.71)	(0.78)	(25.31)	(5.25)	(166.57)	(47.92)	(5.45)	(5.46)	(13.36)	(175.94)
B	4.56	6.98	67.74	23.33	667.45	110.54	39.75	17.66	33.15	971.16
	(3.86)	(4.11)	(21.33)	(1.32)	(3.41)	(29.34)	(5.08)	(1.58)	(11.57)	(39.03)
Cryaquepts										
A	9.04	46.41	135.98	86.80	582.82	89.48	61.01	25.48	25.91	1062.92
	(6.26)	(21.23)	(11.75)	(17.69)	(403.24)	(53.70)	(14.60)	(8.74)	(20.51)	(408.83)
B	0.43	7.71	21.29	23.73	76.50	104.50	18.82	7.50	11.82	272.33
	(0.87)	(4.84)	(20.36)	(13.40)	(63.86)	(69.22)	(4.98)	(1.35)	(9.95)	(98.05)
Typic Cryofluvents										
A	8.97	19.09	130.06	54.27	521.66	71.49	51.89	25.76	18.71	901.90
	(7.00)	(6.68)	(34.12)	(10.33)	(109.76)	(50.23)	(9.40)	(16.55)	(12.42)	(128.27)
B	2.73	10.55	67.47	50.91	447.25	132.49	40.86	14.50	10.97	777.73
	(2.36)	(3.38)	(40.23)	(16.60)	(372.63)	(39.04)	(9.70)	(12.65)	(14.90)	(377.84)
Rock outcrop-Lithic Cryumbrepts										
A	5.23	35.82	24.27 (4.09)	180.90	119.22	299.24	31.86	5.43	19.12	721.08
	(1.54)	(4.63)		(28.33)	(36.75)	(81.43)	(4.10)	(3.45)	(23.98)	(97.10)
B	2.83	12.76	8.64	315.29	51.55	223.44	67.56	10.58	9.22	701.86
	(1.07)	(5.18)	(1.99)	(179.53)	(36.51)	(27.13)	(59.25)	(1.64)	(4.61)	(194.59)
Typic Cryorthods										
A	4.67	17.19	46.95	22.65	144.70	19.02	27.50	13.87	12.57	309.12
	(2.05)	(2.78)	(18.11)	(3.80)	(83.49)	(8.15)	(8.44)	(9.92)	(14.23)	(88.11)
B	4.11	35.24	11.08 (1.24)	57.12	96.47	21.83	22.96	5.26	7.30	261.37
	(2.78)	(3.26)		(3.39)	(42.87)	(3.65)	(3.89)	(2.53)	(5.47)	(43.98)

Table 4.3. Average soil C, N, and P_{sum} concentrations (± standard error) for EC, LC, and TCF sampled from winter through fall 2010. P_{sum}= Resin–P_i + $NaHCO_3$–P_T + NaOH–P_T.

Season	Horizon	n	C (μg g^{-1})	N (μg g^{-1})	P_{sum} (μg g^{-1})	C:N:P_{sum}
Winter	A	6	98,966 ± 22,361	6,387 ± 1,795	594 ± 86	167:11:1
	B	6	47,317 ± 6,364	3,147 ± 1,122	539 ± 78	88:6:1
Spring	A	18	73,369 ± 12,260	5,063 ± 696	459 ± 41	160:11:1
	B	18	26,112 ± 2,192	2,067 ± 385	382 ± 37	68:5:1
Summer	A	18	74,469 ± 6,897	3,921 ± 268	662 ± 31	112:6:1
	B	18	35,950 ± 2,844	2,020 ± 102	471 ± 28	76:4:1
Fall	A	18	50,714 ± 5,319	2,812 ± 355	445 ± 24	114:6:1
	B	18	24,403 ± 2,101	1,563 ± 148	404 ± 34	60:4:1

Table 4.4. Comparison of annual P fluxes and pools (kg) in the Emerald Lake watershed (area=120 ha) and catchment mass balance of P over 10,000 years of soil development adapted from Sickman et al. (2003) and Vicars et al. (2010). For the 10,000 year P mass balance, rock weathering was estimated from the average export of Si from the EML catchment from 1985-1999 (336 moles Si ha^{-1} yr^{-1}), corrected for Si deposition (0.1 kg Si ha^{-1} yr^{-1}; Tegen & Kohfeld (2006)) and the average (± Std. error) Si and P content in granite from EML (n=9; 0.7 mg P g^{-1} ± 0.096 and 297 mg Si g^{-1} ± 6.9). [a]Values obtained from Vicars et al. (2010). [b]Values obtained from Sickman et al. (2003). [c]Basin biomass P was estimated from biomass N (11,146 eq N ha^{-1}; 24 ha; Williams et al. (1995)) using an average N:P ratio of 12 (Güsewell, 2004).

Component	Catchment flux	Catchment pool
Dry deposition	8.6[a]	
Deposition in snowpack	5.3[a]	
Total deposition	13.9[a]	
Catchment export	8.8[b]	
Lake water		0.97[b]
Lake sediment		3,000[b]
Catchment soil		78,600
Freely exchangeable P_i		540
$NaHCO_3$–P_i		3,300
$NaHCO_3$–P_o		3,400

----------10,000 year P mass balance----------

	Inputs (kg)	Outputs/storage (kg)
Rock weathering	24,665	
Atmospheric deposition	139,000[a]	
Catchment export		88,000[b]
Catchment soil		78,600
Lake sediments		3,000[b]
Vegetation		312[c]
Total	163,665	169,912
Atmospheric contribution to soil P pool		53,935−60,400

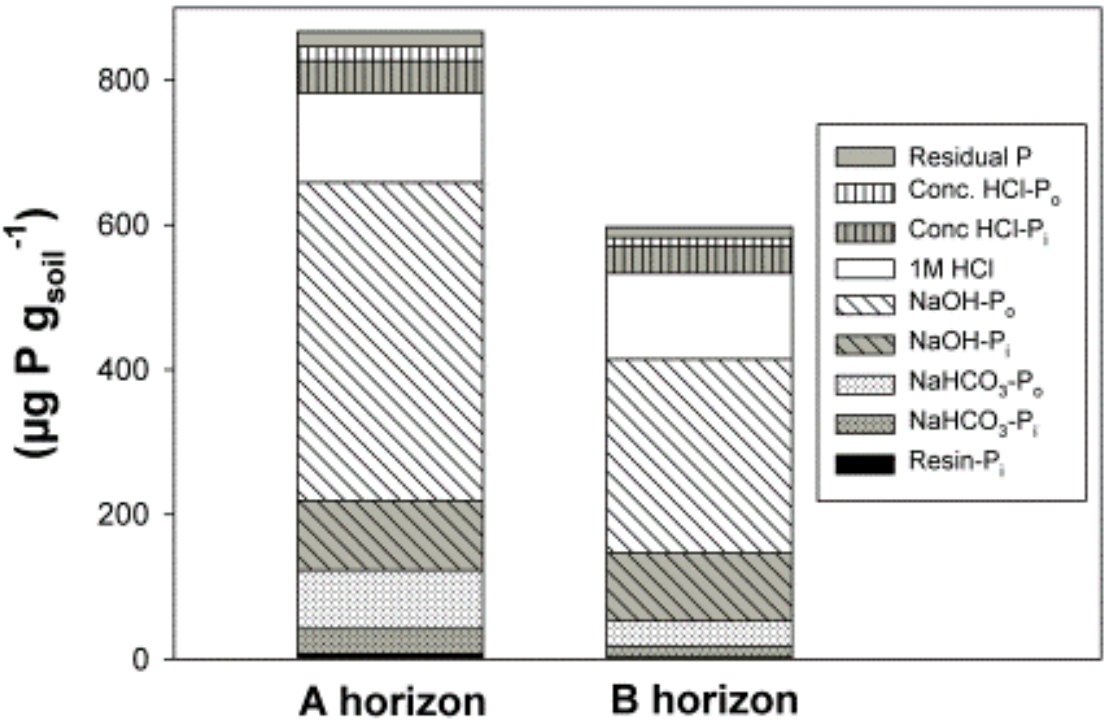

Fig. 4.1. Average P concentrations in Entic Cryumbrepts (EC), Lithic Cryumbrepts (LC), Cryaquepts (C), Typic Cryofluvents (TCF), Rock outrcrop-Lithic Cryumbrepts (RLC), and Typic Cryorthods (TC), following a sequential P fractionation procedure. P_i=inorganic P and P_o=organic P.

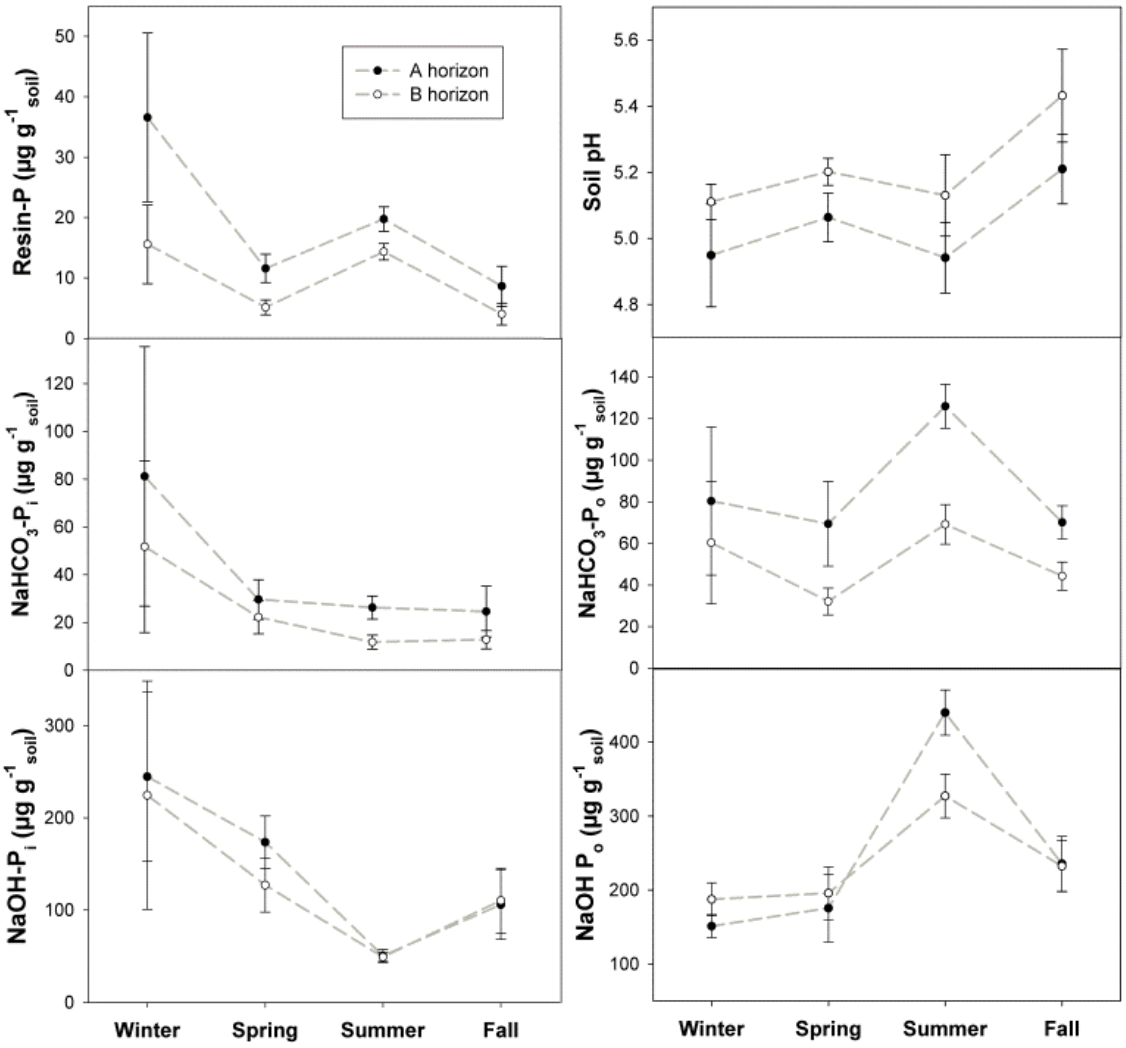

Fig. 4.2. Average seasonal changes in soil P concentrations and pH from LC, EC, and TCF from winter through fall 2010. Error bars denote standard errors.

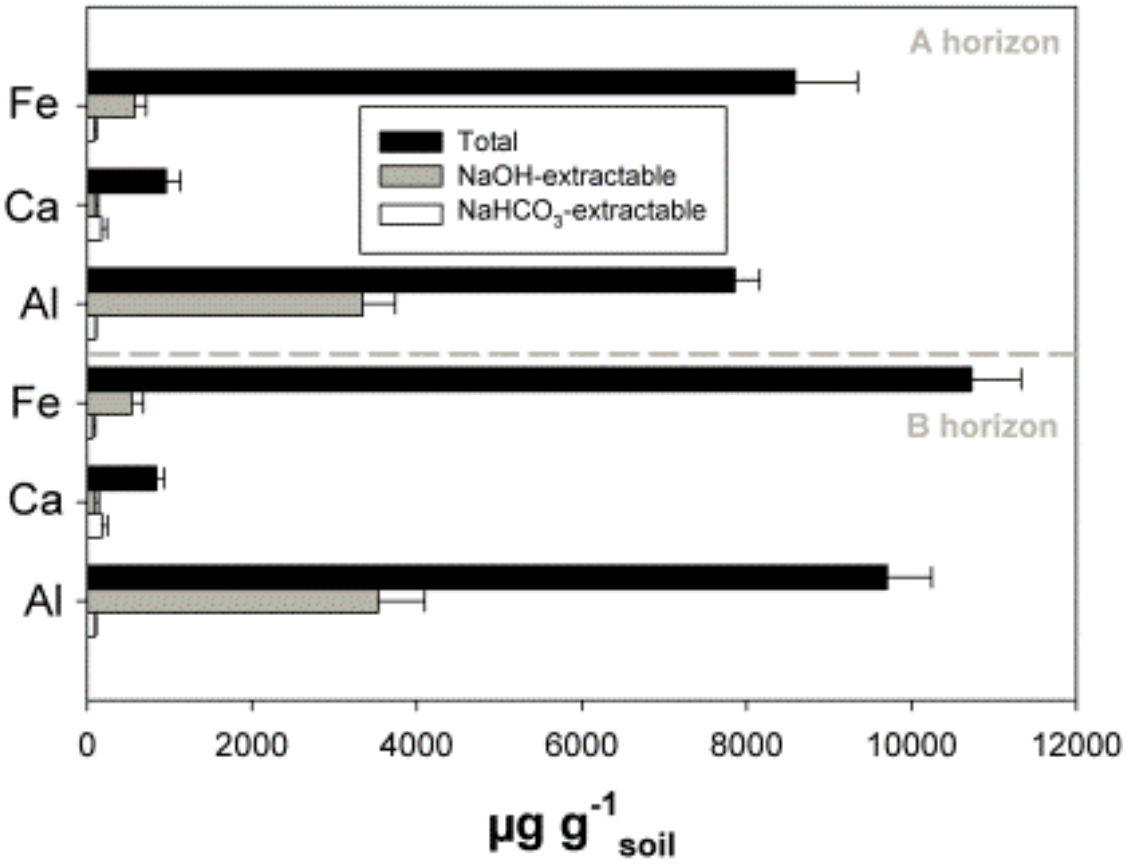

Fig. 4.3. Average soil Ca, Fe, and Al concentrations from LC, EC, and TCF extracted with $NaHCO_3$ and NaOH. Error bars denote standard errors.

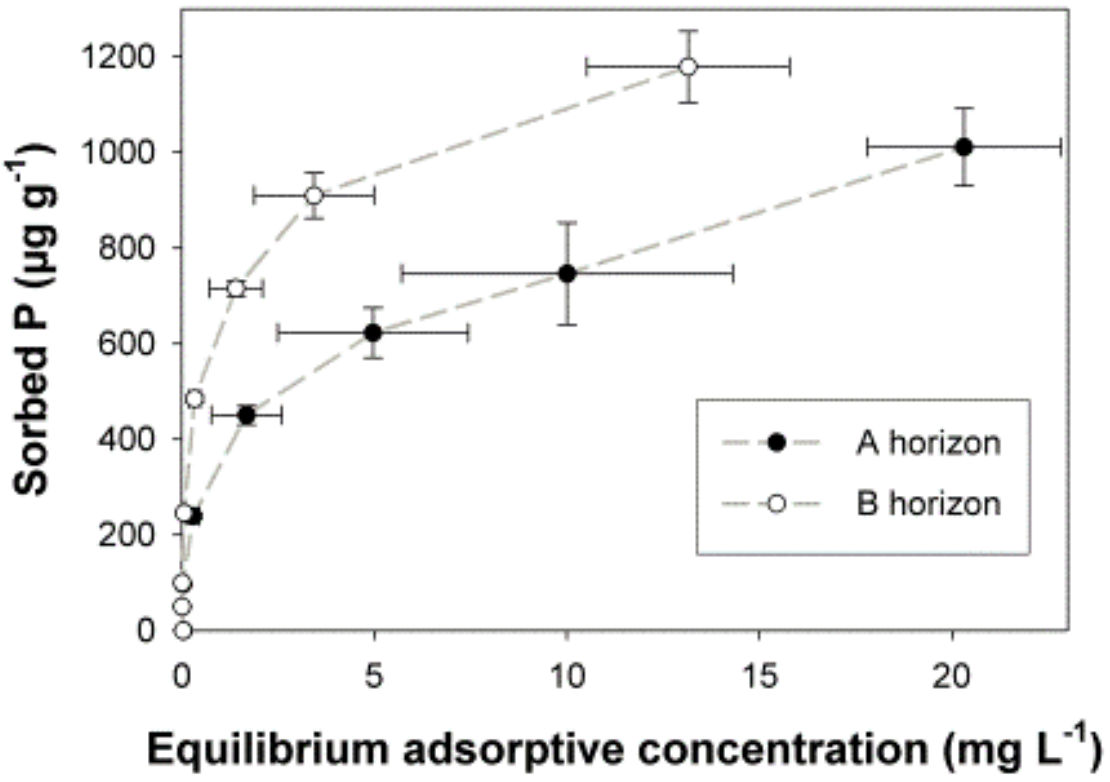

Fig. 4.4. Average P sorption in LC, EC, and TCF at 0, 2, 4, 10, 20, 30, 40, and 60 mg P L^{-1} equilibrating solution concentrations. The equilibrium adsorptive concentration (*x*-axis) is the concentration of P in solution after equilibration with soil. Error bars denote standard errors.

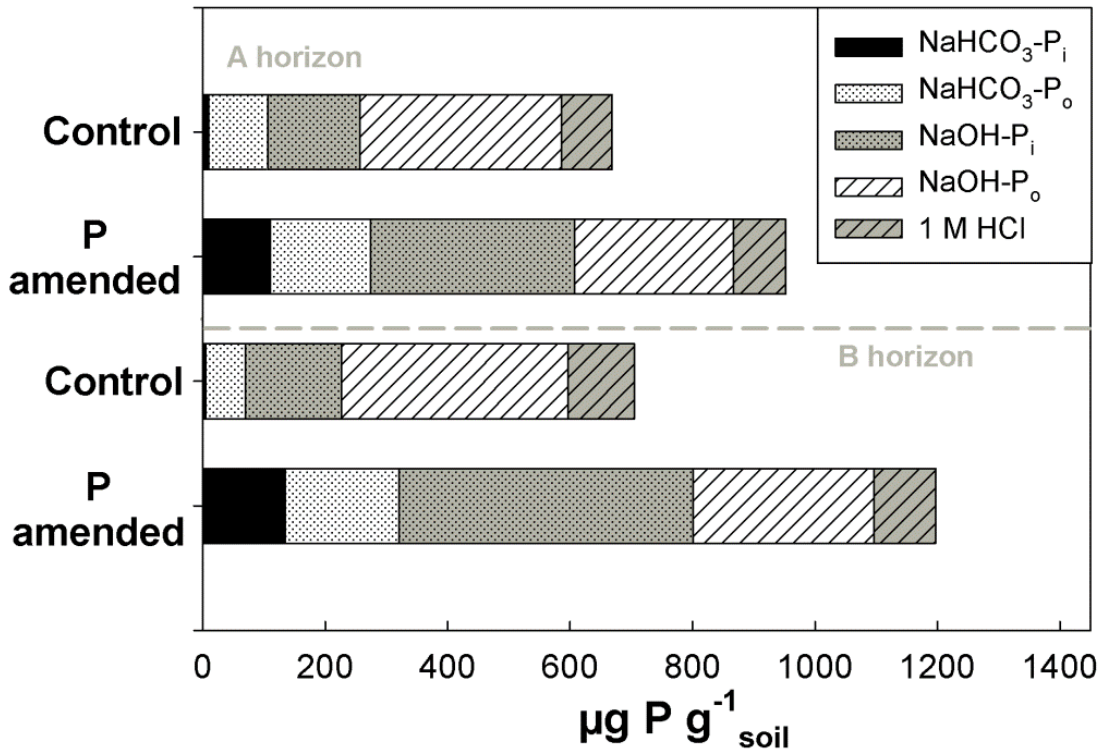

Fig. 4.5. Average recovery of P in soils following P amendments to LC, EC, and TCF

.

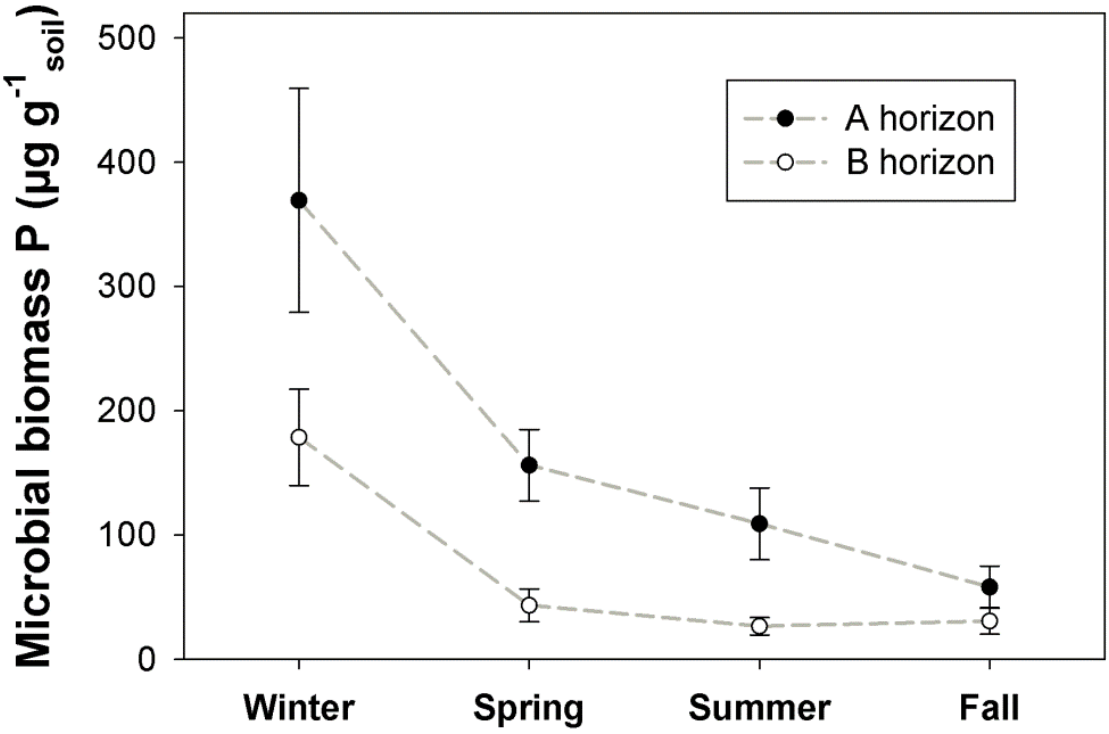

Fig. 4.6. Average change in microbial biomass P for LC, EC, and TCF from winter through fall 2010. Error bars denote standard errors.

5. PHOSPHORUS POOLS IN SEDIMENTS OF HIGH-ELEVATION LAKES OF THE SIERRA NEVADA, CALIFORNIA: IMPLICATIONS FOR INTERNAL LOADING OF P

Abstract

High-elevation lakes in the Sierra Nevada exhibit spatial and temporal variation in the degree of P vs. N limitation of phytoplankton growth. Variation in trophic condition could be the result of changing rates of atmospheric deposition of nutrients and/or climate-induced changes in soil and sediment biogeochemistry. Because atmospheric N inputs have remained relatively constant over the past three decades, I hypothesized that internal P loading from catchment soils and lake sediments are the main controls in trophic variability. However, fundamental information on the size and distribution of sediment P pools is lacking. I evaluated P pools in sediments from 50 Sierra Nevada lakes using a sequential fractionation procedure to gain better understanding of landscape controls on P forms in sediments. I also performed sediment core incubations under both oxic and anoxic conditions and analyzed long-term records of lake chemistry to quantify rates of sediment P release to Emerald Lake. On average, the sediments of Sierra Nevada lakes contain 1445 μg P g^{-1}, of which 5 % is freely exchangeable, 13 % associated with reducible metal hydroxides (NaBD-Pt), 68 % associated with Al hydroxides (NaOH-Pt), and the remaining 14 % stabilized in recalcitrant pools. In general, sediments behaved as net sinks for P during core incubations and were not significant sources of P despite hypolimnetic anoxia. These results are consistent with multiple linear regression analysis

that showed that sediment P fractions are not well correlated with soluble P concentrations in lakes. Due to the high Al content in Sierran sediments, P is strongly retained by Al hydroxides even under anoxia, suggesting that biological P demand in aquatic ecosystems is primarily met by allochthonous inputs and/or water-column recycling of P. Thus, changes in the release of P from lake sediments do not explain observed temporal and spatial patterns of phytoplankton nutrient limitation in the Sierra Nevada.

Introduction

Alpine lakes are particularly sensitive to environmental change and may be used as indicators of the impacts of a warming climate, changing precipitation patterns, and altered atmospheric composition (Parker et al., 2008; Sickman et al., 2003b). Because lakes accumulate materials at the lowest point of the landscape, they integrate watershed processes and can express changes in environmental conditions through a variety of limnological parameters. For example, changes in both dissolved organic carbon (DOC) (Parker et al., 2008) or zooplankton abundance (Fischer et al., 2011) can be used as early warning of the effects of a changing climate on alpine environments. Lake water and sediment chemistry can also be used to assess altered atmospheric composition of nutrients or changes in landscape processes as evidenced by shifts in the trophic status of lakes (Sickman et al., 2003b), as well as aid in understanding past catchment-scale geomorphic and ecological processes (Oldfield, 1977).

In high-elevation lakes of the Sierra Nevada, increases in phosphorus (P) supply over the past 30 years have resulted in mild eutrophication events that have shifted nutrient dynamics from primarily P-limited systems to increasing limitation and co-limitation by nitrogen (N) (Sickman and Melack, 1998). Although increased rates of atmospheric P deposition and enhanced transport of P-bearing terrestrial materials from the catchment are likely contributing to the P enrichment of high-elevation lakes (Chapter 4; Kopacek et al., 1995; Morales-Baquero et al., 1999; Vicars et al., 2010), the contribution of lake sediments to the P budget of alpine Sierran lakes has been understudied. In particular, little is known about the chemistry of P in lake sediments

including fundamental information about the size and distribution of the P pool. Thus, by examining the content and distribution of P in sediment cores, it may be possible to infer whether climatically induced changes in lake physicochemical conditions (e.g., dissolved oxygen, temperature or sulfate) are contributing to the eutrophication of Sierran lakes.

In most freshwater lakes, P is typically in short supply relative to ecosystem demand (Wetzel, 2001). Because P is efficiently cycled and adsorbed to particles in most upland soils (Smeck, 1985), the P supply to fresh water environments is commonly met by internal P loading from sediments, or recycling of P within the water column (Nürnberg, 1985). However, lakes with high catchment to volume ratios typically receive larger nutrient loads than lakes draining smaller watersheds and may significantly contribute terrestrial materials to surface waters.

The transfer of P from sediments to the water column can occur through numerous pathways including chemical and biological processes (Amirbahman et al., 2003; Boström and Petterson, 1982; Campbell, 1994). The classic model for P release from sediments is centered on the presence of reducing conditions at the sediment-water interface that result in the reductive dissolution of Fe hydroxides ($Fe(OH)_3$) and subsequent release of Fe-associated P into solution (Amirbahman et al., 2003; Mortimer, 1941). Although this process was initially conceived as strictly chemically driven (Mortimer, 1941), microbes contain a significant proportion of soluble sediment P (Prairie et al., 2001) and the presence of Fe-reducing bacteria is necessary for the oxidation of organic matter and subsequent Fe and P release to the water column (Lovley, 1991). It has also been shown that the exchange of P between the sediment-water

interface depends on temperature (Anthony and Lewis, 2012; Jensen and Andersen, 1992) as well as on other biological processes during which changes in redox potential can cause microbial cell lysis and subsequent release of soluble P to the water column (Böstrom et al., 1988; Gächter et al., 1988). Importantly, the release of P from sediments can also be influenced by the biogeochemistry of S, in which the microbial reduction of sulfate (SO_4^{2-}) to sulfide (S^{2-}) can form insoluble FeS or FeS_2 and decrease the adsorptive control of Fe on P (Caraco et al., 1993; Hasler and Einsele, 1948).

Although the exchange of P between the sediment-water interface is to a large extent controlled by redox processes, reducing environments do not always result in the desorption of P from sediments (Hupfer et al., 2004; Schindler et al., 1973). In lakes with elevated nitrate (NO_3^-) concentrations and reducing environments, NO_3^- can act as an alternative electron acceptor during the oxidation of organic matter (Böstrom et al., 1988). Under these conditions, Fe-hydroxides are not reduced and P is retained on sediment surfaces. Other processes controlling P release under reducing environments involve the presence of high concentrations of Al in sediments during which P released from the reduction of Fe can be irreversible bound to aluminum hydroxides ($Al(OH)_3$) (Kopacek et al., 2005; Kopacek et al., 2001). Because $Al(OH)_3$ is insensitive to redox, P bound to Al is effectively inactivated from solution where it can be permanently stored (Kopacek et al., 2005). In sediments, P is effectively sorbed by Al when the ratio of Al:Fe extracted in water, $NaHCO_3$-$Na_2S_2O_4$ (BD), and NaOH is > 3 or the ratio of Al_{NaOH}:$P_{(H2O+BD)}$ > 25 (Kopacek et al., 2005). However, because information regarding

the size and distribution of Fe, Al, and P pools in Sierra Nevada lake sediments is lacking, it is unknown whether these mechanisms exert control on sediment P dynamics.

This study was designed to answer the following questions: (i) What is the P, Fe, Al and Ca content and distribution in sediments of high-elevation Sierra Nevada lakes? (ii) What is the rate of P transfer from sediments to the water column during oxic and anoxic conditions? (iii) How does lake chemistry and lake physiography relate to sediment P content? To answer these questions I analyzed sediments form 50 high-elevation lakes distributed throughout the central Sierra Nevada and used a sequential P fractionation procedure to determine the size and distribution of sediment P, Fe, Al, and Ca pools. I also conducted in-situ sediment core incubations at Emerald Lake to determine rates of P release from sediments under both ambient and N_2-induced anoxic environments. Multiple linear regression models with stepwise selection were also used to understand what parameters controlled P in lake water and labile P concentrations in sediments. Lastly, I evaluated long-term limnological record for two high-elevation Sierra Nevada lakes to identify changes in lake water P concentrations during anoxic episodes. I hypothesized that most of the P in lake sediments would be stabilized in Fe- and Al-hydroxides and that little P would be transferred from sediments to the water column during oxic conditions. However, I hypothesized that during anoxic episodes, significant transfers of P from sediments to the water column would occur.

Methods

Site descriptions

The Sierra Nevada is a semi-continuous belt of plutonic rocks stretching north to south for approximately 700 km, from the Mojave Desert in California to northwestern Nevada. Its climate is characterized as Mediterranean, with precipitation occurring mainly during winter months in the form of snow. However, summer thundershowers are not uncommon, and can significantly influence catchment hydrology, especially in high-elevation watersheds (Sadro and Melack, 2012). The Sierra Nevada is mainly composed of granitic and granodioritic bedrock polished by several glacial periods starting approximately 1 million years ago and lasting until about 10 thousand years ago (Taskey, 1995). Given the relatively young age of the Sierran landscape, soils are poorly developed and are commonly classified as Entisols and Inceptisols (Huntington and Akeson, 1987).

In this study I focus on 50 high-elevation lakes (denoted the surveyed lakes) located in the central Sierra Nevada. The surveyed lakes were selected from a lake chemistry database of 500 Sierra Nevada lakes which formed the basis for diatom-inference models of lake chemistry (Bennett et al., *in press*). The lakes range in elevation from 2198 to 3791 m above sea level, have surface area ranging of 0.55 to 83.6 ha, depths from 3 to 35 m, and watershed areas of 40.1 to 944 ha.

In addition to the surveyed lakes, I measured sediment P pools in short sediment cores and performed sediment incubation experiments in Emerald Lake (EML), a representative high-elevation lake located on the western slope of the central Sierra

Nevada within Sequoia and Kings Canyon National Parks (2,800 m a.s.l.; 36°35'49"N, 118°40'29"W). EML is a well studied 2.72 ha oligotrophic glacial cirque lake with a 120 ha watershed area. The lake has a mean depth of 6 m and a maximum depth of 10 m, a volume of approximately 162,000 m^3, and is characterized by weakly buffered waters (Melack et al., 1998). The geology of the EML watershed is dominated by granitic and granodioritic bedrock with mafic intrusions, aplite dikes, and pegmatite veins (Williams et al., 1993). Vegetation is sparse, covering approximately 20% of the basin and characterized by Lodgepole Pine (*Pinus contorta*), Western White Pine (*Pinus monticola*), and low woody shrubs such as Sierra willow (*Salix orestera*) and grasses (*Calamagrostis canadensis*). EML is typically ice-covered from December through June (Sadro et al., 2011b).

We also make use of the long-term limnological record of both EML and Pear Lake (PRL) (J. Sickman, unpublished data), to assess changes in lake water P as a function of hypolimnetic O_2 concentrations. PRL is a 8.0 ha 591,000 m^3 oligotrophic high-elevation lake (2,904 m a.s.l.) located approximately 1 km northeast from EML (36°36'02"N, 118°40'00"W). It has an average depth of 7.4 m with a maximum depth of 27 m, promoting periods of strong stratification and hypolimnetic anoxia. The PRL watershed is 142 ha of which 90% is bedrock, talus, and boulders with a geology dominated by coarse-grained granites containing mafic inclusions of widely variable size and texture. The vegetation is similar to that described for EML, except for the presence of small stands of red fir (*Abies magnifica*).

Lake sediment sampling

During the summer of 2007 and 2008, the top 2 cm of sediment was obtained from each of the 50 surveyed lakes using a gravity corer (Aquatic Research Instruments, Hope Idaho). In the lab, all sediments were freeze-dried and homogenized prior to total C, N, and P measurements. Water samples were co-collected at each of the surveyed lakes analyzed for pH, conductivity (Cond), acid neutralizing capacity (ANC), PO_4^{3-}, Cl^-, NO_3^-, SO_4^{2-}, Ca^{2+}, Mg^{2+}, Na^+, K^+, Si, Fe, particulate C (PC), particulate N (PN), particulate P (PP), total dissolved N (TDN), total dissolved P (TDP), dissolved organic N (DON), and DOC (Bennett et al. 2012 in press).

In summer 2011, three sediment cores were obtained from the deepest part of EML and sectioned into 0-2, 2-5, 5-10, 10-20, and 20-30 cm samples, from which P, Fe, Al, and Ca concentrations were obtained. These samples were stored at 4°C in the dark and not freeze-dried prior to analysis. To express the sediment on a dry weight basis, two 10 g samples from each depth were oven-dried at 104°C from which the water content was determined.

Sediment P sequential fractionation

We used a modified sequential fractionation procedure (Agemian, 1997) to determine the size and distribution of P pools in lake sediments, in which NH_4Cl was replaced with NaCl in the first step of the extraction to minimize the dissolution of Ca-bound P early in the procedure (Lukkari et al., 2007). For each sediment, a 0.5 g (dry weight) sample was sequentially extracted with (i) 0.46 M NaCl under an N_2 environment for 1 h to obtain loosely bound and pore water P; (ii) 0.11 M sodium dithionite ($Na_2S_2O_4$)

in 0.11 M sodium bicarbonate ($NaHCO_3$) buffer (pH 7) under an N_2 environment for 1 h to obtain P bound primarily to redox-sensitive Fe-oxides (NaBD-P_i) and organic P that is easily mineralized (NaBD-P_o); (iii) 0.1 M NaOH for 18 h which yields what is considered to be inorganic P (NaOH–P_i) associated with amorphous and some crystalline Al oxides but that may contain Fe-associated P not extracted in the previous step, as well as organic P (NaOH–P_o) associated with humic compounds and polyphosphates; (iv) 0.5 M HCl for 1 h to extract Ca-associated P found predominantly in apatite minerals (HCl-P_i); and (v) 1 M NaOH at 85 °C for 1 h to extract residual and recalcitrant forms of occluded P (85°NaOH-P). All extracts generated in the sequential fractionation procedure were filtered through Whatman 42 filter paper (2.5 µm). Total phosphorus was determined by a colorimetric method (Murphy and Riley, 1962) to quantify inorganic forms of P (P_i) and by ICP to obtain total P (P_t). For the determination of P in NaBD extractions, samples were sparged with He to remove dithionite prior to colorimetric determination of P, as it interferes with the reducing phosphomolybdate complex by affecting color development (Lukkari et al., 2007). Organic P (P_o) was estimated as the difference between P_t and P_i.

Sediment core incubations

During the ice-free season of 2011 intact sediment cores from EML were incubated in-situ to estimate ambient rates of P flux from sediments to the water column. Incubation experiments were conducted on three occasions: July 12, August 15, and September 13. On July 12, eight sediment cores (ca. 30 cm length) were collected with a gravity corer from the deepest part of EML. Sediment cores were collected in 60 cm

long clear polycarbonate core tubes (6.8 cm ID), so that approximately half of the core was occupied by sediment and the remaining half by lake water (ca. 1 L). Following collection, all cores were carefully brought up to the surface taking care to minimize disturbance. At the surface, the dissolved oxygen (DO) of the overlying water was measured (Yellow Springs Instruments O_2 meter) and a 250 ml water sample was collected from each core, filtered (Whatman GF/F; 0.7 µm), stored in polypropylene bottles and denoted the t_0 sample. To maintain a constant water volume inside the core, an equal volume of filtered lake water (0.2 µm) was added back to the core tube to make up for the volume of the water samples. Make-up lake water was stored in a 10 L container kept inside the lake to minimize any effects associated with sudden changes in temperature during the core refilling process.

Following the collection of t_0 samples, each core was sealed with a plastic cap and waterproof tape. Once capped, the cores were place in a holder and lowered back into the lake (10 m depth) for incubation (water temperature 4.2 °C). All sediment cores were sampled at time 5 h (30 mL), 22 h (250 mL), 28 h (30 mL), 45 h (250 mL), 52 h (30 mL), and 69 h (250 mL). To simplify the water sampling procedure, the plastic caps sealing the core tubes were equipped with fittings (Luer-Lok) to which one end of silicone tube was attached while the other end reached down to approximately 5 cm above the sediment surface inside the core. At each sampling time, the cores were brought back to the surface and a syringe was connected to the fitting attached to the silicone tube and 20 mL of water were initially extracted from the core as a rinse. After the tubing rinse, the syringe was reattached to the cap fitting and the water sample was

slowly withdrawn. A second syringe was used to add the makeup water to the cores and they were returned to the holder and redeployed in the lake. Sampling took less than 1 hour. At the end of the incubation all cores were brought back to the surface during which DO was measured one last time prior to discarding the sediments.

On August 15, four sediment cores were collected, incubated at 7.3 °C (lake water temperature) and processed as previously described. All sediment cores were sampled at time 0 h (250 mL), 15 h (30 mL), 19 h (30 mL), 25h (250 mL), 40 h (30 mL), 44h (30 mL), and 48 h (250 mL). Dissolved oxygen and temperature were monitored inside a single sediment core with D-Opto O_2 sensors (Zebra-Tech, Ltd.) at one minute intervals. The sensors were calibrated using Winkler titrations (Sadro et al., 2011b). On September 13, eight sediment cores were incubated at 12 °C (lake water temperature), but five of the cores were initially sparged with N_2 until the O_2 concentration inside the cores fell to 0.3 mg O_2 L^{-1}. The remaining three cores were not amended with N_2 and served as controls. Temperature and O_2 concentrations inside the cores were monitored in both an N_2-amended and reference core with D-Opto O_2 sensors. All sediment cores were sampled at time 0 h (250 mL), 15 h (30 mL), 19 h (30 mL), 25 h (250 mL), 40 h (30 mL), 44 h (30 mL), and 48 h (250 mL). For the N_2 amended cores, filtered make up water was also sparged with N_2 (0.3 mg O_2 L^{-1}).

Water samples gathered during each incubation period were kept in a nylon bag inside the lake while in the field and transported on ice to the laboratory where they were stored in the dark at 4°C until analyzed. In the laboratory, the 250 mL water samples were analyzed for soluble reactive P (SRP), TDP, NO_3^-, TDN, Fe, Al, SO_4^{2-}, ANC, and

pH, while 30 mL samples were analyzed for SRP and TDP only. All sample concentrations were corrected for the addition of filtered make-up (Bennett et al., *in press*).

Emerald Lake and Pear Lake long-term limnological records

We used long-term limnological records for both EML and PRL (1983 to present), to observe changes in lake water P concentrations during periods of anoxia. Because reducing environments can promote the liberation of P from reducible metal hydroxides (Mortimer, 1941), I expected to find inverse relationships between O_2 and P concentrations.

Multiple linear regression and statistical analyses

We used ordinary least squares multiple linear regression with stepwise model selection to understand what variables control lake water SRP and TDP and sediment labile P (NaCl-P_t + NaBD-P_t) in the surveyed lakes. Models were developed as a function of water chemistry (TDP, SRP, DOC, pH, Cond, ANC, Cl^-, NO_3^-, SO_4^{2-}, Ca^{2+}, Mg^{2+}, Na^+, K^+, Si, Fe, PC, PN, PP, PN:PP, DIN:TP, TDN, DON), lake physiography (elevation, lake depth, lake area, watershed area) and sediment chemistry (% C, % N, C:N, NaCl-P_t, NaBD-P_t, Labile P , NaOH-P_t, Al_t, Ca_t, Fe_t, $Al_{(NaCl+NaBD+NaOH)}$:$Fe_{(NaCl+NaBD+NaOH)}$, $Al_{(NaOH)}$:$P_{(NaCl+NaBD)}$). Predictive models for SRP and TDP included all variables except for (SRP, TDP, PP, PN:PP). For the development of a model to predict sediment labile P, two approaches were used. The first was intended to predict sediment labile P content based on water chemistry and lake

physiography, as a model based on these parameters can be practical for land managers. The second approach incorporated all variables except for NaCl-P_t, NaBD-P_t, Labile P, and NaOH-P_t. Model selection was based on a "significance level to enter" $\alpha = 0.15$ and a "significance level to stay" $\alpha = 0.05$.

To detect whether significant differences existed between treatments and sampling times during in-situ sediment core incubations, I used repeated measures ANOVA with Tukey post-hoc tests. I also used simple linear regression on each individual core to estimate rates of P sorption/desorption from sediments. Linear regression was also used to develop predictive relationships between O_2 and dissolved P concentrations for both the EML and PRL long-term hydrochemical record.

Results

Sequential extraction of sediment cores

On average (± std. dev.), the total P content in sediment from the surveyed lakes was 1,445 ± 491 µg P g^{-1}. Of the total P, 5 % was considered freely exchangeable (NaCl-P_t), 13 % associated with reducible metal hydroxides (NaBD-Pt), 68 % associated with Al hydroxides (NaOH-P_t), and the remaining 14 % stabilized in recalcitrant pools (Fig. 5.1, Table 5.1). In EML, the largest average total P content was found in the 0-2 cm section (1,274 ± 87 µg P g^{-1}) with P concentrations gradually declining as a function of core depth, to a minimum P content of 793 ± 48 µg P g^{-1} in the 20-30 cm core section (Fig. 5.1, Table 5.1). The majority of P was found in the NaOH extractable pool (78 %),

followed by P occluded in recalcitrant pools (15 %), and P found in freely exchangeable pools or associated with reducible metal hydroxides (7 %) (Fig. 5.1, Table 5.1).

Average (± std. dev.) Fe and Al concentration measured in sediments from the surveyed lakes were approximately equal (7,779 ± 2,762 µg Al g^{-1} and 7,621 ± 7,077 µg Fe g^{-1}; Figs. 5.2-5.3, Table 5.1). However, for EML, the average total Al content in sediments was slightly larger than the average total for Fe (8,920 ± 1,906 µg Al g^{-1} and 5,457 ± 1,782 µg Fe g^{-1}; Figs. 5.2-5.3, Table 5.1). For Al, the highest concentrations were found in the 5-10 cm depth range (Fig. 5.2, Table 5.1), while for Fe, concentrations decreased with increasing depth (Fig. 5.3, Table 5.1). Surprisingly, average Ca concentrations in the surveyed lakes (2,880 ± 1,493 µg Ca g^{-1}) were more than double the average concentrations found at EML (1,160 ± 458 µg Ca g^{-1}; Fig. 5.4); on average, more Ca was extracted with NaCl in the surveyed lakes than the total Ca extracted for EML (Fig. 5.4). Though freeze-drying could have altered the measurement of Ca in surveyed lakes, Ca concentrations in 15 freeze-dried sediments from EML were within 10 % of fresh sediments, consistent with other studies indicating minor effects of freeze-drying on Ca analysis (Hjorth, 2004). Unlike Fe and Al, Ca concentrations did not vary as a function of depth, and remained remarkably constant throughout the length of the sediment core (Fig. 5.4, Table 5.1).

In-situ sediment core incubations

Sediment core incubations were used to estimate potential rates of P transfer from sediments to the water column. During the July and August incubations at EML, I generally observed a decreasing trend in both average SRP and TDP concentrations with

time, suggesting that lake sediments behaved as net sinks for P (Fig. 5.5, Table 5.3). In September, SRP concentrations were about an order of magnitude larger than during July and August in reference cores, but I observed no consistent increase in SRP concentrations over time ($p > 0.28$; Fig. 5.6). In N_2-treated cores, a subtle, but not statistically significant ($p = 0.62$) increase in SRP concentrations was observed from t_0 to t_{25} (1.6 to 5.0 µg P L^{-1}; Fig. 5.6), but there was no overall effect of treating cores with N_2 ($p = 0.77$). At t_{40}, SRP concentrations in N_2-treated cores declined to 2.8 µg P L^{-1}, but increased once again to about 5 µg P L^{-1} during measurements made at $t_{44\text{-}48}$. From the average rate of SRP increase among reference and N_2-treated cores during September, I estimated a P desorption rate of 0.05-0.1 µg P L^{-1} h^{-1} as the best approximation for the transfer of P from sediments to the water column (Table 5.3). However, it is important to consider that significant differences in SRP concentrations over time were not detected (Figs. 5.5-5.6) and that the vast majority of slopes reported in table 5.3 are not significantly different from zero.

In July, core water Fe concentrations decreased from 23 µg L^{-1} at t_{22} to 12 µg L^{-1} at t_{69} ($p = 0.08$) and Al concentrations decreased from 15 µg L^{-1} at t_{22} to 7 µg L^{-1} at t_{69} ($p = 0.08$; data not shown). During August, there were no significant differences between sampling times for Fe or Al ($p > 0.16$), during which Fe concentrations averaged 7.9 µg L^{-1} and Al 8.4 µg L^{-1}. In September, N_2-amendment had no overall effect on both Fe and Al concentrations (average Fe = 35 µg L^{-1} and Al = 11 µg L^{-1}; $p > 0.44$), but in N_2-treated cores, there was a significant decline in Fe concentrations from t_{25} to t_{48} (51 to 20 µg Fe L^{-1}; $p = 0.007$). For SO_4^{2-} (data not shown), significant changes in concentration were

not detected over the length of the incubation periods in July, August, and September (average SO_4^{2-} = 0.2 µg L^{-1}; $p > 0.13$). However, in September, SO_4^{2-} concentrations in N_2-treated cores (0.23 µg L^{-1}) were higher than in reference cores (0.19 µg L^{-1} ; $p = 0.02$).

For NO_3^-, concentrations were about an order of magnitude larger in July than during August and September (Figs. 5.5-5.6), but despite the elevated NO_3^- levels, a significant increase in NO_3^- over the length of the July incubation period was not detected ($p > 0.24$). In August, however, the average NO_3^- concentration increased over time (t_0-t_{48}; $p = 0.05$; Fig. 5.5). In September, NO_3^- concentrations did not significantly change over the length of the incubation period ($p > 0.57$) and there were no differences in NO_3^- concentrations between reference and N_2-treated cores ($p = 0.76$). For TDN, concentrations in July significantly increased from t_0 to a maximum at t_{45} (Fig. 5.5; p = 0.003). In August, TDN concentrations significantly increased over time ($p = 0.018$). In September, although there were no significant differences between reference and N_2-treated cores ($p = 0.17$), the average TDN concentration was higher under N_2 treatment and significantly increased over the length of the incubation period ($p = 0.02$; Fig. 5.6).

Both pH and ANC remained relatively constant (pH ≈ 5.8-6.5 ; ANC ≈ 17-25 µEq L^{-1}) during incubations and between sampling times (July, August, and September) without significant changes observed over the length of the incubations ($p > 0.26$; data not shown) or between reference and N_2-treated cores ($p > 0.30$). For DO, concentrations inside the cores during July at t_0 averaged 11 mg O_2 L^{-1} and presumably remained oxic during the incubation period since DO concentrations averaged 8 mg O_2 L^{-1} at the end of the incubation. In August, D-Opto O_2 sensors monitored DO concentrations inside

sediment cores. The initial (t_0) DO concentration was 7.8 mg O_2 L^{-1}, and increased over time to a final DO content of 8.2 mg O_2 L^{-1}. In September, the DO content inside reference cores started at 7.8 mg O_2 L^{-1} and gradually decreased over the length of the incubation period to 5.7 mg O_2 L^{-1} (Fig. 5.6). For N_2-treated cores, the DO began at 0.7 mg O_2 L^{-1} and gradually increased over time to a maximum of 3.2 mg O_2 L^{-1} recorded at the end of the experiment (Fig. 5.6).

Emerald and Pear lake chemistry

The long-term water chemical record for both EML and PRL was used to understand how changes in the DO content of both epilimnion and hypolimnion affected P dynamics in the water column. From the long-term limnological record of EML (1982-2008) I focused on a period between 1984-1985 during which hypolimnetic anoxia (DO as low as 0.1 mg L^{-1}) was observed likely resulting from a large flood during the summer of 1984. For the PRL record (1986-1993), I focused on periods of low hypolimnetic oxygen observed during 1986-1989 (DO as low as 0.2 mg L^{-1}). For EML, there was not a strong relationship between DO and either PO_4^{3-} ($y = -0.0016x + 0.0639$, $r^2 = 0.0017$, $p = 0.76$; Fig. 5.7) or TDP ($y = -0.0089x + 0.1995$, $r^2 = 0.22$, $p = 0.0025$; Fig. 5.7). However, a significant and stronger inverse relationship between NH_4^+ and DO concentrations was detected ($y = -0.6161x + 5.3184$, $r^2 = 0.3971$, $p < 0.0001$; Fig. 5.7). Similar to EML, TDP concentrations in PRL were not strongly affected by anoxic episodes ($y = -0.0260x + 0.3468$, $r^2 = 0.1130$, $p = 0.0113$; Fig. 5.8), while changes in NH_4^+ as a function of DO were best explained by an exponential decay model suggesting a strong relationship between both variables ($y = 245.95\, e^{-0.5866x}$, $r^2 = 0.4960$, $p < 0.0001$; Fig. 5.8).

Multiple linear regression models

Ordinary least squares multiple linear regression models developed for the prediction of both SRP and TDP concentrations in Sierran lakes, did not select any of the sediment variables developed from the sequential extraction procedure (Table 5.4). Sediment N content and lake water Na^+ concentrations explained approximately 38 % of the variation in SRP (Table 5.4). For TDP, 57 % of the variation was explained by Si, particulate C, and DON (Table 5.4). The model developed to predict sediment labile P content as a function of water chemistry and lake physiography did not explain more than 43 % of the observed variation. However, once sediment chemical parameters were included, the model explained 73 % of the variation as a function of Na^+, K^+, and C and N sediment content (Table 5.4).

Discussion

Contribution of lake sediments to the P budget of Sierran lakes

The objective of this study was to quantify the size and distribution of the sediment P pool in Sierra Nevada lakes, and assess whether internal loading is an important factor controlling P supply in high-elevation Sierran lakes. In EML, sediments are estimated to contain approximately 3,000 kg of P (area = 27,000 m^2, depth = 1m, ρ = 0.085 g cm^{-3}, average = 1,300 µg P g^{-1}) (Sickman et al., 2003b). However, using an active sediment depth of 30 cm (P found below this depth is presumed to be of little ecological significance; Carey and Rydin, 2011), a sediment area of 2.7 ha, a bulk density ranging from 0.06-0.2 g cm^{-3} (Sickman, 2001), and the measurements of sediment P

content (Table 5.1), I estimate a total P mass of 1,416 kg of P in EML sediments (Table 5.2). Of the P extracted (average 1,445 µg P g^{-1}), the majority is found in the upper 2 cm, with lower P concentrations detected with increasing sediment depth (Fig. 5.1). Of the total P pool in sediments, 31 % is found in freely exchangeable and reducible metal hydroxide (NaCl-P + NaBD-P) pools, such that the internal loading of P from sediments can contribute to the P enrichment of Sierran lakes.

Although the P content stored in lake sediments can explain the annual export of P from the EML catchment (Table 5.2), this study suggests that sediments are not an important source of P to high-elevation lakes, but rather, a potential sink. In-situ sediment core incubations at EML during July, August, and September indicated either no change or negative fluxes in both SRP and TDP concentrations over time, suggesting that sediments were not a strong P source (Table 5.3). Furthermore, despite inducing anaerobic conditions during September incubations, a significant increase in both SRP and TDP was not observed, supporting the limited contribution of lake sediments to the P budget of high-elevation lakes (Table 5.3). Limited P desorption from sediments under anaerobic conditions was also observed in the long-term records for both EML and PRL, in which increases in P supply were not detected in response to hypolimnetic anoxia (Figs. 5.7-5.8), suggesting that either reducing conditions were not adequate for sediment P release, or that other processes quickly sorbed P from the reduction of Fe-phosphates. Finally, multiple linear regression models revealed that sediment P chemistry was not a significant parameter when modeling lake water SRP and TDP concentrations (Table 5.4). Because P concentrations in surficial sediments can be representative of watershed

P inputs and adsorption onto stable pools (Pettersson, 2001), a presumably important mechanism for P sequestration in EML sediments, surficial sediment P concentrations can be of low predictive power when modeling P concentrations in surface waters (Carey and Rydin, 2011).

From the measurements of lake water Fe and TDN in sediment cores, I suspect that anaerobic conditions were present, such that Fe reduction should have occurred. After 25 hours of incubation, Fe concentrations increased in N_2-treated cores and were significantly greater than concentrations in reference cores ($p = 0.01$) suggesting Fe reduction. Moreover, TDN concentrations in N_2-treated cores increased significantly, presumably due to the accumulation of NH_4^+ during anaerobic conditions that limited nitrification (Rysgaard et al., 1994); a pattern consistent with the long-term chemical records for both EML and PRL (Figs. 5.7-5.8). Thus, I speculate that other mechanisms that quickly adsorb P released from the reduction of Fe, are required to explain P dynamics in Sierran lake sediments.

Nitrate can serve as an electron acceptor during the oxidation of organic matter in reducing environments, such that the reduction of Fe-phosphates and associated P release is averted (Böstrom et al., 1988). However, this mechanism is presumably unimportant in Sierran lakes since a significant decrease in NO_3^- during core incubations was not observed, and NO_3^- concentrations are typically too low to significantly affect redox conditions (0.1 to 0.2 μg L^{-1}). Nevertheless, it is well known that Al exerts control on the solubility of P (Lindsay, 1979), and that unlike Fe, Al is insensitive to redox, such that Al-bound P may be permanently stored in lake sediments (Rydin et al., 2000). In

sediments with an $Al:Fe_{(H2O+BD+NaOH)} > 3$ or an $Al_{NaOH}:P_{(H2O+BD)} > 25$, P release under reducing conditions ceases (Kopacek et al., 2005); Al-hydroxides are readily available to sequester desorbed P. In sediments from the Sierra Nevada surveyed lakes, the average (± std. dev.) $Al:Fe_{(NaCl+NaBD+NaOH)}$ was 1.7 ± 1.7 and the $Al_{NaOH}:P_{(NaCl+NaBD)}$ was 71.6 ± 153.3. For EML, these ratios were also consistent with Al dominated sediments with an $Al:Fe_{(NaCl+NaBD+NaOH)}$ ratio of 1.6 ± 0.5 and an $Al_{NaOH}:P_{(NaCl+NaBD)}$ ratio of 76 ± 6.2 (both ratios increased with sediment depth). Although the $Al:Fe_{(NaCl+NaBD+NaOH)}$ in most Sierran lakes is < 3, presumably due to the competition between organic C and P for available adsorption sites on Al hydroxides (Tipping, 1981), the high $Al_{NaOH}:P_{(NaCl+NaBD)}$ ratios found in most Sierran lakes has been shown sufficient to prevent P desorption from anoxic sediments (Kopacek et al., 2005). Thus, in high-elevation lakes of the Sierra Nevada, Al can be an important regulator of lake P availability, by naturally inactivating P from solution and thereby limiting the contribution of internal P loading to the enrichment of surface waters.

Sediment P, Fe, Al, and Ca content

In comparison with sediments from other remote ecosystems, I find a higher sediment P content in Sierran sediments than in the top 5 cm of oligotrophic alpine lakes in the Tatra Mountains (Slovakia and Poland) (~800 µg P g^{-1}) (Kopacek et al., 2005) or in the top 10 cm in lake sediments of Upper Hadlock Pond (1,041 µg P g^{-1}), a mesotrophic lake located in an undisturbed watershed in Acadia National Park (eastern ME, USA) (SanClements et al., 2009). In contrast, I find lower Al and Fe concentrations in Sierran sediments (surveyed lakes = 7,779 µg Al g^{-1}, EML = 8,918 µg Al g^{-1}, Fig. 5.2; surveyed

lakes = 7,620 µg Fe g^{-1}, EML = 5,546 µg Fe g^{-1}, Fig. 5.3) than in sediments from Tatra Mountain lakes (~18,800 µg Al g^{-1}; ~11,200 µg Fe g^{-1}) or sediments from Upper Hadlock Pond (22,967 µg Al g^{-1}; ~10,000 µg Fe g^{-1}). For Ca, sediment concentrations from the surveyed lakes (2,880 µg Ca g^{-1}) were similar to those found in Upper Hadlock Pond (3,500 µg Ca g^{-1}), but for EML sediments, Ca concentrations were lower (1,160 µg Fe g^{-1}), presumably suggesting low weathering rates in EML when compared to other Sierra Nevada lakes. Calcium was not measured in sediments of the Tatra Mountains.

In comparison to EML watershed soils, EML sediments from the upper 2 cm contain approximately 400 µg g^{-1} more P than soils in A horizons and 670 µg P g^{-1} more than soils in B horizons (Table 5.1). With increases in sediment depth, however, P concentrations decreased, and P concentrations in sediments from the 20-30 cm depth roughly equaled the P content of soils (867 µg P g^{-1} in A horizons and 597 µg P g^{-1} in B horizons; Table 5.1). For Fe, soils had greater concentrations than lake sediments, but for Al, A horizons were depleted while B horizons were enriched relative to lake sediments (Table 5.1). Accumulation of Fe and Al in soils relative to lake sediments may be due to decreases in soil hydraulic conductivity in deeper soils (Brown et al., 1990), creating zones of Fe and Al illuviation and storage (Chapter 4). For Ca, EML sediments had higher concentrations than soils (Table 5.1) and showed consistent patterns of Ca accumulation over the length of the sediment core (Fig. 5.4), suggesting that weathering rates over the 20th century have remained relatively constant in the EML catchment (Table 5.1).

In EML, P and Fe concentrations, and to a lesser extent Al, are greater in surficial sediments when compared to concentrations found at a 20-30 cm depth. Decreasing elemental concentrations with sediment depth can be the result of degradation of organic matter (Rydin, 2000), temporary sequestration of P in Fe-oxyhydroxides in surficial oxic sediments (Mortimer, 1941; Rydin, 2000), or simply the result of increased allochthonous inputs from the watershed (Carey and Rydin, 2011). In eutrophic lakes, the limited capacity of lake sediments to bind P typically results in the pattern observed in EML sediments, exhibiting decreasing elemental concentrations as a function of sediment depth (Carey and Rydin, 2011). However, EML is an oligotrophic lake (TDP < 10 μg L^{-1}) in which lake sediments appear to act as net P sinks (Table 5.3; Fig. 5.5) and have a high P retention capacity ($Al_{NaOH}:P_{(NaCl+NaBD)}$ = 76), suggesting that the accumulation of P in surficial sediments is more the result of increased supply of allochthonous material to the lake rather than a limited capacity of sediments to sequester P. Because both Fe and Al are tightly coupled to the cycling of P in alpine soils (Kana et al., 2011; Chapter 4), the input of allochthonous materials are presumably important in the supply of P to high-elevation lakes (Chapter 4).

Additional support for increased supply of allochthonous materials to alpine lakes can be obtained by comparing the sediment P profile in EML to those of other oligotrophic lakes (TP_{water} < 10 μg L^{-1}). Oligotrophic lake sediments are generally characterized by increasing P concentrations with sediment depth, such that sediments at the surface have lower P concentrations than deeper sediments (i.e., high burial capacity; Carey and Rydin, 2011). Higher P concentrations in deep sediments are attributed to

diffusion, decreases in catchment P export from reduced weathering rates, or to higher Al concentrations for P sequestration (Carey and Rydin, 2011). However, the sediment P profile in EML, with higher P concentrations at the surface (Figs. 5.1-5.2, Table 5.1), is opposite to the pattern typical of most oligotrophic lakes, suggesting that Sierran lakes may be undergoing a transitional period to a more eutrophic state (Carey and Rydin, 2011). Because sediment Ca concentrations remained remarkably constant as a function of core depth (Fig. 5.4, Table 5.1), it is unlikely that changes in watershed weathering rates can simply account for the increased P accumulation in surface sediments. Thus, processes that increase the supply of Fe, Al, and P, while maintaining a constant Ca input, may explain the increase in P supply to Sierran lakes.

Increased P supply from terrestrial sources is consistent with the P mass balance for the watershed, which indicates that the freely exchangeable sediment P pool (NaCl-Pt) is not sufficiently large to account for the watershed P export (Table 5.2), and that the reducible metal hydroxide P pool (NaBD- and NaOH-Pt) must be mobilized. However, because sediments acted as net P sinks (Table 5.3) and reducing environments did not significantly release P from sediments (Figs. 5.6, 5.7, and 5.8), it is suggested that allochthonous P inputs are an important component of the P budget in high-elevation lakes.

Conceptual model for the P enrichment of Sierra Nevada high-elevation lakes

Phosphorus can be supplied to montane lakes through direct atmospheric P deposition (Vicars et al., 2010), transfer of P-bearing material from the watershed (Kopacek et al., 2011; Chapter 4), or through internal P loading (Nürnberg, 1985). This

study demonstrates that the transfer of P from sediments is small and not likely to meet the P requirements of phytoplankton and algae in Sierra Nevada lakes. Hence I conclude that atmospheric P deposition, as well as terrestrial inputs from the watershed, are the two most important processes regulating P supply to alpine lakes. However, P enrichment through atmospheric pathways, alone, cannot account for the increases in P supply to Sierran lakes, as soils in the EML catchment and other alpine sites have been shown to be highly retentive of P (Kana et al., 2011; Chapter 4). Based on the average P deposition rate for EML (40 µg P m^{-2} d^{-1}) (Vicars et al., 2010) and a lake area of 2.7 ha, I estimate an annual P input of 0.4 kg P directly to the lake, an amount too small to account for the annual watershed P export of 8.8 kg (Table 5.2).

Soils of the EML catchment are characterized by relatively large organic P pools, of which the Fe- and Al-associated P_o pools account for the majority of the total P (53-62 %; Chapter 4). Because soil P_o pools can be relatively mobile and labile (Celi and Barberis, 2005; Frossard et al., 1989), significant transfers of P from soils to surface waters can actually occur (Sadro and Melack, 2012; Sadro et al., 2011a). Transfers of terrestrial materials to surface waters can also be enhanced by acidic deposition (Driscoll et al., 2003; Kram et al., 1995; Likens et al., 1996); an issue affecting western U.S. landscapes from chronic N pollution (Pardo et al., 2011). In summer of 2009, an intense rainfall event at EML flooded the catchment with 15-20 cm of rain within a 24 h period, increasing dissolved organic P concentrations by 50% and TP by 61% (Sadro and Melack, 2012). During precipitation events of lesser magnitude, sufficient terrestrial material was transferred from the catchment to account for a 20-30 µM increase in DOC

(Sadro et al., 2011a). Because DOC has been linked with increases in allochthonous supply to other high-elevation lakes (Kopacek et al., 2011) it may serve as a vehicle for P supply to Sierran lakes. In lakes, photochemical reactions can liberate dissolved organically-bound metals acting as an important mechanism for the accumulation of Fe, Al, and P in lake sediments (Kopacek et al., 2006).

The input of allochthonous materials to lakes, as a process to explain increases in lake P availability and accumulation in surficial sediments, is consistent with the selection of sediment % C and N to model sediment labile P, suggesting that organic materials exert control in the accumulation of P in sediments (Table 5.4). Moreover, the positive relationship between Na^+ concentrations in lake water with both SRP and sediment labile P and Si with TDP (Table 5.4) may be indicative of volcanic glass weathering (Burkins et al., 1999) and desilification of high-elevation Sierran soils (Dahlgren et al., 1997), highlighting the importance of terrestrial materials to surface waters. The inverse relationship between K^+ and sediment labile P may result from the weathering of biotite to vermiculite, during which interlayer K^+ is lost (Farmer and Wilson, 1970), and P may be effectively adsorbed by the high cation exchange capacity of vermiculite.

Importantly, the transport of terrestrial materials to surface waters can be affected by changes in climate. Climate change forecasts for the Sierra Nevada predict shifts in precipitation patterns, resulting in less snow and more rain with concomitant increases in temperature (Kim, 2005; Knowles et al., 2006). In oligotrophic montane lakes, warmer water temperatures have been shown to increase the rate of P supply from sediments to

the water column (Anthony and Lewis, 2012). In soils, warmer temperatures are projected to enhance the advancement of the treeline to higher elevations (Dahlgren et al., 1997), which coupled with atmospheric N and P deposition, may synergistically interact to develop the soil organic matter pool (Dahlgren et al., 1997; Luckman and Kavanagh, 2000) and increase the transport of DOC and nutrients to alpine lakes. Development of the soil organic matter pool with concomitant supply of Fe, Al, and P to surface waters can occur without necessarily enhancing rates of Ca weathering, remaining consistent with the findings in this study. Therefore, I hypothesize that changes in climate can enhance the contribution of allochthonous P inputs to surface waters by developing the soil organic matter pool, and through shifts in hydrology during snowmelt and summer rainfall, favor the transport of allochthonous materials to high-elevation lakes.

Summary and conclusions

Sediments of high-elevation lakes in the Sierra Nevada have a high P content relative to Sierran soils or to lake sediments from other remote ecosystems. However, despite a relatively high degree of P availability, sediments appear to be sinks for P regardless of the development of reducing conditions during hypolimnetic anoxia, as documented in sediment core incubations and long-term limnological records of two high-elevation Sierran lakes. Moreover, I find that multiple linear regression models with stepwise variable selection, fail to include sediment P measurements as significant parameters for the prediction of SRP and TDP in surface waters. I conclude that due to the high Al content in Sierran lake sediments, P is effectively deactivated and is of little

ecological significance in the P budget of alpine lakes. Rather, I hypothesize that a synergistic effect between a warming climate and enhanced rates of atmospheric N and P deposition, have interacted to develop the soil organic matter pool in alpine catchments, thereby increasing the supply of P from landscapes to Sierran lakes through the transport of DOC.

.

Tables and Figures

Table 5.1. Emerald Lake sediment and soil P, Fe, Al, and Ca concentrations. Exchangeable P includes P extracted with water and 0.5 M $NaHCO_3$ in soils and 0.46 M NaCl and 0.11 M $Na_2S_2O_4$ in 0.11 M $NaHCO_3$ for sediments. Residual P includes P extracted with concentrated HCl and a microwave digestion for soils and hot (85°C) 1M NaOH for sediments. Total P corresponds to the sum of all fractions in both soils and lake sediments. Soil estimates were obtained from Chapter 4.

Soil horizon	P (µg g^{-1})								
	Exchangeable		$NaHCO_3$		NaOH		Dilute HCl	Residual	Total
	P_i	P_o	P_i	P_o	P_i	P_o	P_i		
A	7.4	--	34.7	80.7	96.6	439.0	123.8	84.5	867
B	2.9	--	14.7	35.2	94.1	267.9	118.6	57.7	597
Sediment depth									
0-2	0.3	3.2	47.9	37.0	467.0	532.6	84.3	101.4	1273
2-5	0.4	2.8	57.3	26.8	401.1	562.6	85.7	88.9	1225
5-10	0.5	2.0	52.6	24.0	498.8	443.6	78.5	83.0	1183
10-20	0.5	1.6	48.6	17.2	391.7	343.3	99.7	77.8	981
20-30	0.7	1.4	42.0	14.7	339.3	272.7	77.6	44.8	793

Soil horizon	Al (µg g^{-1})					
A	--	105.1	3344.0	--	--	7859
B	--	96.6	3528.6	--	--	9706
Sediment depth						
0-2	238.1	60.0	5940.5	1200.1	1967.7	9406
2-5	219.4	45.9	6296.3	1188.8	1833.4	9584
5-10	181.6	38.4	6357.9	1148.3	2004.1	9730
10-20	144.8	24.6	5374.1	967.6	1871.0	8382
20-30	109.7	19.2	4789.7	817.3	1756.2	7492

Soil horizon	Fe (µg g^{-1})					
A	--	86.4	580.3	--	--	8587
B	--	70.8	544.4	--	--	10728
Sediment depth						
0-2	9.7	4821.0	1163.7	1605.9	51.8	7652
2-5	13.8	3842.3	1213.9	1588.9	57.8	6717
5-10	15.4	2715.5	1005.0	1376.5	65.4	5178
10-20	23.0	1850.6	736.0	1223.1	105.0	3938
20-30	15.6	1889.2	621.3	1147.2	125.7	3799

Soil horizon	Ca (µg g^{-1})					
A	--	174.9	105.8	--	--	959
B	--	182.4	99.2	--	--	841
Sediment depth						
0-2	607.7	84.3	92.7	369.2	25.0	1179
2-5	587.0	69.5	89.2	391.0	23.5	1160
5-10	567.5	83.1	94.4	384.7	23.3	1153
10-20	521.9	78.6	81.4	417.1	42.6	1142
20-30	596.1	92.2	87.3	344.9	44.4	1165

Table 5.2. Comparison of annual P fluxes and pools in Emerald Lake (2.7 ha) and its watershed (120 ha). Adapted from Sickman et al. (2003) and Vicars et al. (2010). [a]Values obtained from Vicars et al. (2010). [b]Values obtained from Sickman et al. (2003). Soil estimates obtained from Chapter 4.

Component	Catchment flux (kg)	Catchment pool (kg)
Dry deposition	8.6[a]	
Deposition in snowpack	5.3[a]	
Total deposition	13.9[a]	
Catchment export	8.8[b]	
Lake water		0.97[b]
Lake sediment (30 cm)		1416
Freely exchangeable P_i		3.4
NaBD–P		96.2
0.1 M NaOH–P		1093
Total Catchment soil		78600
Freely exchangeable P_i		540
$NaHCO_3$–P_i		3300
$NaHCO_3$–P_o		3400

Table 5.3. Rates of P transfer from lacustrine sediments to the water column obtained from the average slope and standard deviation for linear regressions performed on each sediment core incubated during July, August, and September 2011.

Parameter	Date	Treatment	n	Average slope ($\mu g\ P\ L^{-1}\ h^{-1}$)	Std. dev.
SRP	July	--	8	-0.0064	0.0045
	August	--	4	-0.00025	0.0097
	September	Control	3	0.104	0.0678
		N_2-treated	5	0.0520	0.0214
TDP	July	--	8	-0.0163	0.0139
	August	--	4	-0.0293	0.0285
	September	Control	3	-0.0284	0.0280
		N_2-treated	5	-0.0384	0.0188

Table 5.4. Ordinary least squares multiple liner regression models with stepwise selection for the prediction of SRP, TDP, and sediment labile P ($NaCl\text{-}P_t$ + $NaBD\text{-}P_t$). Models were developed based on parameters for water chemistry, lake physiography, and sediment chemistry. *Sediment P measurements were not included in sediment chemistry.

Predicted variable	Variables included in model	Parameters selected by model	Parameter estimate	*p* value	R^2	Adjusted R^2
SRP	Water chemistry	Intercept	0.0449	<0.0001	0.3807	0.3512
	Lake physiography	Na^+	0.000533	0.0034		
	Sediment chemistry	% N	0.0103	0.0108		
TDP	Water chemistry	Intercept	- 0.0359	0.0288	0.5743	0.5431
	Lake physiography	Si	0.000651	0.0085		
	Sediment chemistry	Part. C	0.00112	0.0206		
		DON	0.00506	<0.0001		
Sediment labile P	Water chemistry	Intercept	- 62.091	0.5962	0.4318	0.3902
	Lake physiography					
		TDP	3753.3763	0.0029		
		ANC	5.1512	0.0008		
		K^+	- 56.0738	0.0018		
	Water chemistry	Intercept	- 76.8838	0.3526	0.7298	0.7028
	Lake physiography	Na^+	8.7850	0.0010		
	Sediment chemistry*	K^+	- 29.9966	0.0116		
		% C	- 68.3589	<0.0001		
		% N	908.4035	<0.0001		

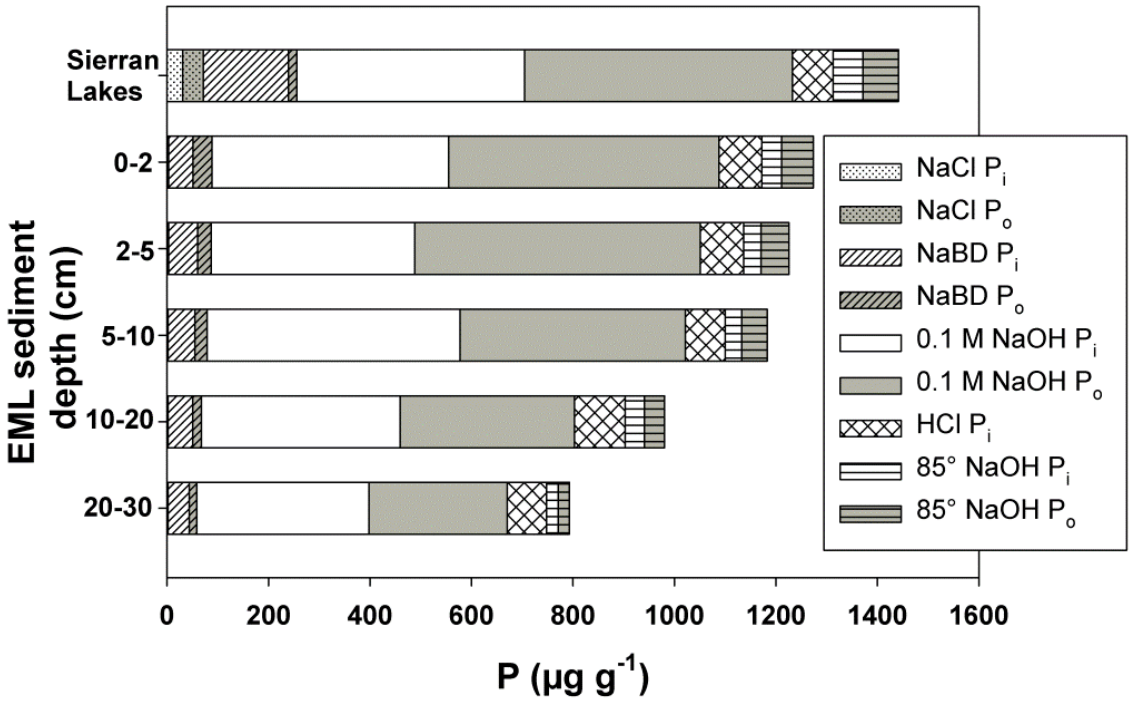

Fig. 5.1. Average P concentrations by sequential extraction in sediments of the surveyed lakes (top bar) and Emerald Lake (depth increments)

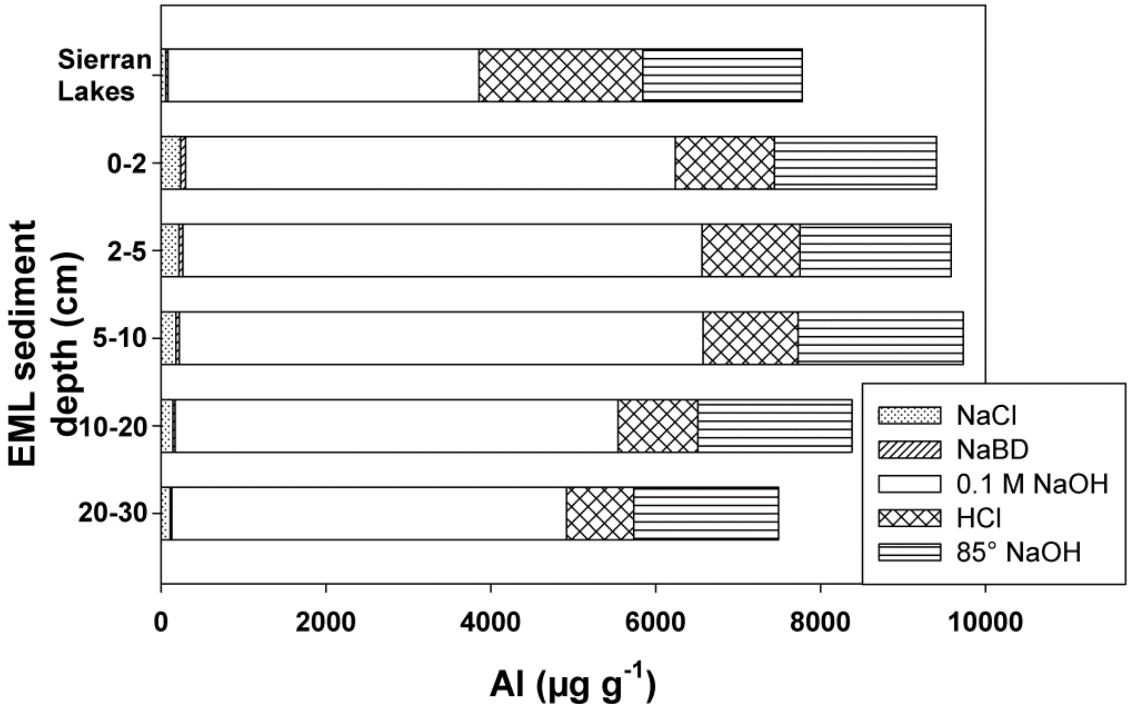

Fig. 5.2. Average Al concentrations by sequential extraction in sediments of the surveyed lakes (top bar) and Emerald Lake (depth increments).

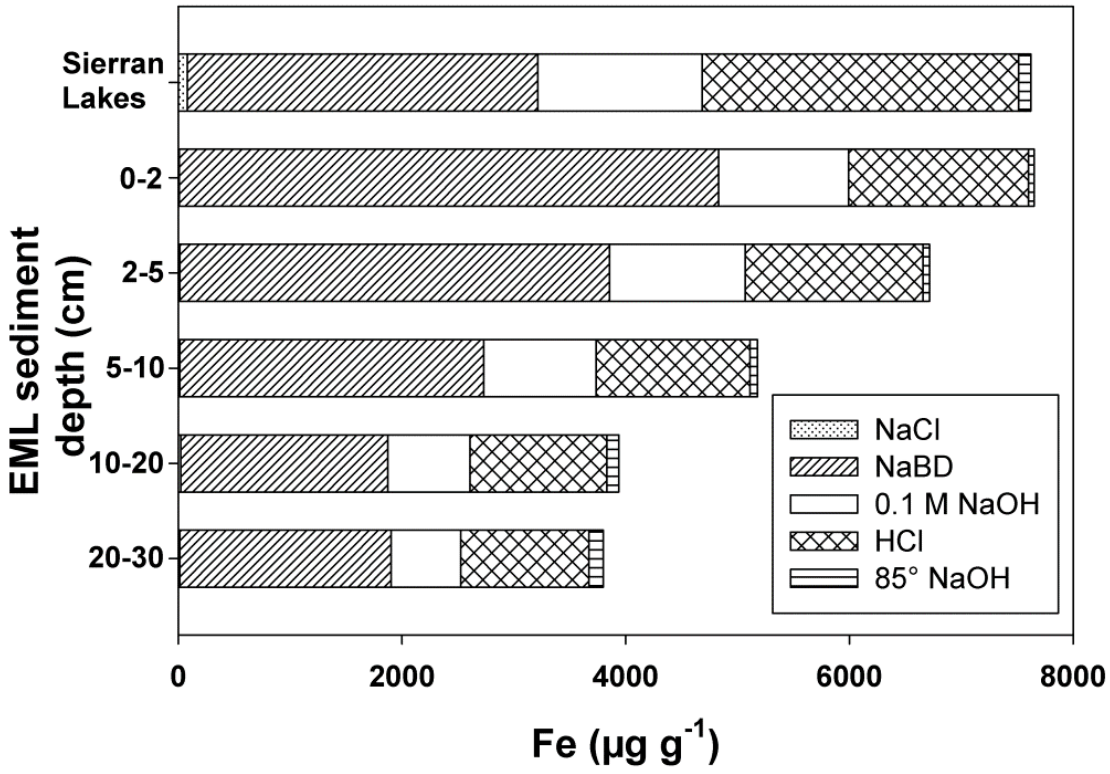

Fig. 5.3. Average Fe concentrations by sequential extraction in sediments of the surveyed lakes (top bar) and Emerald Lake (depth increments).

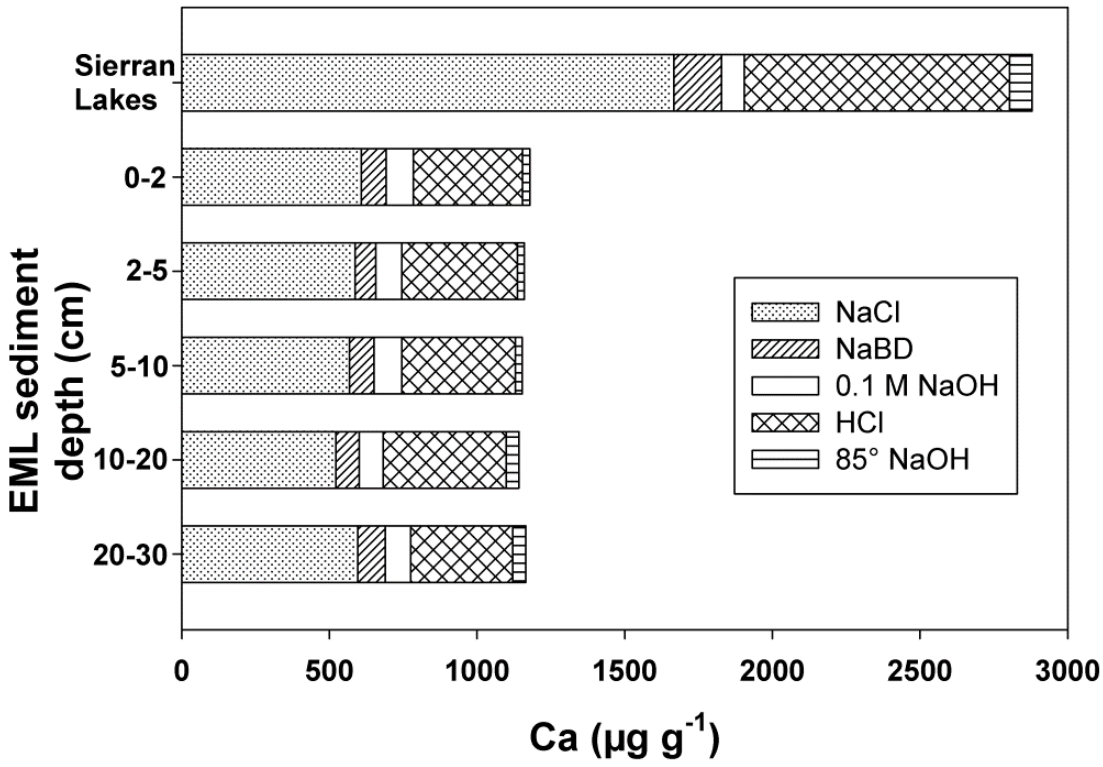

Fig. 5.4. Average Ca concentrations by sequential extraction in sediments of the surveyed lakes (top bar) and Emerald Lake (depth increments).

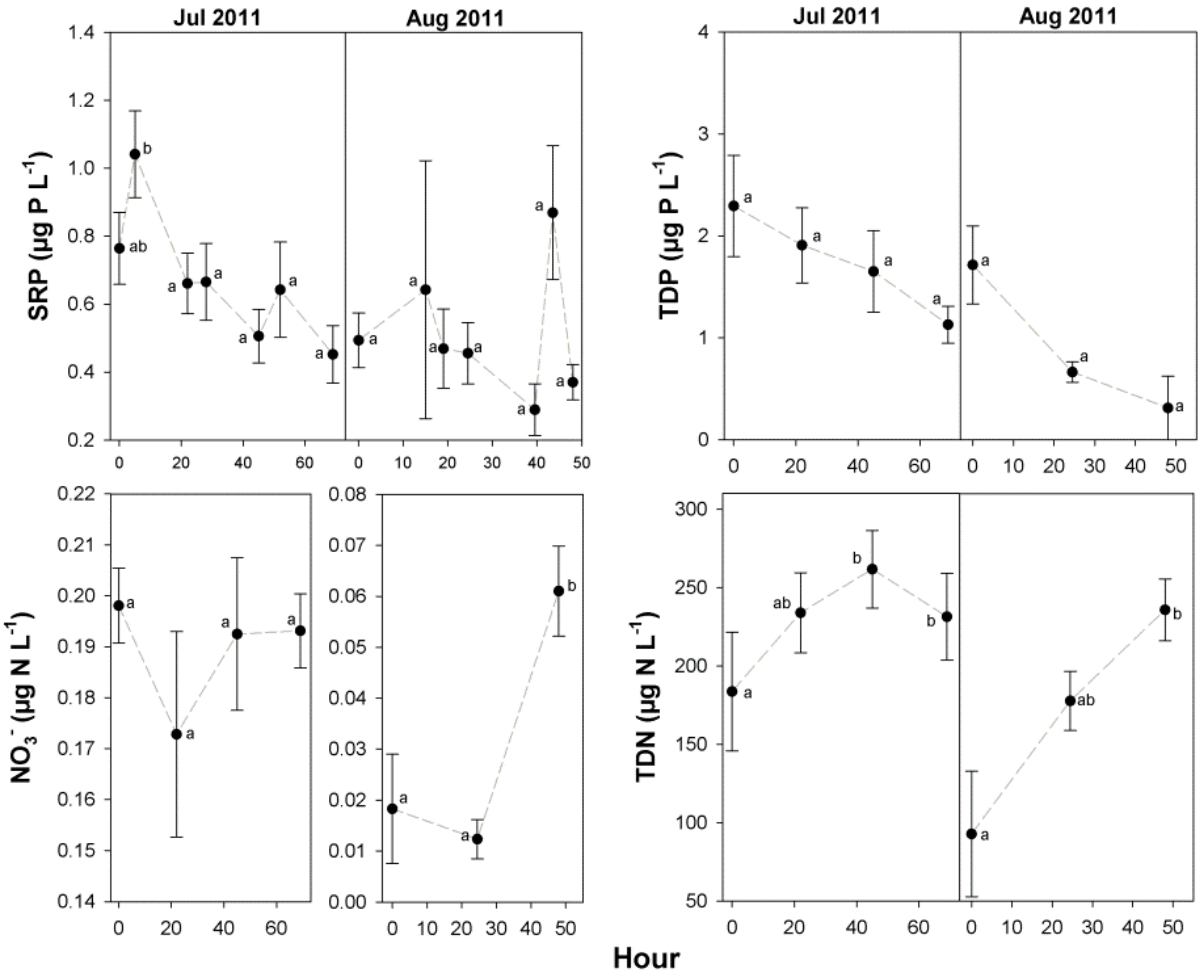

Fig. 5.5. Average (± std. error) SRP, TDP, NO_3^-, and TDN concentrations for sediment cores incubated in-situ at Emerald Lake during July and August, 2011. Significant differences between sampling times are denoted by lower-case letters (α = 0.05).

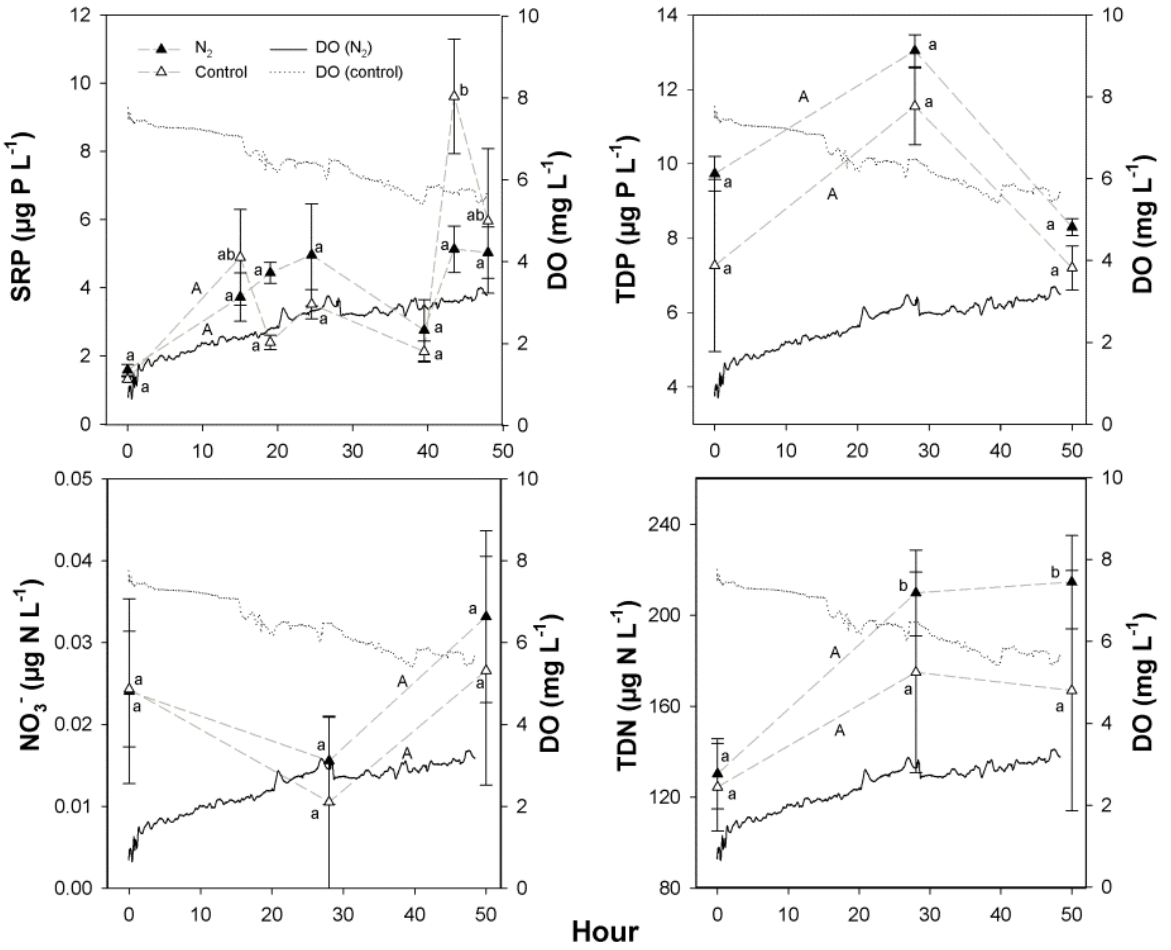

Fig. 5.6. Average (± std. error) SRP, TDP, NO_3^-, and TDN concentrations for sediment cores incubated in-situ at Emerald Lake during September 2011. Significant differences between sampling times are denoted by lower-case letters ($\alpha = 0.05$). Significant differences between treatments are denoted by upper-case letters (A and B; $\alpha = 0.05$). DO concentrations in N_2-treated cores are shown by the solid black line and for reference cores by the dotted line.

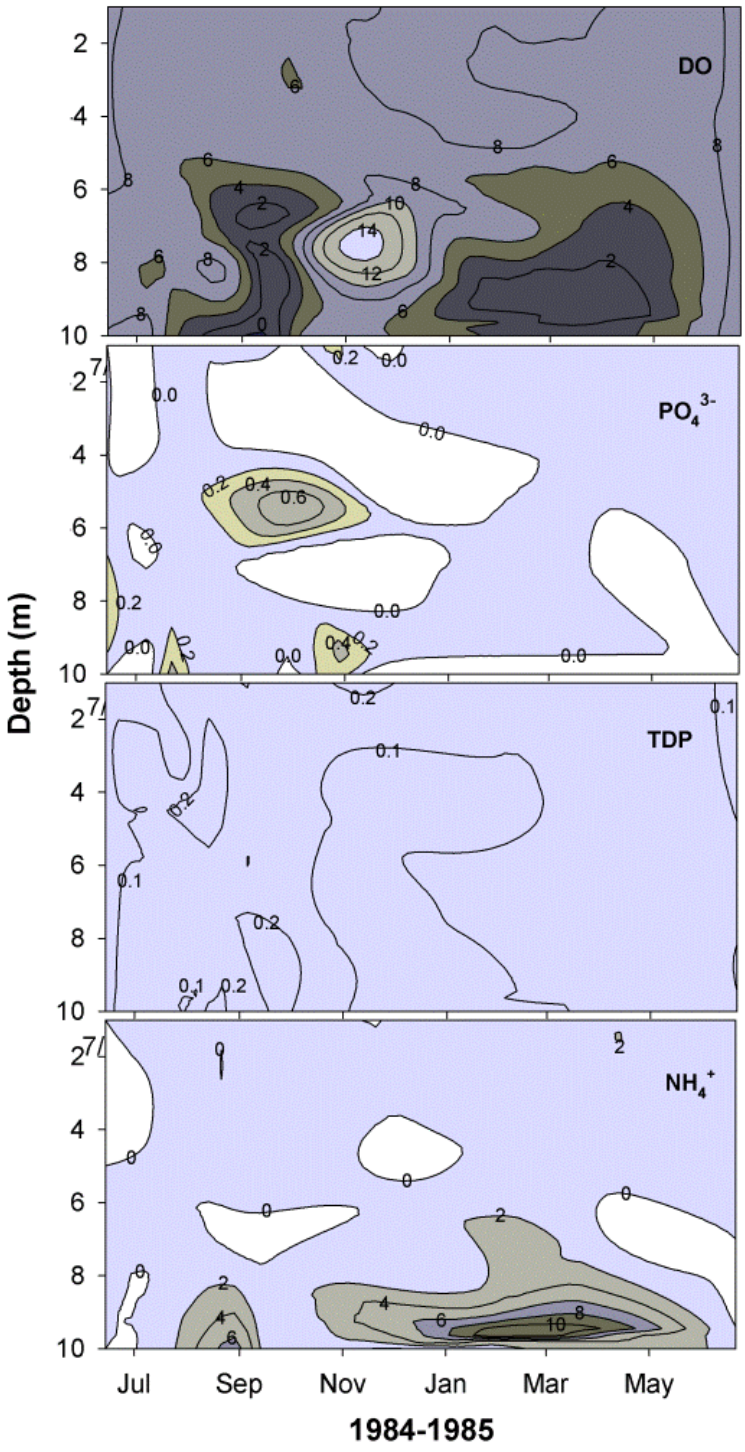

Fig. 5.7. Average time-depth profile for DO, PO_4^{3-}, TDP, and NH_4^+ concentrations in Emerald Lake from June 1984 through July 1985 (J. Sickman, unpublished data). Concentrations are expressed in µg L^{-1} for N and P and mg O_2 L^{-1} for DO.

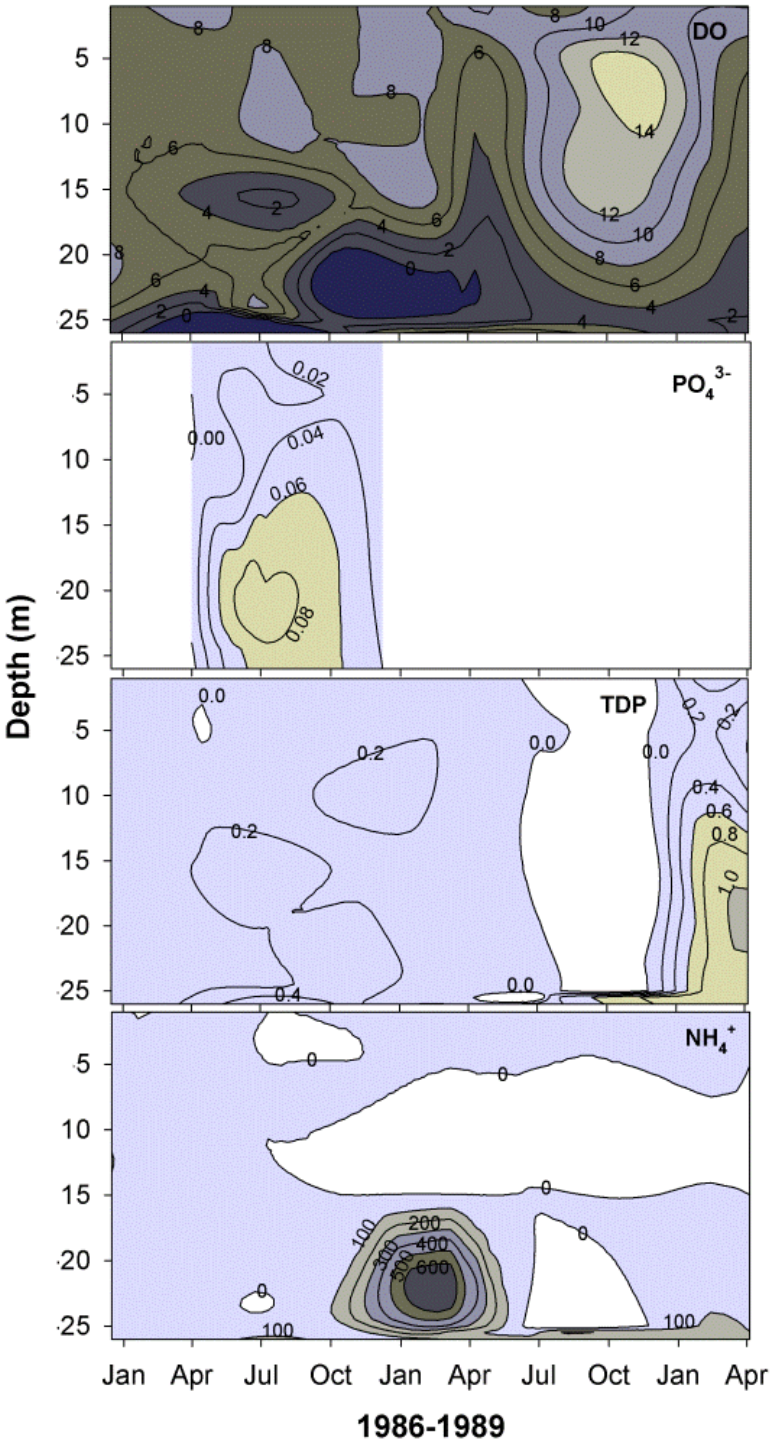

Fig. 5.8. Average time-depth profile for DO, PO_4^{3-}, TDP, and NH_4^+ concentrations in Pear Lake from December 1986 through April 1989 (J. Sickman, unpublished data). Concentrations are expressed in µg L^{-1} for N and P and mg O_2 L^{-1} for DO.

6. OVERARCHING CONCLUSIONS

In summary, chaparral ecosystems are characterized by large hydrologic and gaseous N losses during transitional periods from dry to wet soil conditions, as controlled by C limitation and asynchrony between N availability and plant demand. In chaparral ecosystems, kinetic N saturation is observed in catchments with atmospheric N inputs of 9 kg N ha^{-1} yr^{-1} underscoring the need to establish critical loads that reflect these observations. However, this study highlights potential limitations to the use of N saturation theory on xeric landscapes, as inconsistencies can develop depending on the season in which hydrologic and gaseous N measurements are made. Because of the intrinsic nature of semiarid systems to maintain N limitation, capacity N saturation may be difficult to observe in ecosystems in which most of the N inputs occur during summer and the majority of the N export occurs at the onset of the wet season prior to plant N uptake.

Although the internal loading of P from lacustrine sediments is generally an important mechanism regulating P supply to aquatic environments, in sediments of the Sierra Nevada, P is strongly bound to Al-oxides limiting the contribution of sediments to the eutrophication of alpine lakes. However, because rates of P transfer from sediments to the water column are enhanced by warmer temperatures, future warming, as predicted by climate change models, may increase the contribution of sediments to the P supply of surface waters. From this study, it can be concluded that increases in P supply to alpine lakes are not controlled by internal loading, but rather, I hypothesize that observed increases in P supply are controlled by direct atmospheric P deposition, and presumably,

by a synergistic mechanism between warmer temperatures and shifting hydrology that can mobilize P from catchment soils to surface waters.

This research underscores the importance of seasonal transitions in understanding how the indirect effects of anthropogenic pollution affect Mediterranean-type ecosystems in both chaparral and alpine catchments. Because temperature, extended droughts, and the frequency of extreme rainfall events are predicted to increase for Mediterranean regions, coupled with increased atmospheric N and P deposition, periods of soil rewetting together with hydrologic flushing are likely to significantly influence the biogeochemistry of the Sierra Nevada landscape. In chaparral, continued export of N along with soil acidification and potential vegetation type conversions are expected to intensify, while at higher elevations, increased contribution of aeolian P inputs, development of the soil organic matter pool in response to warmer temperatures, altered cycling of P, and increased frequency of extreme precipitation events are likely to continue to contribute allochthonous materials to high-elevation lakes.

References

Aber, J.D., McDowell, W., Nadelhoffer, K.J., Magill, A., Berntson, G., Kamakea, M., McNulty, S., Currie, W., Rustad, L., Fernandez, I., 1998. Nitrogen saturation in temperate forest ecosystems: hypothesis revisited. BioScience 48, 921-934.

Aber, J.D., Nadelhoffer, K.J., Steudler, P., Melillo, J.M., 1989. Nitrogen saturation in northern forest ecosystems. Bioscience 39, 378-386.

Aber, J.D., Ollinger, S.V., Driscoll, C.T., Likens, G.E., Holmes, R.T., Freuder, R.J., Goodale, C.L., 2002. Inorganic N losses from a forested ecosystem in response to physical, chemical, biotic and climatic perturbations. Ecosystems 5, 648-658.

Agemian, H., 1997. Determination of nutrients in aquatic sediments, In: Mudroch, A., Azcue, J.M., Mudroch, P. (Eds.), Manual of physico-chemical analysis of aquatic sediments. CRC Press, Boca Raton, FL, pp. 175-227.

Allen, E.B., Padgett, P.E., Bytnerowicz, A., Minnich, R., 1998. Nitrogen deposition effects on coastal sage vegetation of southern California. Proceedings of the international symposium on air pollution and climate change effects on forest ecosystems, Riverside, CA February 5-9, 1996. USDA Forest Service, Pacific Southwest Research Station, PSW-GTR-166, 131-140.

Allen, M.F., Sexton, J.C., Moore, T.S., Christensen, M., 1981. Influence of Phosphate Source on Vesicular-Arbuscular Mycorrhizae of Bouteloua-Gracilis. New Phytologist 87, 687-694.

Allison, F.E., 1963. Losses of gaseous nitrogen from soils by chemical mechanisms involving nitrous acid and nitrites. Soil Science 96, 404-409.

Amirbahman, A., Pearce, A.R., Bouchard, R.J., Norton, S.A., Kahl, J.S., 2003. Relationship between hypolimnetic phosphorus and iron release from eleven lakes in Maine, USA. Biogeochemistry 65, 369-385.

Anderson, G., 1974. The nature of alkali-soluble soil organic phosphates. Journal of Soil Science 25, 282-297.

Anderson, G., 1980. Assessing organic phosphorus in soils, In: Khasawneh, F.E., Sample, E.C., Kamprath, E.J. (Eds.), The role of phosphorus in agriculture. American Society of Agronomy, Madison, Wisconsin.

Anderson, G., Arlidge, E.Z., 1962. The adsorption of inositol phosphates and glycerophosphate by soil clays, clay minerals and hydrated sequioxides in acid media. Journal of Soil Science 13, 216-224.

Anderson, G., Williams, E.G., Moir, J.O., 1974. A comparison of the sorption of inorganic phosphate and inositol-hexaphosphate by six acid soils. Journal of Soil Science 25, 51-62.

Anderson, I.C., Levine, J.S., 1986. Relative Rates of Nitric-Oxide and Nitrous-Oxide Production by Nitrifiers, Denitrifiers, and Nitrate Respirers. Applied and Environmental Microbiology 51, 938-945.

Anderson, I.C., Levine, J.S., 1987. Simultaneous field measurements of biogenic emissions of nitric oxide and nitrous oxide. Journal of Geophysical Research 92, 965-976.

Anderson, I.C., Levine, J.S., Poth, M.A., Riggan, P.J., 1988. Enhanced biogenic emissions of nitric oxide and nitrous oxide following surface biomass burning. Journal of Geophysical Research-Atmospheres 93, 3893-3898.

Anderson, I.C., Poth, M.A., 1989. Semiannual losses of nitrogen as NO and N_2O from unburned and burned chaparral. Global Biogeochemical Cycles 3, 121-135.

Anthony, J.L., Lewis, W.M., 2012. Low boundary layer response and temperature dependence of nitrogen and phosphorus releases from oxic sediments of an oligotrophic lake. Aquatic Sciences 74, 611-617.

Bateman, P.C., Clark, L.D., Huber, N.K., Moore, J.G., Rinehart, C.D., 1963. The Sierra Nevada batholith: A synthesis of recent work across the central part. U.S. Geological Survey Paper 414-D.

Belser, L.W., Mays, E.L., 1980. Specific-inhibition of nitrite oxidation by chlorate and its use in assessing nitrification in soils and sediments. Applied and Environmental Microbiology 39, 505-510.

Bennett, D.M., Sickman, J.O., Lucero, D.M., Whitmore, T.J., *in press*. Diatom-interference models for acid-neutralizing capacity and nitrate based on a 50-lake calibration dataset from the Sierra Nevada, California, USA. Jounal of Paleolimnology.

Berg, P., Klemedtsson, L., Rosswall, T., 1982. Inhibitory effect of low partial pressures of acetylyne on nitrification. Soil Biology & Biochemistry 14, 301-303.

Bernal, S., Butturini, A., Sabater, F., 2005. Seasonal variations of dissolved nitrogen and DOC : DON ratios in an intermittent Mediterranean stream. Biogeochemistry 75, 351-372.

Billings, S.A., Schaeffer, S.M., Evans, R.D., 2002. Trace N gas losses and N mineralization in Mojave desert soils exposed to elevated CO2. Soil Biology & Biochemistry 34, 1777-1784.

Blackmer, A.M., Bremner, J.M., 1976. Potential of Soil as a Sink for Atmospheric Nitrous-Oxide. Geophysical Research Letters 3, 739-742.

Blackwell, M.S.A., Brookes, P.C., de la Fuente-Martinez, N., Murray, P.J., Snars, K.E., Williams, J.K., Haygarth, P.M., 2009. Effects of soil drying and rate of re-wetting on concentrations and forms of phosphorus in leachate. Biology and Fertility of Soils 45, 635-643.

Bobbink, R., Hicks, K., Galloway, J., Spranger, T., Alkemade, R., Ashmore, M., Bustamante, M., Cinderby, S., Davidson, E., Dentener, F., Emmett, B., Erisman, J.W., Fenn, M., Gilliam, F., Nordin, A., Pardo, L., De Vries, W., 2010. Global assessment of nitrogen deposition effects on terrestrial plant diversity: a synthesis. Ecological Applications 20, 30-59.

Bollmann, A., Conrad, R., 1997. Enhancement by acetylene of the decomposition of nitric oxide in soil. Soil Biology & Biochemistry 29, 1057-1066.

Borken, W., Matzner, E., 2009. Reappraisal of drying and wetting effects on C and N mineralization and fluxes in soils. Global Change Biology 15, 808-824.

Bormann, F.H., Likens, G.E., Siccama, T.G., Pierce, R.S., Eaton, J.S., 1974. The export of nutrients and recovery of stable conditions following deforestation at Hubbard Brook. Ecological Monographs 44, 255-277.

Böstrom, B., Andersen, J.M., Fleischer, S., Jansson, M., 1988. Exchange of phosphorus across the sediment-water interface. Hydrobiologia 170, 229-244.

Boström, B., Petterson, K., 1982. Different patterns of phosphorus release from lake sediments in laboratory experiments. Hydrobiologia 92, 415-429.

Bowman, R.A., Cole, C.V., 1978a. An exploratory method for fractionation of organic phosphorus from grassland soils. Soil Science 125, 95-101.

Bowman, R.A., Cole, C.V., 1978b. Transformations of organic phosphorus substrates in soils as evaluated by $NaHCO_3$ extraction. Soil Science 125, 49-54.

Brookes, P.C., Landman, A., Pruden, G., Jenkinson, D.S., 1985. Chloroform Fumigation and the Release of Soil-Nitrogen - a Rapid Direct Extraction Method to Measure Microbial Biomass Nitrogen in Soil. Soil Biology & Biochemistry 17, 837-842.

Brooks, P.D., Williams, M.W., Schmidt, S.K., 1996. Microbial activity under alpine snowpacks, Niwot Ridge, Colorado. Biogeochemistry 32, 93-113.

Brooks, P.D., Williams, M.W., Schmidt, S.K., 1998. Inorganic nitrogen and microbial biomass dynamics before and during spring snowmelt. Biogeochemistry 43, 1-15.

Brookshire, E.N.J., Valett, H.M., Thomas, S.A., Webster, J.R., 2007. Atmospheric N deposition increases organic N loss from temperate forests. Ecosystems 10, 252-262.

Brown, A.D., Lund, L.J., Lueking, M.A., 1990. Integrated soil processes studies at Emerald Lake watershed. Final Report, California Air Resources Board contract A5-204-32.

Burkins, D.L., Blum, J.D., Brown, K., Reynolds, R.C., Erel, Y., 1999. Chemistry and mineralogy of a granitic, glacial soil chronosequence, Sierra Nevada Mountains, California. Chemical Geology 162, 1-14.

Burns, D.A., Murdoch, P.S., 2005. Effects of a clearcut on the net rates of nitrification and N mineralization in a northern hardwood forest, Catskill Mountains, New York, USA. Biogeochemistry 72, 123-146.

Butterly, C.R., McNeill, A.M., Baldock, J.A., Marschner, P., 2011. Rapid changes in carbon and phosphorus after rewetting of dry soil. Biology and Fertility of Soils 47, 41-50.

Campbell, P., 1994. Phorphorus budgets and stoichiometry during the open-water season in two unmanipulated lakes in the Experimental Lakes Area, northwestern Ontario. Canadian Journal of Fisheries and Aquatic Sciences 51, 2739-2755.

Caraco, N.F., 1993. Disturbance of the Phosphorus Cycle - a Case of Indirect Effects of Human Activity. Trends in Ecology & Evolution 8, 51-54.

Caraco, N.F., Cole, J.J., Likens, G.E., 1993. Sulfate control of phosphorus availability in lakes. A test and re-evaluation of Hasler and Einsele's model. Hydrobiologia 253, 275-280.

Carey, C.C., Rydin, E., 2011. Lake trophic status can be determined by the depth distribution of sediment phosphorus. Limnology and Oceanography 56, 2051-2063.

Cassagne, N., Remaury, M., Gauquelin, T., Fabre, A., 2000. Forms and profile distribution of soil phosphorus in alpine Inceptisols and Spodosols (Pyrenees, France). Geoderma 95, 161-172.

Celi, L., Barberis, E., 2005. Abiotic stabilization of organic phosphorus in the environment, In: Turner, B.L., Frossard, E., Baldwin, D.S. (Eds.), Organic phosphorus in the environment. CAB International, Cambridge, MA, pp. 113-132.

Celi, L., Lamacchia, S., Marsan, F.A., Barberis, E., 1999. Interaction of inositol hexaphosphate on clays: Adsorption and charging phenomena. Soil Science 164, 574-585.

Chadwick, O.A., Derry, L.A., Vitousek, P.M., Huebert, B.J., Hedin, L.O., 1999. Changing sources of nutrients during four million years of ecosystem development. Nature 397, 491-497.

Chapuis-Lardy, L., Wrage, N., Metay, A., Chotte, J.L., Bernoux, M., 2007. Soils, a sink for N_2O? A review. Global Change Biology 13, 1-17.

Cisneros, R., Bytnerowicz, A., Schweizer, D., Zhong, S.R., Traina, S., Bennett, D.H., 2010. Ozone, nitric acid, and ammonia air pollution is unhealthy for people and ecosystems in southern Sierra Nevada, California. Environmental Pollution 158, 3261-3271.

Cleveland, C.C., Liptzin, D., 2007. C : N : P stoichiometry in soil: is there a "Redfield ratio" for the microbial biomass? Biogeochemistry 85, 235-252.

Cline, D., 1995. Snow surface energy exchanges and snowmelt at a continental alpine site, In: Tonnessen, K.A., Williams, M.W., Tranter, M. (Eds.), Biogeochemistry of seasonally snow-covered basins. International Association for Hydrological Sciences, pp. 157-166.

Cohn, T.A., 1995. Recent advances in statistical methods for the estimation of sediment and nutrient transport in rivers. Reviews of Geophysics 33, 1117-1123.

Cole, C.V., Elliott, E.T., Hunt, H.W., Coleman, D.C., 1978. Trophic Interactions in Soils as They Affect Energy and Nutrient Dynamics .V. Phosphorus Transformations. Microbial Ecology 4, 381-387.

Conant, R.T., Ryan, M.G., Agren, G.I., Birge, H.E., Davidson, E.A., Eliasson, P.E., Evans, S.E., Frey, S.D., Giardina, C.P., Hopkins, F.M., Hyvonen, R., Kirschbaum, M.U.F., Lavallee, J.M., Leifeld, J., Parton, W.J., Steinweg, J.M., Wallenstein, M.D., Wetterstedt, J.A.M., Bradford, M.A., 2011. Temperature and soil organic matter decomposition rates - synthesis of current knowledge and a way forward. Global Change Biology 17, 3392-3404.

Condron, L.M., Tiessen, H., 2005. Interactions of organic phosphorus in terrestrial ecosystems, In: Turner, B.L., Frossard, E., Baldwin, D.S. (Eds.), Organic phosphorus in the environment. CAB International, Cambridge, MA, pp. 295-307.

Conrad, R., 1994. Compensation Concentration as Critical Variable for Regulating the Flux of Trace Gases between Soil and Atmosphere. Biogeochemistry 27, 155-170.

Conrad, R., 1996. Soil microorganisms as controllers of atmospheric trace gases (H_2, CO, CH_4, OCS, N_2O, and NO). Microbiological Reviews 60, 609-640.

Coplen, T.B., Bohke, J.K., Casciotti, K.L., 2004. Using dual-bacterial denitrification to improve delta N-15 determinations of nitrates containing mass-independent 17O. Rapid Communications in Mass Spectrometry 18, 245-250.

Correll, D.L., 1998. The role of phosphorus in the eutrophication of receiving waters: a review. Journal of Environmental Quality 27, 261-266.

Coxson, D.S., Parkinson, D., 1987. The Pattern of Winter Respiratory Response to Temperature, Moisture, and Freeze Thaw Exposure in Bouteloua-Gracilis Dominated Grassland Soils of Southwestern Alberta. Canadian Journal of Botany-Revue Canadienne De Botanique 65, 1716-1725.

Cross, A.F., Schlesinger, W.H., 1995. A literature review and evaluation of the Hedley fractionation: applications to the biogeochemical cycle of soil phosphorus in natural ecosystems. Geoderma 64, 197-214.

Crutzen, P.J., 1979. Role of NO and NO_2 in the Chemistry of the Troposphere and Stratosphere. Annual Review of Earth and Planetary Sciences 7, 443-472.

Curtis, C.J., Evans, C.D., Goodale, C.L., Heaton, T.H.E., 2011. What Have Stable Isotope Studies Revealed About the Nature and Mechanisms of N Saturation and Nitrate Leaching from Semi-Natural Catchments? Ecosystems 14, 1021-1037.

Dahlgren, R.A., Boettinger, J.L., Huntington, G.L., Amundson, R.G., 1997. Soil development along an elevational transect in the western Sierra Nevada, California. Geoderma 78, 207-236.

Dail, B.D., Davidson, E.A., Chorover, J., 2001. Rapid abiotic transformatoin of nitrate in an acid forest soil. Biogeochemistry 54, 131-146.

Davidson, E.A., 1992. Sources of nitric oxide and nitrous oxide following wetting of dry soil. Soil Science Society of America Journal 56, 95-102.

Davidson, E.A., Keller, M., Erickson, H.E., Verchot, L.V., Veldkamp, E., 2000. Testing a conceptual model of soil emissions of nitrous and nitric oxides. Bioscience 50, 667-680.

Davidson, E.A., Kingerlee, W., 1997. A global inventory of nitric oxide emissions from soils. Nutrient Cycling in Agroecosystems 48, 37-50.

Davidson, E.A., Matson, P.A., Vitousek, P.M., Riley, R., Dunkin, K., Garciamendez, G., Maass, J.M., 1993. Processes regulating soil emissions of NO and N_2O in a seasonally dry tropical forest. Ecology 74, 130-139.

Davidson, E.A., Schimel, J.P., 1995. Microbial processes of production and consumption of nitric oxide, nitrous oxide and methane, In: Matson, P.A., Harriss, R.C. (Eds.), Biogenic trace gases: measuring emissions from soil and water. Oxford: Blackwell Scientific Publications Ltd, pp. 327-357.

Davidson, E.A., Vitousek, P.M., Matson, P.A., Riley, R., Garcia-Mendez, G., Maass, M., 1991. Soil emissions of nitric oxide in a seasonally dry tropical forest of Mexico. Journal of Geophysical Research 96, 15439-15445.

Del Grosso, S.J., Parton, W.J., Mosier, A.R., Walsh, M.K., Ojima, D.S., Thornton, P.E., 2006. DAYCENT national-scale simulations of nitrous oxide emissions from cropped soils in the United States. Journal of Environmental Quality 35, 1451-1460.

Dickens, S.J.M., 2011. Exotic plant invasion alters chaparral ecosystem resistance, resilience and succession, Botany and Plant Sciences. University of California, Riverside, Riverside, CA.

DiStefano, J.F., Gholz, J.L., 1986. A proposed use of ion exchange resin to measure nitrogen mineralization and nitrification in intact soil cores. Communications in Soil and Plant Analysis 17, 989-998.

Doyle, A., Weintraub, M.N., Schimel, J.P., 2004. Persulfate digestion and simultaneous colorimetric analysis of carbon and nitrogen in soil extracts. Soil Science Society of America Journal 68, 669-676.

Driscoll, C.T., Driscoll, K.M., Mitchell, M.J., Raynal, D.J., 2003. Effects of acidic deposition on forest and aquatic ecosystems in New York State. Environmental Pollution 123, 327-336.

Edmondson, W.T., Anderson, G.C., Peterson, D.R., 1956. Artificial eutrophication of Lake Washington. Limnology and Oceanography 1, 47-53.

Edwards, K.A., McCulloch, J., Kershaw, G.P., Jefferies, R.L., 2006. Soil microbial and nutrient dynamics in a wet Arctic sedge meadow in late winter and early spring. Soil Biology & Biochemistry 38, 2843-2851.

Ellis, B.A., Kummerow, J., 1989. The importance of N_2 fixation in *Ceanothus* seedlings in early postfire chaparral, In: Keeley, S.C. (Ed.), The California chaparral: paradigms reexamined. Natural History Museum of Los Angeles County, Science Series No. 34, Los Angeles, CA, USA, pp. 115-116.

Erickson, H., Davidson, E.A., Keller, M., 2002. Former land-use and tree species affect nitrogen oxide emissions from a tropical dry forest. Oecologia 130, 297-308.

Erisman, J.W., Galloway, J., Seitzinger, S., Bleeker, A., Butterbach-Bahl, K., 2011. Reactive nitrogen in the environment and its effect on climate change. Current Opinion in Environmental Sustainability 3, 281-290.

Evans, C., Davies, T.D., 1998. Causes of concentration/discharge hysteresis and its potential as a tool for analysis of episode hydrochemistry. Water Resources Research 34, 129-137.

Fang, Y.T., Zhu, W.X., Gundersen, P., Mo, J.M., Zhou, G.Y., Yoh, M., 2009. Large Loss of Dissolved Organic Nitrogen from Nitrogen-Saturated Forests in Subtropical China. Ecosystems 12, 33-45.

Farmer, V.C., Wilson, M.J., 1970. Experimental conversion of biotite to hydrobiotite. Nature 226, 841-842.

Fenn, M.E., Allen, E.B., Geiser, L.H., 2011. Mediterranean California, In: Pardo, L.H., Robin-Abbott, M.J., Driscoll, C.T. (Eds.), Assessment of the nitrogen deposition effects and empirical critical loads of nitrogen for ecoregions of the United States. U.S. Forest Service, Newton Square, PA, pp. 143-169.

Fenn, M.E., Allen, E.B., Weiss, S.B., Jovan, S., Geiser, L.H., Tonnesen, G.S., Johnson, R.F., Rao, L.E., Gimeno, B.S., Yuan, F., Meixner, T., Bytnerowicz, A., 2010. Nitrogen critical loads and management alternatives for N-impacted ecosystems in California. Journal of Environmental Management 91, 2404-2423.

Fenn, M.E., Baron, J.S., Allen, E.B., Rueth, H.M., Nydick, K.R., Geiser, L., Bowman, W.D., Sickman, J.O., Meixner, T., Johnson, D.W., Neitlich, P., 2003a. Ecological effects of nitrogen deposition in the western United States. Bioscience 53, 404-420.

Fenn, M.E., Haeuber, R., Tonnesen, G.S., Baron, J.S., Grossman-Clarke, S., Hope, D., Jaffe, D.A., Copeland, S., Geiser, L., Rueth, H.M., Sickman, J.O., 2003b. Nitrogen emissions, deposition, and monitoring in the western United States. Bioscience 53, 391-403.

Fenn, M.E., Poth, M.A., 1999. Temporal and spatial trends in streamwater nitrate concentrations in the San Bernardino Mountains, southern California. Journal of Environmental Quality 28, 822-836.

Fenn, M.E., Poth, M.A., 2004. Monitoring nitrogen deposition in throughfall using ion exchange resin columns: A field test in the San Bernardino Mountains. Journal of Environmental Quality 33, 2007-2014.

Fenn, M.E., Poth, M.A., Aber, J.D., Baron, J.S., Bormann, B.T., Johnson, D.W., Lemly, A.D., McNulty, S.G., Ryan, D.E., Stottlemyer, R., 1998. Nitrogen excess in North American ecosystems: Predisposing factors, ecosystem responses, and management strategies. Ecological Applications 8, 706-733.

Fenn, M.E., Poth, M.A., Bytnerowicz, A., Sickman, J.O., Takemoto, B.K., 2003c. Effects of ozone, nitrogen deposition, and other stressors on montane ecosystems in the Sierra Nevada, In: Bytnerowicz, A., Arbaugh, M.J., Alonso, R. (Eds.), Ozone air pollution in the Sierra Nevada: distribution and effects on forests. Elsevier, Amsterdam (Netherlands), pp. 111-155.

Fenn, M.E., Poth, M.A., Dunn, P.H., Barro, S.C., 1993. Microbial N and biomass, respiration and N-mineralization in soils beneath two chaparral species along a fire-induced age gradient. Soil Biology & Biochemistry 25, 457-466.

Fenn, M.E., Poth, M.A., Johnson, D.W., 1996. Evidence for nitrogen saturation in the San Bernardino Mountains in southern California. Forest Ecology and Management 82, 211-230.

Fierer, N., Schimel, J.P., 2002. Effects of drying-rewetting frequency on soil carbon and nitrogen transformations. Soil Biology & Biochemistry 34, 777-787.

Fierer, N., Schimel, J.P., 2003. A proposed mechanism for the pulse in carbon dioxide production commonly observed following the rapid rewetting of a dry soil. Soil Science Society of America Journal 67, 798-805.

Filippa, G., Freppaz, M., Williams, M.W., Helmig, D., Liptzin, D., Seok, B., Hall, B., Chowanski, K., 2009. Winter and summer nitrous oxide and nitrogen oxides fluxes from a seasonally snow-covered subalpine meadow at Niwot Ridge, Colorado. Biogeochemistry 95, 131-149.

Firestone, M.K., Davidson, E.A., 1989. Microbial basis of NO and N_2O production and consumption in soil, In: Andreae, M.O., Schimel, D.S. (Eds.), Exchange of trace gases between terrestrial ecosystems and the atmosphere. John Wiley & Sons, New York, pp. 7-21.

Fischer, J.M., Olson, M.H., Williamson, C.E., Everhart, J.C., Hogan, P.J., Mack, J.A., Rose, K.C., Saros, J.E., Stone, J.R., Vinebrooke, R.D., 2011. Implications of climate change for Daphnia in alpine lakes: predictions from long-term dynamics, spatial distribution, and a short-term experiment. Hydrobiologia 676, 263-277.

Fitzhugh, R.D., Lovett, G.M., Venterea, R.T., 2003. Biotic and abiotic immobilization of ammonium, nitrite, and nitrate in soils developed under different tree species in the Catskill Mountains, New York, USA. Global Change Biology 9, 1591-1601.

Freppaz, M., Williams, B.L., Edwards, A.C., Scalenghe, R., Zanini, E., 2007. Simulating soil freeze/thaw cycles typical of winter alpine conditions: Implications for N and P availability. Applied Soil Ecology 35, 247-255.

Frossard, E., Stewart, J.W.B., Starnaud, R.J., 1989. Distribution and Mobility of Phosphorus in Grassland and Forest Soils of Saskatchewan. Canadian Journal of Soil Science 69, 401-416.

Gächter, R., Meyer, J.S., Mares, A., 1988. contribution of bacteria to release and fixation of phosphorus in lake sediments. Limnology and Oceanography 33, 1542-1558.

Galloway, J.N., Dentener, F.J., Capone, D.G., Boyer, E.W., Howarth, R.W., Seitzinger, S.P., Asner, G.P., Cleveland, C.C., Green, P.A., Holland, E.A., Karl, D.M., Michaels, A.F., Porter, J.H., Townsend, A.R., Vorosmarty, C.J., 2004. Nitrogen cycles: past, present, and future. Biogeochemistry 70, 153-226.

Garcia, C., Hernandez, T., Costa, F., 1994. Microbial activity in soils under Mediterranean environmental conditions. Soil Biology & Biochemistry 26, 1185-1191.

Gelfand, I., Feig, G., Meixner, F.X., Yakir, D., 2009. Afforestation of semi-arid shrubland reduces biogenic NO emission from soil. Soil Biology & Biochemistry 41, 1561-1570.

Gelfand, I., Yakir, D., 2008. Influence of nitrite accumulation in association with seasonal patterns and mineralization of soil nitrogen in a semi-arid pine forest. Soil Biology & Biochemistry 40, 415-424.

Goldberg, S.D., Knorr, K.H., Gebauer, G., 2008. N2O concentration and isotope signature along profiles provide deeper insight into the fate of N2O in soils. Isotopes in Environmental and Health Studies 44, 377-391.

Goodale, C.L., Aber, J.D., McDowell, W.H., 2000. The long-term effects of disturbance on organic and inorganic nitrogen export in the White Mountains, New Hampshire. Ecosystems 3, 433-450.

Grulke, N.E., Dobrowolski, W., Mingus, P., Fenn, M.E., 2005. California black oak response to nitrogen amendment at a high O_3, nitrogen-saturated site. Environmental Pollution 137, 536-545.

Güsewell, S., 2004. N:P ratios in terrestrial plants: variation and functional significance. New Phytologist 164, 243-266.

Gurevitch, J., Scheiner, S.M., Fox, G.A., 2002. The ecology of plants. Sinauer Associates Inc., Sunderland, MA.

Hall, S.J., Huber, D., Grimm, N.B., 2008. Soil N2O and NO emissions from an arid, urban ecosystem. Journal of Geophysical Research-Biogeosciences 113, 11.

Hall, S.J., Matson, P.A., 2003. Nutrient status of tropical rain forests influences soil N dynamics after N additions. Ecological Monographs 73, 107-129.

Hall, S.J., Matson, P.A., Roth, P.M., 1996. NOx emissions from soil: Implications for air quality modeling in agricultural regions. Annual Review of Energy and the Environment 21, 311-346.

Hanes, T.L., 1971. Succession after fire in the chaparral of southern California. Ecological Monographs 41, 27-52.

Harrison, A.F., 1987. Soil organic phosphorus: A review of world literature. CAB International, Wallingford, UK.

Hasler, A.D., Einsele, W.G., 1948. Fertilization for increasing productivity of natural inland waters. Trans. N. Amer. Wildl. Conf. 13, 527-555.

Hedin, L.O., Armesto, J.J., Johnson, A.H., 1995. Patterns of nutrient loss from unpolluted, old-growth temperate forests: evaluation of biogeochemical theory. Ecology 76, 493-509.

Hendershot, W.H., Lalande, H., Duquette, M., 2008. Soil reaction and exchangeable acidity, In: Carter, M.R., Gregorich, E.G. (Eds.), Soil sampling and methods of analysis. Canadian Society of Soil Science, Boca Raton, Fl.

Hesterberg, D., 2010. Macroscale chemical properties and X-ray absorption spectroscopy of soil phosphorus, In: Singh, B., Gräfe, M. (Eds.), Developments in soil science: Synchrotron-based techniques in soils and sediments. Elsevier B.V., The Netherlands, pp. 313-356.

Hjorth, T., 2004. Effects of freeze-drying on partitioning patterns of major elements and trace metals in lake sediments. Analytica Chimica Acta 526, 95-102.

Homyak, P.M., Yanai, R.D., Burns, D.A., Briggs, R.D., Germain, R.H., 2008. Nitrogen immobilization by wood-chip application: Protecting water quality in a northern hardwood forest. Forest Ecology and Management 255, 2589-2601.

House, W.A., Denison, F.H., 2002. Total phosphorus content of river sediments in relationship to calcium, iron and organic matter concentrations. Science of the Total Environment 282, 341-351.

Huntington, G.L., Akeson, M.A., 1987. Soil resource inventory of Sequoia National Park Central Part. Department of Interior National Park Service, California, U.S. Order No. 8005-2-0002.

Hupfer, M., Rube, B., Schmieder, P., 2004. Origin and diagenesis of polyphosphate in lake sediments: A ^{31}P-NMR study. Limnology and Oceanography 49, 1-10.

IPCC, 2007. Climate change 2007: the physical science basis, Geneva, 1-18 pp.

Jensen, H.S., Andersen, F.O., 1992. Importance of temperature, nitrate, and pH for phosphate release from aerobic sediments of four shallow, eutrophic lakes. Limnology and Oceanography 37, 577-589.

Judd, K.E., Likens, G.E., Groffman, P.M., 2007. High nitrate retention during winter in soils of the hubbard brook experimental forest. Ecosystems 10, 217-225.

Kana, J., Kopacek, J., 2006. Impact of soil sorption characteristics and bedrock composition on phosphorus concentrations in two Bohemian Forest lakes. Water Air and Soil Pollution 173, 243-259.

Kana, J., Kopacek, J., Camarero, L., Garcia-Pausas, J., 2011. Phosphate Sorption Characteristics of European Alpine Soils. Soil Science Society of America Journal 75, 862-870.

Keeley, J.E., Davis, F.W., 2007. Chaparral, In: Barbour, M.J., Keeler-Wolf, T., Schoenherr, A.A. (Eds.), Terrestrial vegetation of California. University of California Press, Berkeley, CA, pp. 339-366.

Keeley, J.E., Lubin, D., Fotheringham, C.J., 2003. Fire and grazing impacts on plant diversity and alien plant invasions in the southern Sierra Nevada. Ecological Applications 13, 1355-1374.

Kendall, C., 1998. Tracing nitrogen sources and cycles in catchments, In: Kendall, C., McDonnell, J.J. (Eds.), Isotope Tracers in Catchment Hydrology. Elsevier Science, Amsterdam, The Netherlands, pp. 519-576.

Kieft, T.L., Soroker, E., Firestone, M.K., 1987. Microbial biomass response to a rapid increase in water potential when dry soil is wetted. Soil Biology & Biochemistry 19, 119-126.

Kim, J., 2005. A projection of the effects of climate change induced by increased CO_2 on extreme hydrologic events in the western US. Climate Change 68, 153-168.

Knowles, N., Dettinger, M.D., Cayan, D.R., 2006. Trends in snowfall versus rainfall in the Western United States. Journal of Climate 19, 4545-4559.

Kopacek, J., Borovec, J., Hejzlar, J., Ulrich, K.U., Norton, S.A., Amirbahman, A., 2005. Aluminum control of phosphorus sorption by lake sediments. Environmental Science & Technology 39, 8784-8789.

Kopacek, J., Hejzlar, J., Vrba, J., Stuchlik, E., 2011. Phosphorus loading of mountain lakes: Terrestrial export and atmospheric deposition. Limnology and Oceanography 56, 1343-1354.

Kopacek, J., Maresova, M., Norton, S.A., Porcal, P., Vesely, J., 2006. Photochemical source of metals for sediments. Environmental Science & Technology 40, 4455-4459.

Kopacek, J., Prochazkova, L., Stuchlik, E., Blazka, P., 1995. The Nitrogen-Phosphorus Relationship in Mountain Lakes - Influence of Atmospheric Input, Watershed, and Ph. Limnology and Oceanography 40, 930-937.

Kopacek, J., Ulrich, K.U., Hejzlar, J., Borovec, J., Stuchlik, E., 2001. Natural inactivation of phosphorus by aluminum in atmospherically acidified water bodies. Water Research 35, 3783-3790.

Kram, P., Hruska, J., Driscoll, C.T., Johnson, C.E., 1995. Biogeochemistry of aluminum in a forest catchment in the Czech Republic impacted by atmospheric inputs of strong acids. Water Air and Soil Pollution 85, 1831-1836.

Kummerow, J., Alexander, J.V., Neel, J.W., Fishbeck, K., 1978. Symbiotic nitrogen fixation in Ceanothus roots. American Journal of Botany 65, 63-69.

Le Bissonnais, Y., 1996. Aggregate stability and assessment of soil crustability and erodibility: I. Theory and methodology. European Journal of Soil Science 47, 425-437.

Li, X.Y., Meixner, T., Sickman, J.O., Miller, A.E., Schimel, J.P., Melack, J.M., 2006. Decadal-scale dynamics of water, carbon and nitrogen in a California chaparral ecosystem: DAYCENT modeling results. Biogeochemistry 77, 217-245.

Likens, G.E., Bormann, F.H., Johnson N. M., Fisher D. W., S., P.R., 1970. Effects of forest cutting and herbicide treatment on nutrient budgets in the Hubbard Book watershed-ecosystem. Ecological Monographs 40, 23-47.

Likens, G.E., Driscoll, C.T., Buso, D.C., 1996. Long-term effects of acid rain: Response and recovery of a forest ecosystem. Science 272, 244-246.

Lindsay, W.L., 1979. Chemical equilibria in soils. John Wiley & Sons, New York.

Lipson, D.A., Schmidt, S.K., Monson, R.K., 2000. Carbon availability and temperature control the post-snowmelt decline in alpine soil microbial biomass. Soil Biology & Biochemistry 32, 441-448.

Litaor, M.L., Seastedt, T.R., Walker, M.D., Carbone, M., Townsend, A., 2005. The biogeochemistry of phosphorus across an alpine topographic/snow gradient. Geoderma 124, 49-61.

Lovett, G.M., Goodale, C.L., 2011. A New Conceptual Model of Nitrogen Saturation Based on Experimental Nitrogen Addition to an Oak Forest. Ecosystems 14, 615-631.

Lovley, D.R., 1991. Dissimilatory Fe(III) and Mn(IV) reduction. Microbiological Reviews 55, 259-287.

Luckman, B., Kavanagh, T., 2000. Impact of climate fluctuations on mountain environments in the Canadian Rockies. Ambio 29, 371-380.

Ludwig, J., Meixner, F.X., Vogel, B., Forstner, J., 2001. Soil-air exchange of nitric oxide: An overview of processes, dnvironmental vactors, and modeling studies. Biogeochemistry 52, 225-257.

Lukkari, K., Hartikainen, H., Leivuori, M., 2007. Fractionation of sediment phosphorus revisited. I: Fractionation steps and their biogeochemical basis. Limnology and Oceanography-Methods 5, 433-444.

Lund, L.J., Brown, A.D., Lueking, M.A., Nodvin, S.C., Page, A.L., Sposito, G., 1987. Soil processes at Emerald Lake watershed. Final Report, California Air Resources Board, contract A3-105-32. 114 p.

Maurer, E.P., Stewart, I.T., Bonfils, C., Duffy, P.B., Cayan, D., 2007. Detection, attribution, and sensitivity of trends toward earlier streamflow in the Sierra Nevada. Journal of Geophysical Research-Atmospheres 112.

McCalley, C.K., Sparks, J.P., 2008. Controls over nitric oxide and ammonia emissions from Mojave Desert soils. Oecologia 156, 871-881.

McCalley, C.K., Sparks, J.P., 2009. Abiotic Gas Formation Drives Nitrogen Loss from a Desert Ecosystem. Science 326, 837-840.

Meehl, G.A., Stocker, T.F., Collins, W.D., *et al.*, 2007. Global climate projections, In: Solomon, S., Qin, D., Manning, M., *al., e.* (Eds.), Climate change 2007: The physical

science basis. Contribution of working group I to the fourth assessment report of the intergovernmental panel on climate change. Cambridge University Press, Cambridge, UK, pp. 747-845.

Meixner, F.X., Yang, W.X., 2006. Biogenic emissions of nitric oxide and nitrous oxide from arid and semi-arid land, In: D'Odorico, P., Porporato, A. (Eds.), Dryland Ecohydrology. Springer, pp. 233-255.

Meixner, T., Fenn, M., 2004. Biogeochemical budgets in a Mediterranean catchment with high rates of atmospheric N deposition - importance of scale and temporal asynchrony. Biogeochemistry 70, 331-356.

Melack, J.M., Sickman, J.O., Leydecker, A., 1998. Comparative analyses of high-altitude lakes and catchments in the Sierra Nevada: susceptibility to acidification. Final Report. California Air Resources Board contract A032-188. 615p.

Michalski, G., Meixner, T., Fenn, M., Hernandez, L., Sirulnik, A., Allen, E., Thiemens, M., 2004. Tracing atmospheric nitrate deposition in a complex semiarid ecosystem using $\Delta^{17}O$. Environmental Science & Technology 38, 2175-2181.

Mikan, C.J., Schimel, J.P., Doyle, A.P., 2002. Temperature controls of microbial respiration in arctic tundra soils above and below freezing. Soil Biology & Biochemistry 34, 1785-1795.

Miller, A.E., Schimel, J.P., Meixner, T., Sickman, J.O., Melack, J.M., 2005. Episodic rewetting enhances carbon and nitrogen release from chaparral soils. Soil Biology & Biochemistry 37, 2195-2204.

Miller, A.E., Schimel, J.P., Sickman, J.O., Meixner, T., Doyle, A.P., Melack, J.M., 2007. Mineralization responses at near-zero temperatures in three alpine soils. Biogeochemistry 84, 233-245.

Miller, A.E., Schimel, J.P., Sickman, J.O., Skeen, K., Meixner, T., Melack, J.M., 2009. Seasonal variation in nitrogen uptake and turnover in two high-elevation soils: mineralization responses are site-dependent. Biogeochemistry 93, 253-270.

Miller, A.J., Schuur, E.A.G., Chadwick, O.A., 2001. Redox control of phosphorus pools in Hawaiian montane forest soils. Geoderma 102, 219-237.

Minami, K., 1997. Atmospheric methane and nitrous oxide: sources, sinks and strategies for reducing agricultural emissions. Nutrient Cycling in Agroecosystems 49, 203-211.

Mooney, H.A., Rundel, P.W., 1979. Nutrient relations of the evergreen shrub, *Adenostoma fasciculatum*, in the California chaparral. Botanical Gazette 140, 109-113.

Morales-Baquero, R., Carrillo, R., Reche, I., Sanchez-Castillo, P., 1999. Nitrogen-phosphorus relationship in high mountain lakes: effects of the size of catchment basins. Canadian Journal of Fisheries and Aquatic Sciences 56, 1809-1817.

Morales-Baquero, R., Pulido-Villena, E., Reche, I., 2006. Atmospheric inputs of phosphorus and nitrogen to the southwest Mediterranean region: Biogeochemical responses of high mountain lakes. Limnology and Oceanography 51, 830-837.

Mortimer, C.H., 1941. The exchange of dissolved substances between mud and water in lakes. Journal of Ecology 29, 280-329.

Murphy, J., Riley, J.P., 1962. A modified single solution method for the determination of phosphate in natural waters. Analytica Chimica Acta 27, 31-36.

Mutch, L.S., Rose, M.G., Heard, A.M., Cook, R.R., Entsminger, G.L., 2008. Sierra Nevada network vital signs monitoring plan. National Park Service. U.S. Department of the Interior. Natural Resource Report NPS/SIEN/NRR-2008/072.

Nadelhoffer, K.J., Giblin, A.E., Shaver, G.R., Laundre, J.A., 1991. Effects of Temperature and Substrate Quality on Element Mineralization in 6 Arctic Soils. Ecology 72, 242-253.

NADP, 2010. National atmospheric deposition network. Inorganic nitrogen wet deposition from nitrate and ammonium 2010. http://nadp.sws.uiuc.edu/maplib/pdf/2010/TotalN_10.pdf.

Navarro-Garcia, F., Casermeiro, M.A., Schimel, J.P., 2012. When structure means conservation: Effect of aggregate structure in controlling microbial responses to rewetting events. Soil Biology & Biochemistry 44, 1-8.

Nürnberg, G.K., 1985. Availability of phosphorus upwelling from iron-rich anoxic hypolimnia. Archiv Fur Hydrobiologie 104, 459-476.

Oberson, A., Joner, E.J., 2005. Microbial turnover of phosphorus in soil, In: Turner, B.L., Frossard, E., Baldwin, D.S. (Eds.), Organic phosphorus in the environment. CAB International, Cambridge, MA, pp. 133-164.

Oldfield, F., 1977. Lakes and their drainage basins as units of sediment based ecological study. Progress in Physical Geography 1, 460-504.

Padgett, P.E., Allen, E.B., 1999. Differential responses to nitrogen fertilization in native shrubs and exotic annuals common to Mediterranean coastal sage scrub of California. Plant Ecology 144, 93-101.

Padgett, P.E., Allen, E.B., Bytnerowicz, A., Minich, R.A., 1999. Changes in soil inorganic nitrogen as related to atmospheric nitrogenous pollutants in southern California. Atmospheric Environment 33, 769-781.

Pant, H.K., Edwards, A.C., Vaughan, D., 1994. Extraction, Molecular Fractionation and Enzyme Degradation of Organically Associated Phosphorus in Soil Solutions. Biology and Fertility of Soils 17, 196-200.

Pardo, L.H., Fenn, M.E., Goodale, C.L., Geiser, L.H., Driscoll, C.T., Allen, E.B., Baron, J.S., Bobbink, R., Bowman, W.D., Clark, C.M., Emmett, B., Gilliam, F.S., Greaver, T.L., Hall, S.J., Lilleskov, E.A., Liu, L.L., Lynch, J.A., Nadelhoffer, K.J., Perakis, S.S., Robin-Abbott, M.J., Stoddard, J.L., Weathers, K.C., Dennis, R.L., 2011. Effects of nitrogen deposition and empirical nitrogen critical loads for ecoregions of the United States. Ecological Applications 21, 3049-3082.

Parker, B.R., Vinebrooke, R.D., Schindler, D.W., 2008. Recent climate extremes alter alpine lake ecosystems. Proceedings of the National Academy of Sciences of the United States of America 105, 12927-12931.

Parker, E.R., Sandford, R.L., 1999. The effects of mobile tree islands on soil phosphorus concentrations and distribution in an alpine tundra ecosystem an Niwot Ridge, Colorado Front Range, USA. Arctic Antarctic and Alpine Research 31, 16-20.

Parker, S.S., Schimel, J.P., 2011. Soil nitrogen availability and transformations differ between the summer and the growing season in a California grassland. Applied Soil Ecology 48, 185-192.

Parsons, D.A.B., Scholes, M.C., Scholes, R.J., Levine, J.S., 1996. Biogenic NO emissions from savanna soils as a function of fire regime, soil type, soil nitrogen, and water status. Journal of Geophysical Research-Atmospheres 101, 23683-23688.

Parton, W.J., Neff, J., Vitousek, P.M., 2005. Modelling phosphorus, carbon and nitrogen dynamics in terrestrial ecosystems, In: Turner, B.L., Frossard, E., Baldwin, D.S. (Eds.),

Organic phosphorus in the environment. CAB International, Cambridge, MA, pp. 325-347.

Payne, W.J., 1981. The status of nitric oxide and nitrous oxide as intermediates in denitrification, In: Delwiche, C.C. (Ed.), Denitrification, nitrification, and atmospheric nitrous oxide. Wiley, New York, pp. 85-103.

Perakis, S.S., Hedin, L.O., 2002. Nitrogen loss from unpolluted South American forests mainly via dissolved organic compounds. Nature 415, 416-419.

Perakis, S.S., Sinkhorn, E.R., 2011. Biogeochemistry of a temperate forest nitrogen gradient. Ecology 92, 1481-1491.

Pettersson, K., 2001. Phosphorus characteristics of settling and suspended particles in Lake Erken. Science of the Total Environment 266, 79-86.

Poth, M., 1982. Biological dinitrogen fixation in chaparral., In: Conrad, C.E., Oechel, W.C. (Eds.), Proceedings of the symposium on dynamics and management of Mediterranean-type ecosystems, US Forest Service, Pacific Southwest Forest and Range Experimental Station, General Technical Report PSW-58, Berkeley, CA, pp. 285-290.

Prairie, Y.T., De Montigny, C., Del Giorgio, P.A., 2001. Anaerobic phosphorus release from sediments: a paradigm revisited. Verh. Internat. Verein. Limnol. 27, 4013-4020.

Quiquampoix, H., Mousain, D., 2005. Enzymatic hydrolosis of organic phosphorus, In: Turner, B.L., Frossard, E., baldwin, D.S. (Eds.), Organic phosphorus in the environment. CAB International, Cambridge, MA, pp. 89-112.

Rao, L.E., Allen, E.B., Meixner, T., 2010. Risk-based determination of critical nitrogen deposition loads for fire spread in southern California deserts. Ecological Applications 20, 1320-1335.

Riggan, P.J., Lockwood, R.N., Lopez, E.N., 1985. Deposition and processing of airborne nitrogen pollutants in Mediterranean-type ecosystems of southern-California. Environmental Science & Technology 19, 781-789.

Robertson, G.P., Groffman, P.M., 2007. Nitrogen transformations, In: Paul, E.A. (Ed.), Soil microbiology, ecology, and biochemistry, third ed. Academic Press, New York, pp. 341-364.

Robertson, L.A., Kuenen, J.G., 1984. Aerobic Denitrification - Old Wine in New Bottles. Antonie Van Leeuwenhoek Journal of Microbiology 50, 525-544.

Romanovsky, V.E., Osterkamp, T.E., 2000. Effects of unfrozen water on heat and mass transport processes in the active layer and permafrost. Permafrost and Periglacial Processes 11, 219-239.

Ron Vaz, M.D., Edwards, A.C., Shand, C.A., Cresser, M.S., 1994. Changes in the Chemistry of Soil Solution and Acetic-Acid Extractable-P Following Different Types of Freeze-Thaw Episodes. European Journal of Soil Science 45, 353-359.

Rundel, P.W., Parsons, D.J., 1979. Structural changes in chamise (*Adenostoma fasciculatum*) along a fire-induced age gradient. Journal of Range Management 32, 462-466.

Rydin, E., 2000. Potentially mobile phosphorus in Lake Erken sediment. Water Research 34, 2037-2042.

Rydin, E., Huster, B., Welch, E.B., 2000. Amount of phosphorus inactivated by alum treatments in Washington lakes. Limnology and Oceanography 45, 226-230.

Rysgaard, S., Risgaard-Petersen, N., Sloth, N., Jensen, K., Nielsen, L., 1994. Oxygen regulation of nitrification and denitrification in sediments. Limnology and Oceanography 39, 1643-1652.

Sadro, S., Melack, J.M., 2012. The effect of an extreme rain event on the biogeochemistry and ecosystem metabolism of an oligotrophic high-elevation lake. Arctic, Antarctic, and Alpine Research.

Sadro, S., Melack, J.M., MacIntyre, S., 2011a. Depth-integrated estimates of ecosystem metabolism in a high-elevation lake (Emerald Lake, Sierra Nevada, California). Limnology and Oceanography 56, 1764-1780.

Sadro, S., Melack, J.M., MacIntyre, S., 2011b. Spatial and Temporal Variability in the Ecosystem Metabolism of a High-elevation Lake: Integrating Benthic and Pelagic Habitats. Ecosystems 14, 1123-1140.

SanClements, M.D., Fernandez, I.J., Norton, S.A., 2009. Soil and sediment phosphorus fractions in a forested watershed at Acadia National Park, ME, USA. Forest Ecology and Management 258, 2318-2325.

SanClements, M.D., Fernandez, I.J., Norton, S.A., 2010. Phosphorus in Soils of Temperate Forests: Linkages to Acidity and Aluminum. Soil Science Society of America Journal 74, 2175-2186.

Sardans, J., Penuelas, J., Estiarte, M., 2008. Changes in soil enzymes related to C and N cycle and in soil C and N content under prolonged warming and drought in a Mediterranean shrubland. Applied Soil Ecology 39, 223-235.

Schimel, J., Balser, T.C., Wallenstein, M., 2007. Microbial stress-response physiology and its implications for ecosystem function. Ecology 88, 1386-1394.

Schimel, J.P., Bennett, J., 2004. Nitrogen mineralization: Challenges of a changing paradigm. Ecology 85, 591-602.

Schindler, D.W., 1977. Evolution of Phosphorus Limitation in Lakes. Science 195, 260-262.

Schindler, D.W., Kling, H., Schmidt, R.V., Prokopowich, J., Frost, V.E., Reid, R.A., Capel, M., 1973. Eutrophication of lake 227 by addition of phosphate and nitrage: The second, third, and fourth years of enrichment, 1970, 1971, and 1972. Journal of the Fisheries Research Board of Canada 30, 1415-1440.

Schlesinger, W.H., 1997. Biogeochemistry: An analysis of global change, second ed. Academic Press, San Diego.

Schmidt, I., van Spanning, R.J.M., Jetten, M.S.M., 2004. Denitrification and ammonia oxidation by *Nitrosomonas europaea* wild-type, and NirK- and NorB-deficient mutants. Microbiology 150, 4107-4114.

Schmidt, S.K., Lipson, D.A., 2004. Microbial growth under the snow: Implications for nutrient and allelochemical availability in temperate soils. Plant and Soil 259, 1-7.

Sharpley, A.N., Kleinman, P.J.A., Weld, J.L., 2008. Environmental soil phosphorus indices, In: Carter, M.R., Gregorich, E.G. (Eds.), Soil sampling and methods of analysis, Second ed. CRC Press, Boca Raton, FL, pp. 141-159.

Shiels, A.B., Sanford, R.L., 2001. Soil nutrient differences between two krummholz-form tree species and adjacent alpine tundra. Geoderma 102, 205-217.

Sickman, J.O., 2001. Comparative analyses of nitrogen biogeochemistry in high-elevation ecosystems of the Sierra Nevada and Rocky Mountains. Ph.D. dissertation, Ecology, Evolution and Marine Biology. University of California, Santa Barbara.

Sickman, J.O., Leydecker, A., Chang, C.C.Y., Kendall, C., Melack, J.M., Lucero, D.M., Schimel, J.P., 2003a. Mechanisms underlying export of N from high-elevation catchments during seasonal transitions. Biogeochemistry 64, 1-32.

Sickman, J.O., Leydecker, A., Melack, J.M., 2001. Nitrogen mass balance and abiotic controls on N retention and yield in high-elevation catchments of the Sierra Nevada, California, United States. Water Resources Research 37, 1445-1461.

Sickman, J.O., Melack, J.M., 1998. Nitrogen and sulfate export from high elevation catchments of the Sierra Nevada, California. Water, Air and Soil Pollution 1051-2, 217-226.

Sickman, J.O., Melack, J.M., Clow, D.W., 2003b. Evidence for nutrient enrichment of high-elevation lakes in the Sierra Nevada, California. Limnology and Oceanography 48, 1885-1892.

Sigman, D.M., Casciotti, K.L., Andreani, M., Barford, C., Galanter, M., Bohlke, J.K., 2001. A bacterial method for the nitrogen isotopic analysis of nitrate in seawater and freshwater. Analytical Chemistry 73, 4145-4153.

Simard, R.R., Beauchemin, S., Haygarth, P.M., 2000. Potential for preferential pathways of phosphorus transport. Journal of Environmental Quality 29, 97-105.

Skiba, U., Smith, K.A., Fowler, D., 1993. Nitrification and Denitrification as Sources of Nitric-Oxide and Nitrous-Oxide in a Sandy Loam Soil. Soil Biology & Biochemistry 25, 1527-1536.

Smart, D.R., Stark, J.M., Diego, V., 1999. Resource limitations to nitric oxide emissions from a sagebrush-steppe ecosystem. Biogeochemistry 47, 63-86.

Smeck, N.E., 1973. Phosphorus: an indicator of pedogenic weathering processes. Soil Science 115, 199-206.

Smeck, N.E., 1985. Phosphorus dynamics in soils and landscapes. Geoderma 36, 185-199.

Sokal, R.R., Rohlf, R.J., 1981. Biometry: The principles and practice of statistics in biological research. W.H. Freeman, New York.

Stark, J.M., Firestone, M.K., 1995. Mechanisms for soil moisture effects on activity of nitrifying bacteria. Applied and Environmental Microbiology 61, 218-221.

Stewart, I.T., Cayan, D.R., Dettinger, M.D., 2005. Changes toward earlier streamflow timing across western North America. Journal of Climate 18, 1136-1155.

Stoddard, J.L., 1994. Long-term changes in watershed retention of nitrogen. Its causes and aquatic consequences, In: Baker, L.A. (Ed.). Amer Chemical Society, pp. 223-284.

Stohlgren, T.J., Parsons, D.J., Rundel, P.W., 1984. Population-structure of *Adenostoma fasciculatum* in mature stands of chamise chaparral in the southern Sierra Nevada, California. Oecologia 64, 87-91.

Su, H., Cheng, Y.F., Oswald, R., Behrendt, T., Trebs, I., Meixner, F.X., Andreae, M.O., Cheng, P., Zhang, Y., Poschl, U., 2011. Soil Nitrite as a Source of Atmospheric HONO and OH Radicals. Science 333, 1616-1618.

Swarowsky, A., Dahlgren, R.A., O'Geen, A.T., 2012. Linking Subsurface Lateral Flowpath Activity with Streamflow Characteristics in a Semiarid Headwater Catchment. Soil Science Society of America Journal 76, 532-547.

Taskey, R.D., 1995. Soil survey of high Sierra area, California. U.S. Department of Agriculture, USFS, Pacific Southwest Research Station, CA.

Taylor, B.R., Jones, H.G., 1990. Litter Decomposition under Snow Cover in a Balsam Fir Forest. Canadian Journal of Botany-Revue Canadienne De Botanique 68, 112-120.

Taylor, P.G., Townsend, A.R., 2010. Stoichiometric control of organic carbon-nitrate relationships from soils to the sea. Nature 464, 1178-1181.

Tegen, I., Kohfeld, K.E., 2006. Atmospheric transport of silicon, In: Ittekkot, V., Unger, D., Humbog, C., Tac An, N. (Eds.), The silicon cycle: human perturbations and impacts on aquatic systems. Island Press, Washington, D.C., pp. 81-91.

Tessier, L., Gregorich, E.G., Topp, E., 1998. Spatial variability of soil microbial biomass measured by the fumigation extraction method, and K-EC as affected by depth and manure application. Soil Biology & Biochemistry 30, 1369-1377.

Theisen, A.A., Harward, M.E., 1962. A paste method for preparation of slides for clay mineral identification by x-ray diffraction. Soil Science Society of America Proceedings 26, 90-91.

Tiessen, H., Moir, J.O., 2008. Characterization of available P by sequential extraction, In: Carter, M.R., Gregorich, E.G. (Eds.), Soil sampling and methods of analysis, Second ed. CRC Press, Boca Raton, FL, pp. 293-306.

Tiessen, H., Stewart, J.W.B., Moir, J.O., 1983. Changes in organic and inorganic phosphorus composition of two grassland soils and their particle size fractions during 60-90 years of cultivation. Journal of Soil Science 34, 815-823.

Tipping, E., 1981. The Adsorption of Aquatic Humic Substances by Iron-Oxides. Geochimica Et Cosmochimica Acta 45, 191-199.

Turner, B.L., 2005. Organic phosphorus transfer from terrestrial to aquatic environments, In: Turner, B.L., Frossard, E., Baldwin, D.S. (Eds.), Organic phosphorus in the environment. CAB International, Cambridge, MA, pp. 269-294.

Turner, B.L., 2007. Inositol phosphates in soil: amounts, forms and significance of the phosphorylated inositol stereoisomers, In: Turner, B.L., Richardson, A.E., Mullaney, E.J. (Eds.), Inositol phosphates. Linking agriculture and the environment. CAB International, Wallingford, pp. 186-206.

Turner, B.L., Driessen, J.P., Haygarth, P.M., Mckelvie, I.D., 2003. Potential contribution of lysed bacterial cells to phosphorus solubilisation in two rewetted Australian pasture soils. Soil Biology & Biochemistry 35, 187-189.

Turner, B.L., Haygarth, P.M., 2001. Biogeochemistry - Phosphorus solubilization in rewetted soils. Nature 411, 258-258.

Vance, E.D., Brookes, P.C., Jenkinson, D.S., 1987. An Extraction Method for Measuring Soil Microbial Biomass-C. Soil Biology & Biochemistry 19, 703-707.

Venterea, R.T., Groffman, P.M., Verchot, L.V., Magill, A.H., Aber, J.D., Steudler, P.A., 2003. Nitrogen oxide gas emissions from temperate forest soils receiving long-term nitrogen inputs. Global Change Biology 9, 346-357.

Venterea, R.T., Rolston, D.E., Cardon, Z.G., 2005. Effects of soil moisture, physical, and chemical characteristics on abiotic nitric oxide production. Nutrient Cycling in Agroecosystems 72, 27-40.

Vicars, W.C., Sickman, J.O., 2011. Mineral dust transport to the Sierra Nevada, California: Loading rates and potential source areas. Journal of Geophysical Research-Biogeosciences 116, 14.

Vicars, W.C., Sickman, J.O., Ziemann, P.J., 2010. Atmospheric phosphorus deposition at a montane site: Size distribution, effects of wildfire, and ecological implications. Atmospheric Environment 44, 2813-2821.

Vitousek, P.M., Aber, J.D., Howarth, R.W., Likens, G.E., Matson, P.A., Schindler, D.W., Schlesinger, W.H., Tilman, D., 1997. Human alteration of the global nitrogen cycle: Sources and consequences. Ecological Applications 7, 737-750.

Vitousek, P.M., Field, C.B., 2001. Input/output balances and nitrogen limitation in terrestrial ecosystems, In: Schulze, E.D., Heimann, M., Harrison, S., Holland, E., Lloyd, J., Prentice, I.C., Schimel, D. (Eds.), Global biogeochemical cycles in the climate system. Academic Press, New York, pp. 217-225.

Vitousek, P.M., Melillo, J.M., 1979. Nitrate Losses from Disturbed Forests - Patterns and Mechanisms. Forest Science 25, 605-619.

Voroney, R.P., 2007. The soil habitat, In: Paul, E.A. (Ed.), Soil microbiology, ecology, and biochemistry, Third ed. Academic Press, Burlington MA.

Voroney, R.P., Brookes, P.C., Beyaert, R.P., 2008. Soil microbial biomass C, N, P, and S, In: Carter, M.R., gregorich, E.G. (Eds.), Soil sampling and methods of analysis, Second ed. CRC Press, Boca Raton, FL, pp. 637-651.

Vourlitis, G.L., Pasquini, S., Zorba, G., 2007a. Plant and soil N response of southern californian semi-arid shrublands after 1 year of experimental N deposition. Ecosystems 10, 263-279.

Vourlitis, G.L., Pasquini, S.C., Mustard, R., 2009. Effects of Dry-Season N Input on the Productivity and N Storage of Mediterranean-Type Shrublands. Ecosystems 12, 473-488.

Vourlitis, G.L., Zorba, G., 2007. Nitrogen and carbon mineralization of semi-arid shrubland soil exposed to long-term atmospheric nitrogen deposition. Biology and Fertility of Soils 43, 611-615.

Vourlitis, G.L., Zorba, G., Pasquini, S.C., Mustard, R., 2007b. Chronic nitrogen deposition enhances nitrogen mineralization potential of semiarid shrubland soils. Soil Science Society of America Journal 71, 836-842.

Walker, T.W., Syers, J.K., 1976. The fate of phosphorus during pedogenesis. Geoderma 15, 1-19.

Wetzel, R., 2001. Limnology: Lake and River Ecosystems, Third Ed. ed. Academic Press, San Diego.

Williams, M.R., Brown, A.D., Melack, J.M., 1993. Geochemical and hydrologic controls on the composition of surface water in a high-elevation basin, Sierra Nevada, California. Limnology and Oceanography 38, 775-797.

Williams, M.W., Bales, R.C., Brown, A.D., Melack, J.M., 1995. Fluxes and transformations of nitrogen in a high-elevation catchment, Sierra Nevada. Biogeochemistry 28, 1-31.

Williams, M.W., Brooks, P.D., Seastedt, T., 1998. Nitrogen and carbon soil dynamics in response to climate change in a high-elevation ecosystem in the Rocky Mountains, USA. Arctic and Alpine Research 30, 26-30.

Wood, H.B., Olivier, K.L., Ryan, T.M., 1992. Surface soil acidification in smog-polluted chaparral ecosystems in the San Gabriel Mountains, California. Bulletin of the Ecological Society of America 73, 392.

Wood, S.H., 1977. Distribution, correlation, and cadiocarbon dating of late Holocene tephra, Mono and Inyo craters, eastern California. Geological Society of America Bulletin 88, 89-95.

Wood, Y.A., Fenn, M., Meixner, T., Shouse, P.J., Breiner, J., Allen, E., Wu, L.S., 2007. Smog nitrogen and the rapid acidification of forest soil, San Bernardino Mountains, southern California. Thescientificworldjournal 7, 175-180.

Wood, Y.A., Meixner, T., Shouse, P.J., Allen, E.B., 2006. Altered ecohydrologic response drives native shrub loss under conditions of elevated nitrogen deposition. Journal of Environmental Quality 35, 76-92.

Wu, X., Bruggemann, N., Gasche, R., Shen, Z.Y., Wolf, B., Butterbach-Bahl, K., 2010. Environmental controls over soil-atmosphere exchange of N2O, NO, and CO2 in a temperate Norway spruce forest. Global Biogeochemical Cycles 24, 16.

Xiang, S.R., Doyle, A., Holden, P.A., Schimel, J.P., 2008. Drying and rewetting effects on C and N mineralization and microbial activity in surface and subsurface California grassland soils. Soil Biology & Biochemistry 40, 2281-2289.

Yanai, R.D., 1992. Phosphorus Budget of a 70-Year-Old Northern Hardwood Forest. Biogeochemistry 17, 1-22.

Yoshida, T., Alexander, M., 1970. Nitrous oxide formation by *Nitrosomonas europaea* and heterotrophic microorganisms. Soil Science Society of America Proceedings 34, 880-882.

Yu, J.B., Meixner, F.X., Sun, W.D., Mamtimin, B., Xia, C.H., Xie, W.J., 2010. Biogenic Nitric Oxide Emission of Mountain Soils Sampled from Different Vertical Landscape Zones in the Changbai Mountains, Northeastern China. Environmental Science & Technology 44, 4122-4128.

Zedler, P.H., Gautier, C.R., McMaster, G.S., 1983. Vegetation change in response to extrem events--The effect of a short interval between fires in California chaparral and coastal scrub. Ecology 64, 809-818.

Zhang, L., Wu, Y., Wu, N., Luo, P., Liu, L., Hu, H.Y., 2011. Impacts of vegetation type on soil phosphorus availability and fractions near the alpine timberline of the Tibetan Plateau. Polish Journal of Ecology 59, 307-316.

APPENDIX A. X-RAY DIFFRACTION ANALYSIS

X-ray diffraction (XRD) was conducted on single soil samples from Lithic Cryumbrepts and Typic Cryofluvents from both the A and B horizons using the paste method (Theisen and Harward, 1962) to gain insight on the clay mineralogy of the EML catchment. The fine clay (<0.2 μm) and coarse clay (0.2-2 μm) fractions were separated by centrifugation and the medium silt (5-20 μm) by sedimentation, followed by treatment with sodium hypochlorite for organic matter removal. The < 2 μm fraction was saturated with K (heated at 25, 350, and 550°C) and Mg, and Mg saturation with ethylene glycol (Mg EG). Analyses were performed on an x-ray diffractometer with a graphite crystal monochromator using CuKα radiation (40 kV and 30 mA). Samples were step scanned for 10 s from 2 to 32° 2θ with a step size of 0.02° 2θ.

XRD analysis indicated the presence of smectite, chlorite, vermiculite, hydroxyinterlayered minerals, mica, and potentially kaolinite.

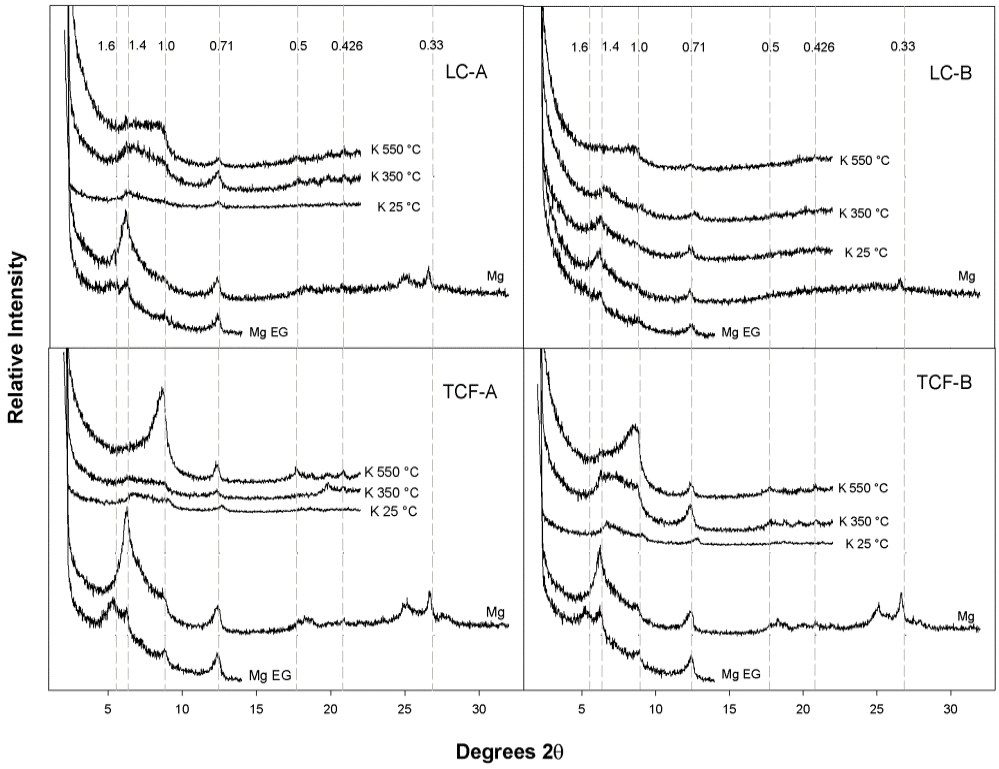

Fig. A.1. XRD analysis of A and B horizons for Lithic Cryumbrepts (LC) and Typic Cryofluvents (TCF).